



MASTER OF SCIENCE IN MECHANICAL ENGINEERING

***Improvement of Machinability of Steel during Turning
Operation by Magnetic Cutting***

by

Mohammad Nauzef Mahmood

Department of Mechanical and Chemical Engineering
Islamic University of Technology (IUT)
Gazipur-1704, Bangladesh.

August, 2012

CERTIFICATE OF APPROVAL

The thesis titled “*Improvement of Machinability of Steel during Turning Operation by Magnetic Cutting*” submitted by Mohammad Nuzef Mahmood bearing Student No. 101603 of Academic Year 2010-2011 has been found as satisfactory and accepted as partial fulfillment of the requirement for the degree of Master of Science in Mechanical Engineering on 05 August 2012.

BOARD OF EXAMINERS

- 1. **Dr. Md. Anayet Ullah Patwari** Chairman
(Supervisor)
Associate Professor
Department of Mechanical and Chemical Engineering
Islamic University of Technology (IUT)
Gazipur, Bangladesh.

- 2. **Dr. Md. Abdur Razzaq Akhanda** Member
(Ex-Officio)
Professor and Head
Department of Mechanical and Chemical Engineering
Islamic University of Technology (IUT)
Gazipur, Bangladesh.

- 3. **Dr. Md. Nurul Absar Chowdhury** Member
Professor
Department of Mechanical and Chemical Engineering
Islamic University of Technology (IUT)
Gazipur, Bangladesh.

- 4. **Dr. Mohammed Alauddin** Member
(External)
Professor and Head
Department of Industrial and Production Engineering
Dhaka University of Engineering and Technology (DUET)
Gazipur, Bangladesh.

DECLARATION OF CANDIDATE

It is hereby declared that this Thesis or any part of it has not been submitted elsewhere for the award of any Degree or Diploma.

(Signature)

Dr. Md. Anayet Ullah Patwari

(Supervisor)

Associate Professor

Department of Mechanical and Chemical Engineering

Islamic University of Technology (IUT)

Gazipur-1704, Bangladesh.

(Signature)

Mohammad Nauzef Mahmood

Student No. 101603

Academic Year: 2010-2011

DEDICATION

This thesis is dedicated to my beloved parents, wife and all my well wishers helping me to accomplish this work.

TABLE OF CONTENTS

No.	Topic	Page
Chapter 1	Introduction	
1.1	Inserts	3
1.2	Tool wear	4
1.3	Surface Structure and Properties	15
1.4	Objective of the study	20
1.5	Thesis Organization	20
Chapter 2	Review of Relevant Literatures	
2.1	General Discussion	23
2.1.1	Contemporary Research about Tool Wear	24
2.1.2	Contemporary Research about Surface Roughness	26
2.1.3	Contemporary Research about Magnetic Cutting	31
2.2	Problem Statement	33
2.3	Scope of Current Work	33
Chapter 3	Experimental Set up and Procedure	
3.1	Experimental setup	37
3.2	Process variables	38
3.3	Equipments and apparatus used	38
3.4	Measurement Techniques	44
3.4.1	Measurement of Tool Wear	44
3.4.2	Measurement of Surface Roughness	46
3.4.3	Observation of chip Behavior	48
3.4.4	Measurement of Temperature	50
3.4.5	Measurement of Cutting Force	50
Chapter 4	Results and Discussions	
4.1	Distribution of Magnetic Field	54
4.2	Study of the Effect on Tool wear	55
4.3	Study of the Effect on Surface Roughness	73
4.4	Study of the Effect on Cutting Temperature	77
4.5	Study of the Effect on Chip Behavior	80
4.6	Study of the Effect on Cutting Force	83

Chapter 5	Conclusions and Recommendations	
5.1	Conclusions	87
5.2	Recommendations	88
References		90
Appendix A		96
Appendix B		97

LIST OF TABLES

No.	Title	Page
Chapter 3		
3.1	Process Variables and their values	38
3.2	Detail specification of the microscope	39
3.3	Chemical composition of the mild steel used in the experimentation	40
3.4	Detail specification of permanent magnet	41
3.5	Technical details of SM1010 digital strain display	52
Chapter 4		
4.1	Accuracy and repeatability of the automated tool wear analysis technique	55
4.2	Sample pictures of tool wear at 860 RPM and 0.75 DOC under different cutting environment	56
4.3	Sample pictures of tool wear at Different depth of cut under different cutting environment	62

LIST OF FIGURES

No.	Title	Page
Chapter 1		
1.1	Photograph of different types of carbide tool inserts	4
1.2	Tool wear phenomena	5
1.3	Photograph of Attrition wear	6
1.4	Photograph of Abrasive wear	6
1.5	Photograph of Diffusion wear	7
1.6	Photograph of Built up edge	7
1.7	Photograph of Chipping wear	8
1.8	Photograph of Flaking	8
1.9	Photograph of Spalling	9
1.10	Photograph of Fracture	9
1.11	Photograph of Flank / nose wear	10
1.12	Photograph of Notching wear	10
1.13	Photograph of Thermal cracking	11
1.14	Photograph of Crater wear	11
1.15	Photograph of Deformation wear	12
1.16	Typical stages of tool wear in normal cutting situation	14
1.17	Schematic of a cross-section of the surface structure of metals	15
1.18	Schematic diagram of surface characteristics	17
Chapter 3		
3.1	Flow sequence of the experimentation	36
3.2	Photograph of experimental setup for a) permanent magnet, b) electromagnet.	37
3.3	Photograph and details of the optical microscope	38
3.4	Photograph of Insert with dimension.	39
3.5	CAD model of Work piece with dimension	40
3.6	Photograph of permanent magnet used in the study	41
3.7	Photograph of electro magnet used in the study	43
3.8	CAD Model of the core of electromagnet	43
3.9	Photograph of electrical Circuit to produce electromagnetic field	43
3.10	Process logic sequence flowchart for measuring tool wear	44
3.11	Image processing result sample for measuring tool wear	46
3.12	Flow diagram of image processing for surface roughness	47
3.13	DIP results (work-piece surface roughness, without magnet) (a) 10x zoom RGB microphotograph, (b) grayscale, (c) profile plot, (d) 2-D coloured contour plot, (e) 3-D coloured contour plot	48
3.14	Photograph of samples of mounted chip	49
3.15	Photograph of instruments used for chip analysis. a) Polishing wheel, b) optical microscope	49

3.16	Photograph of arrangement for measuring cutting temperature a) thermocouple b) experimental setup c) thermocouple hot end attached with insert tip	50
3.17	Photograph of arrangement for measuring cutting force with half bridge circuit and strain meter	51
3.18	SM 1010 Digital Strain Display	51
3.19	Circuit used to connect strain gauges to the strain meter	52

Chapter 4

4.1	Comparison of field distribution between permanent magnet and electromagnetic condition	54
4.2	Comparison of tool wear at 530rpm and depth of cut 0.5 mm	57
4.3	Comparison of tool wear at 860rpm and depth of cut 0.5 mm	57
4.4	Comparison of tool wear at 1400rpm and depth of cut 0.5 mm	58
4.5	Comparison of tool wears at 530rpm and depth of cut 0.75 mm	58
4.6	Comparison of tool wears at 530rpm and depth of cut 1.0 mm	59
4.7	Comparison of tool wears at 860rpm and depth of cut 0.75 mm	59
4.8	Comparison of tool wears at 860rpm and depth of cut 1.0 mm	60
4.9	Comparison of tool wears at 1400rpm and depth of cut 0.75 mm	60
4.10	Comparison of tool wears at 1400rpm and depth of cut 1.0 mm with constant feed	61
4.11	Comparison of tool wear at 530rpm in electromagnetic condition with different depth of cut	62
4.12	Comparison of tool wear at 530rpm in permanent magnetic condition with different depth of cut	63
4.13	Comparison of tool wear at 530rpm in without magnet condition with different depth of cut	63
4.14	Comparison of tool wears at 860rpm in electromagnetic condition with different depth of cut	64
4.15	Comparison of tool wears at 1400rpm in electromagnetic condition with different depth of cut	64
4.16	Comparison of tool wears at 860rpm in permanent magnetic condition with different depths of cut	65
4.17	Comparison of tool wears at 1400rpm in permanent magnetic condition with different depths of cut	65
4.18	Comparison of tool wears at 860rpm in without magnet condition with different depths of cut	66
4.19	Comparison of tool wears at 1400rpm in without magnet condition with different depths of cut	66
4.20	Comparison of tool wear at 0.75mm DOC in electromagnet condition with different cutting speeds	68
4.21	Comparison of tool wear at 0.75mm DOC in permanent magnet condition with different cutting speeds	68

4.22	Comparison of tool wear at 0.75mm DOC in permanent magnet condition with different cutting speeds	69
4.23	Comparison of tool wears at 0.5mm DOC in electromagnet condition with different cutting speeds	69
4.24	Comparison of tool wears at 1.0mm DOC in electromagnet condition with different cutting speeds	70
4.25	Comparison of tool wears at 0.5mm DOC in permanent magnet condition with different cutting speeds	70
4.26	Comparison of tool wears at 1.0mm DOC in permanent magnet condition with different cutting speeds	71
4.27	Comparison of tool wears at 0.5mm DOC in without magnet condition with different cutting speeds	71
4.28	Comparison of tool wears at 1.0mm DOC in without magnet condition with different cutting speeds	72
4.29	Contour plot of the machined surface under different conditions	73
4.30	Sample photographs of surfaces of the work piece at different cutting speed at 0.5 Depth of cut after cutting 1000mm	74
4.31	Comparison of surface roughness at 0.5mm DOC and different cutting environment	74
4.32	Comparison of surface roughness at 0.5mm DOC and different cutting environment	75
4.33	Comparison of surface roughness at 0.5mm DOC and different cutting environment	75
4.34	sample photograph of built up edge taken in electromagnetic cutting condition at 530 RPM and 0.5mm depth of cut	76
4.35	Variation of temperature with depth of cut at 530rpm after 200mm cut	77
4.36	Variation of temperature with depth of cut at 860rpm after 200 mm cut	77
4.37	Variation of temperature with depth of cut at 0.5mm DOC after 200mm cut	78
4.38	Variation of temperature with depth of cut at 0.75mm DOC after 200mm cut	79
4.39	Variation of temperature with depth of cut at 1.0 mm DOC after 200mm cut	79
4.40	Photograph of continuity of chip at different magnetic conditions	80
4.41	Section of chip formed at different cutting conditions	81
4.42	Cross section view of chip formed at different cutting conditions obtained at 530 rpm and 0.5mm DOC	81
4.43	Enlarged view of tooth of chip formed at different cutting conditions obtained at 530 rpm and 0.5mm DOC	82
4.44	Change of shrinkage co efficient at different cutting conditions	82
4.45	Photograph of different colour of chip at different conditions	83
4.46	Change of strain of tool holder and tangential cutting force with respect to Cutting Speed	84
4.47	Change of strain of tool holder and tangential cutting force with respect to depth of cut	85

LIST OF ABBREVIATIONS OF TECHNICAL SYMBOLS AND TERMS

BUE	Built up Edge
DOC	Depth of cut
CBN	Cubic Boron Nitride
SiN	Silicon Nitride
PCBN	Poly Crystalline Boron Nitride
HSS	High Speed Steel
WC	Tungsten Carbide
2D	Two Dimension
3D	Three Dimension

ACKNOWLEDGEMENTS

Every honor and every victory on earth is due to the Great Almighty, descended from Him and must be ascribed to Him. He has given me the capability to do all this work. This thesis is a result of research of one and a half year and this is by far the most significant scientific accomplishment in my life. It would be almost impossible without support and appreciation of those who mattered most. I would like to express my heartiest gratitude to my supervisor, Associate. Prof. Dr. Md. Anayet Ullah Patwari for his supervision, inspiration and unbounded support for doing this work. I would also like to pay my heartiest gratitude to Mr. Shakhawat Hossain, for his support in taking pictures of the inserts and machine operation. I would like to extend my thanks to Mr. Muammer Din Arif for helping with the algorithm for digital image processing. I convey my gratitude to Shafi Noor, Md. Ziaul Haque Shovon and Md. Tawfiqullah for helping me during experimentation. I am also thankful to the Head of the Department Prof. Dr. Abdur Razzaq Akhanda for his guideline and support for my thesis. Last but not the least I am thankful to my parents, my wife and my respected elder brothers, colleagues, friends and relatives who have always supported me in my work.

ABSTRACT

This study presents the results of an investigation of machinability improvement in turning of mild steel (0.25% C) by magnetic cutting. Turning experiments were done by using a precision lathe both without application of magnetic field and with the application of magnetic field. The external magnetic field was implemented using two different magnetic setups: one created by permanent magnet another by electro magnet. Poor machinability results in surface defects and dimensional inaccuracy of the work piece as well as reduction of useful tool life and damage to machine. A recent and promising way to improve the machinability of steel is to reduce the vibration effect of machine-tool-work system by applying external damping effect using magnetic cutting technique. In this investigation the effect of external magnetic field (both permanent magnet and electromagnet) was evaluated on machinability parameters such as tool life, surface roughness, cutting temperature and cutting force. The characteristics of chip produced during turning were also observed to further study the magnetic effect on cutting mechanism. Improvements in tool life, reduction in average surface roughness, increase in cutting temperature and decrease in cutting force were observed during the experimentation by magnetic cutting. Certain changes of chip formation characteristics were also observed when the mild steel was being cut. It has been observed that the chip serration nature has been changed significantly in magnetic cutting. Experiments were carried out by changing cutting speed and depth of cut to determine the optimal magnetic field to be applied which would translate into greatest amount of benefits. Due to the limitation of feed variation within the existing facilities of lathe, the feed value was kept constant at 0.095 mm/rev. The observations of effect of magnetic field on machinability parameters, lead to the conclusion that magnetic cutting improves the machinability factors of mild steel significantly and further enhance the possibility of using magnetic effects to reduce machining costs.

Chapter 1

Introduction

Background Information

Tool wear adversely affects productivity, dimensional accuracy, as well as product quality in most machining processes. Because of tool wear the surface finish of the product also deteriorates. So it is one of the primary concerns to reduce tool wear in any machining process. There have been several ways to determine tool wear specially flank wear but all of them are either costly or complex process. To reduce tool wear the effect of external electromagnetic force is studied by many contemporary researchers. All of those studies have been carried out in particular cutting condition and using electromagnets. This study further investigates the effect of external magnetic field over a wide range of cutting conditions. As setting up electromagnet is often complex this study introduces permanent magnet in turning and compares the result with non magnetic and electromagnetic cutting conditions over the whole range of cutting conditions. To facilitate the measurement of tool wear easily, this study also proposes the use of digital image processing technique to determine tool wear. Finally this study aims to establish the advantages of magnetic cutting over non magnetic cutting and proposes the most suitable cutting environment in different cutting conditions.

Introduction

Turning is a metal cutting process used for the generation of cylindrical surfaces. Typically the work piece is rotated on a spindle and the tool is fed into it radially, axially or both ways simultaneously to give the required surface. The term turning, in the general sense, refers to the generation of any cylindrical surface with a single point tool. More specifically, it is often applied just to the generation of external cylindrical surfaces oriented primarily parallel to the work piece axis. The generation of surfaces oriented primarily perpendicular to the work piece axis are called facing. In turning, the direction of the feeding motion is predominantly axial with respect to the machine spindle. In facing a radial feed is dominant. Tapered and contoured surfaces require both modes of tool feed at the same time often referred to as profiling. The cutting characteristics of most turning applications are similar. For a given surface only one cutting tool is used.

This tool must overhang its holder to some extent to enable the holder to clear the rotating work piece. Once the cut starts, the tool and the work piece are usually in contact until the surface is completely generated. During this time the cutting speed and cut dimensions will be constant when a cylindrical surface is being turned. In the case of facing operations the cutting speed is proportional to the work diameter, the speed decreasing as the center of the piece is approached. Sometimes a spindle speed changing mechanism is provided to increase the rotating speed of the work piece as the tool moves to the center of the part.

In general, turning is characterized by steady conditions of metal cutting. Except at the beginning and end of the cut, the forces on the cutting tool and the tool tip temperature are essentially constant. For the special case of facing, the varying cutting speed will affect the tool tip temperature. Higher temperatures will be encountered at the larger diameters on the work piece. However, since cutting speed has only a small effect on cutting forces, the forces acting on a facing tool may be expected to remain almost constant during the cut.

1.1 Inserts

A tipped tool generally refers to any cutting tool where the cutting edge consists of a separate piece of material, either brazed, welded or clamped on to a separate body. Common materials for tips include tungsten carbide, polycrystalline diamond, and cubic boron nitride. The advantage of tipped tools is only a small insert of the cutting material is needed to provide the cutting ability. The small size makes manufacturing of the insert easier than making a solid tool of the same material. This also reduces cost because the tool holder can be made of a less-expensive and tougher material. In some situations a tipped tool is better than its solid counterpart because it combines the toughness of the tool holder with the hardness of the insert. Inserts are removable cutting tips, which mean they are not brazed or welded to the tool body. They are usually indexable, meaning that they can be rotated or flipped without disturbing the overall geometry of the tool (effective diameter, tool length offset, etc.). This saves time in manufacturing by allowing fresh cutting edges to be presented periodically without the need for tool grinding and setup changes.



Fig: 1.1 Photograph of different types of carbide tool inserts

Cutting Tool Material:

- + High speed steels (HSS)**
- + Cast Cobalt alloys**
- + Carbides**

Coatings:

Coatings are frequently applied to carbide tool tips to improve tool life or to enable higher cutting speeds. Coated tips typically have lives 10 times greater than uncoated tips. Common coating materials include titanium nitride, titanium carbide and aluminum oxide, usually 2 - 15 micro-m thick.

1.2 Tool wear

The change of shape of the tool from its original shape, during cutting, resulting from the gradual loss of tool material is defines as tool wear. Cutting tools are subjected to an extremely severe rubbing process. They are in metal-to-metal contact between the chip and work piece, under conditions of very high stress at high temperature. The situation is further aggravated (worsened) due to the existence of extreme stress and temperature gradients near the surface of the tool. During machining, cutting tools remove material

from the component to achieve the required shape, dimension and surface roughness (finish). However, wear occurs during the cutting action, and it will ultimately result in the failure of the cutting tool. When the tool wear reaches a certain extent, the tool or active edge has to be replaced to guarantee the desired cutting action. The high contact stress between the tool rake-face and the chip causes severe friction at the rake face, as well; there is friction between the flank and the machined surface. The result is a variety of wear patterns and scars which can be observed at the rake face and the flank face.

1.2.1 Effects of Tool Wear

Some General effects of tool wear include:

- Increased cutting forces
- Increased cutting temperatures
- Poor surface finish
- Decreased accuracy of finished part

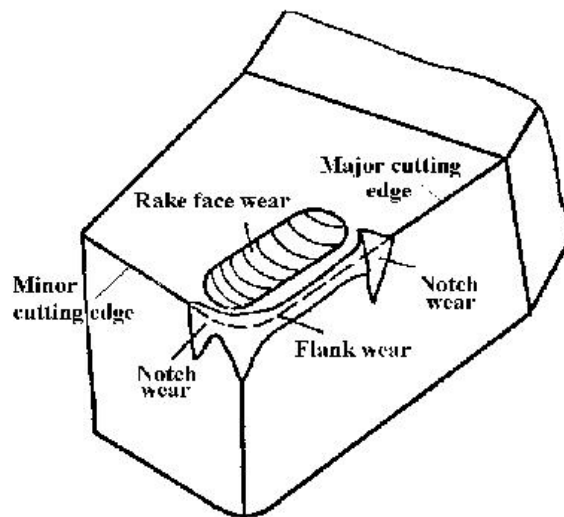


Fig: 1.2 Tool wear phenomena

1.2.2 Different Types of Tool Wear

Attrition wear

Sometimes called Adhesion wear, this pattern is found on very slow surface feed operations. It is characterized by a very rough surface on the land and face of the tool. Usually, a built up edge (BUE) is observed. Chips will be thick and not curl. Severe streaking of the finished part will be apparent.

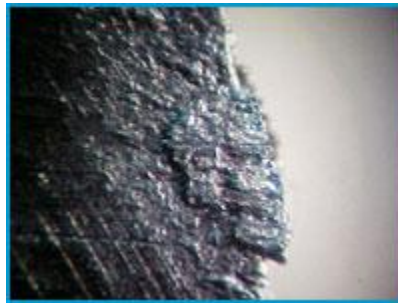


Fig: 1.3 Photograph of Attrition wear [Courtesy: www.armg.com, 2011]

Abrasive wear

Deep, multiple scratches or scores are observed on the land (flank) of the tool. The scoring may appear predominantly on front rows of cutting teeth or it may appear randomly anywhere on the broach tool. The scoring will not appear uniform in length and will be at different positions across the land of the tool.

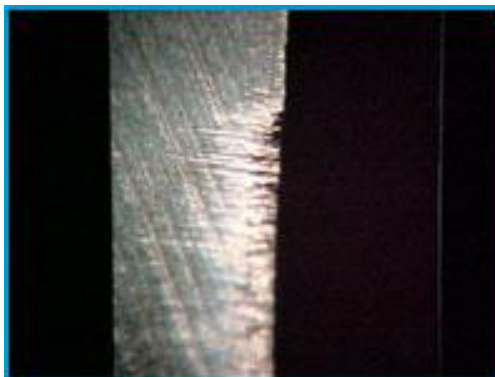


Fig: 1.4 Photograph of Abrasive wear [Courtesy: www.armg.com, 2011]

Diffusion wear

A smooth cutting edge with a dark burned appearance very close to the edge will characterize the diffusion wear on a broach. Cratering of the tool face will be visible. Often, whole rows of cutting teeth will be broken away removing all evidence.

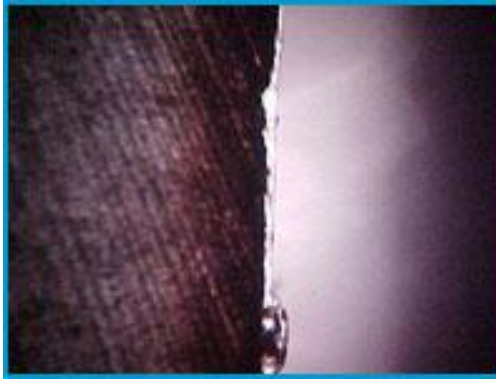


Fig: 1.5 Photograph of Diffusion wear [Courtesy: www.armg.com, 2011]

Built Up Edge

This common problem is identified by work piece material sticking to the face of the tool. The BUE often leads to chipping of the tool cutting edges. Often it will be an irregular wear pattern and will generate poor surface micro-finish on the part. Remnants of a built up edge may show on the finished part as a streak left behind when the tool is extracted from the work piece.

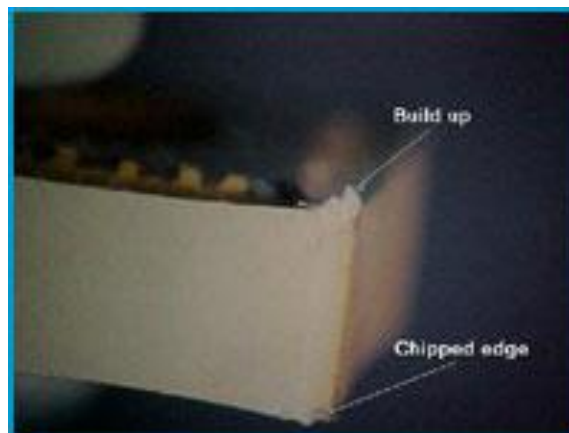


Fig: 1.6 Photograph of Built up edge [Courtesy: www.armg.com, 2011]

Chipping Wear

This common problem is identified by sharp ragged edges on the used insert. The wear pattern is irregular along the edge of the tool. Often, chipping wear leads to a catastrophic failure early in the life of the tool which masks the failure mode. Surface finish is usually streaked and uneven.

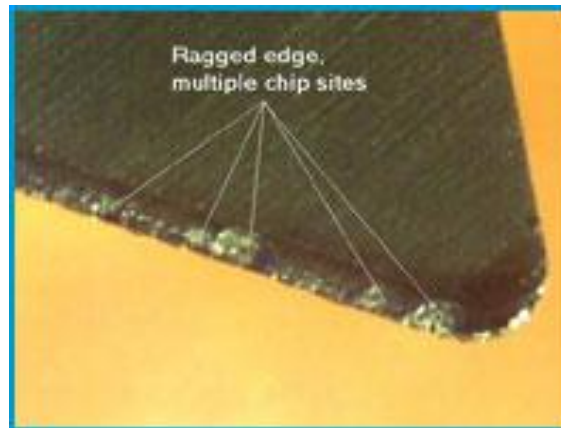


Fig: 1.7 Photograph of Chipping wear [Courtesy: www.armg.com, 2011]

Flaking

Flaking appears to be a large chip in tool. There will be one or two large areas missing the tool face.

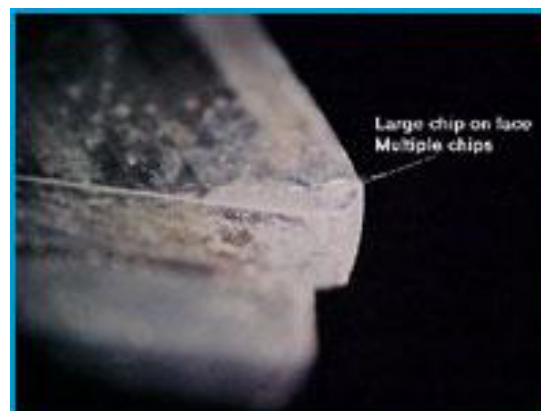


Fig: 1.8 Photograph of Flaking [Courtesy: www.armg.com, 2011]

Spalling

This wear pattern is difficult to observe as it occurs relatively early in the life of the tool. If left in place, the tool will eventually demonstrate failure modes such as Crater, Flaking, Flank or Fracture wear. If Spalling and Thermal Cracking are both observed, condition should be treated as thermal shock first. Since spalling occurs early, other wear patterns develop that mask and may mislead the observer.

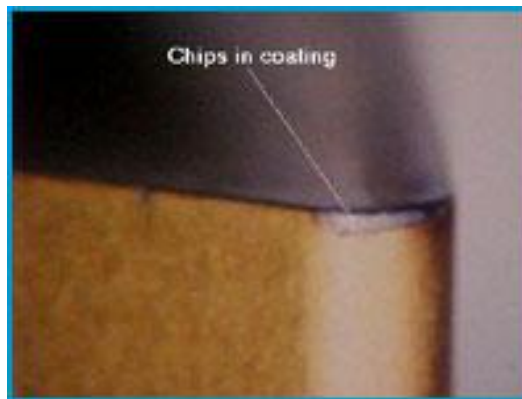


Fig: 1.9 Photograph of Spalling [Courtesy: www.armg.com, 2011]

Fracture

Often the evidence is lost when the insert is shattered. It may be the result of over use or severe overload. If it occurs very late in the life of the tool, other wear patterns probably existed such as Chipping, Crater, Deformation or Flaking and the tool was overrun.

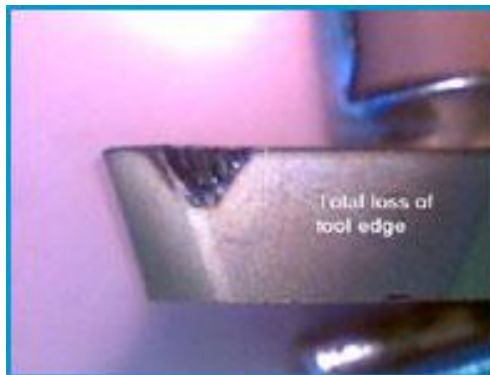


Fig: 1.10 Photograph of Fracture [Courtesy: www.armg.com, 2011]

Flank / Nose / Face Wear

This is the most common wear pattern. It is uniform over a localized area and accelerates with higher temperatures. It appears as a rough surface primarily on the flank of the tool and to a lesser extent on the face of the tool. There will be a slight burn mark at the trailing edge of the wear pattern. This type of wear pattern is the most favourable mode when it is uniform and progresses slowly.

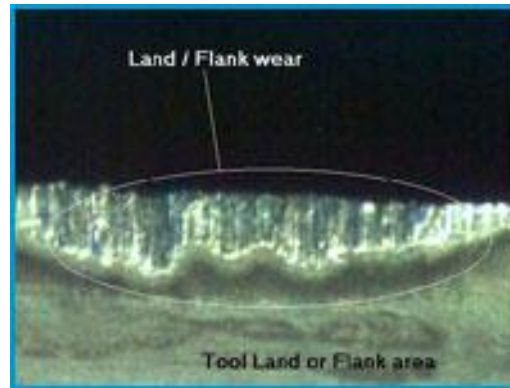


Fig: 1.11 Photograph of Flank / nose wear [Courtesy: www.armg.com, 2011]

Notching Wear

Notching wear is a single groove formation that occurs simultaneously on the face and flank of the tool at the depth of cut. This notch will cause poor micro-finish on the part and may precede a fracture failure mode.

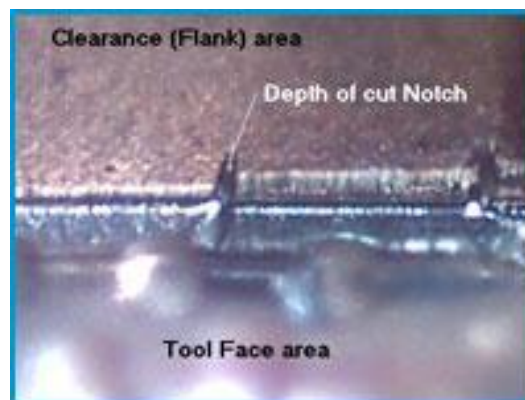


Fig: 1.12 Photograph of Notching wear [Courtesy: www.armg.com, 2011]

Thermal Cracking

This wear pattern is unique as shows up as hairline cracks that are perpendicular to the cutting edge. Many times the parallel cracks are uniformly distributed long the cutting edge. These edge chips will appear to be very uniform in depth and are in line with the direction of tool travel.

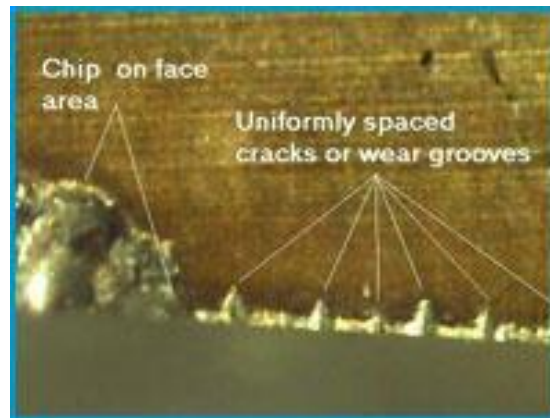


Fig: 1.13 Photograph of Thermal cracking [Courtesy: www.armg.com, 2011]

Crater Wear

On the tool face, crater wear appears as a shallow trough in localized areas. Crater wear will increase until it reaches the cutting edge causing chipping or fracture. Chipping or fracture is an advanced crater wear condition and often misleading.

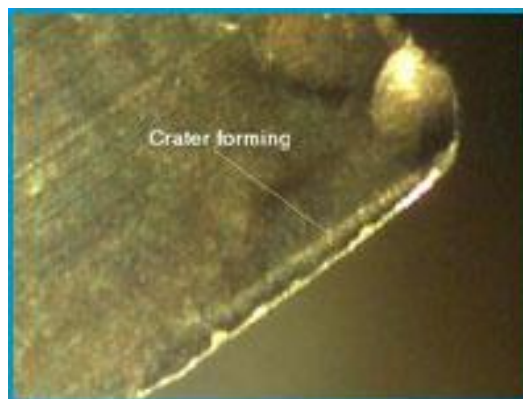


Fig: 1.14 Photograph of Crater wear [Courtesy: www.armg.com, 2011]

Deformation Wear

Deformation wear is always accompanied by a bulge of tool material in the flank / land area. There will be evidence of thermal lines seen as discoloration. This severe deformation is quickly followed by fracture. Micro-finish on the part may be very acceptable, while maintaining dimensional stability is difficult.

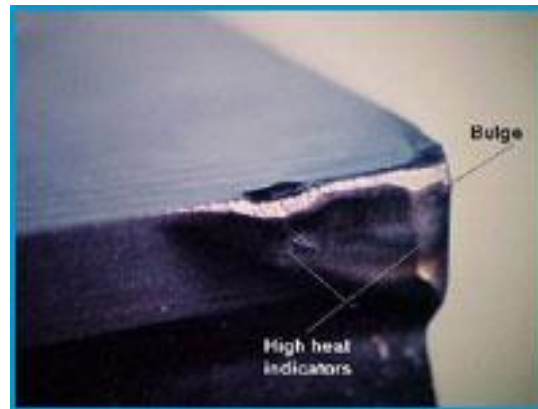


Fig: 1.15 Photograph of Deformation wear [Courtesy: www.armg.com, 2011]

1.2.3 Wear of Tungsten Carbide (WC) tools

It is well accepted that, during machining of steel work materials with WC tools, several wear mechanisms such as abrasion, adhesion, oxidation, diffusion, etc. can operate simultaneously [1–6]. Thus under a given set of machining conditions, determination of the dominant wear mechanism is difficult. However, Hastings and Oxley [1] and Opitz and Konig [2] have pointed out that, the most likely dominant wear mechanisms and the corresponding cutting speeds/ temperatures are: abrasion at low speeds/temperatures, followed by adhesion at moderate speeds/temperatures and then diffusion at high speeds/temperatures. By superposition of these wear mechanisms; they were able to explain the observed variations of tool wear¹ over a wide range of cutting speeds [1, 2]. That is, the total wear occurring on a tool contact face (e.g. flank face) is equal to the sum of the wear occurring due to the separate effects of the above wear mechanisms. It should be noted that all of the above wear processes will not occur

simultaneously. Moreover, the dominant wear mechanism will depend on the cutting conditions and, tool and work materials.

1.2.4 Tool wear/life relationships

The well-known Taylor equation [7] which is the most widely used tool life relation in machining can be written as:

$$T = \frac{A_t}{V^{b_t}} \quad (1.1)$$

Where T is tool life, V is cutting speed and A_t , b_t are constants. Although this equation was originally developed for machining with high-speed steel tools, it has been applied in machining with WC as well as PCD and PCBN tools. On the other hand, it has been shown that, for a given tool/work material combination, the above equation does not agree well with experimental results over wide ranges of cutting conditions [8]. This has been attributed to the changes in the dominant tool wear mechanism with changes in cutting conditions. Nevertheless, reasonable agreement has been shown over ranges of speeds normally used in practice [4].

It has also been shown that there is considerable evidence, both theoretical and experimental, that the tool temperature has a great influence on tool wear rate and tool life [1, 9]. In fact, in Eq. (1), cutting speed seems to influence tool life through temperature. The evidence also supports the observation that, for a particular tool/work material combination, the tool life and tool temperature are related by the empirical equation [1, 9].

$$T = AT_t^{-B} \quad (1.2)$$

Where T_t is tool temperature and A and B are constants. The validity of Eq. (1.2) depends on the existence of a dominant, temperature dependant wear mechanism [1, 9]. It has been shown that, for carbide tools, at practical cutting speeds (where no built-up edge

is observed and the tool temperatures are normally above 800°C), the dominant wear mechanism is diffusion [1, 9–11].

Wear on the flank (relief) face is called Flank wear and results in the formation of a wear land. Wear land formation is not always uniform along the major and minor cutting edges of the tool. Flank wear most commonly results from abrasive wear of the cutting edge against the machined surface. Flank wear can be monitored in production by examining the tool or by tracking the change in size of the tool or machined part. Flank wear can be measured by using the average and maximum wear land size V_B and V_{Bmax} .

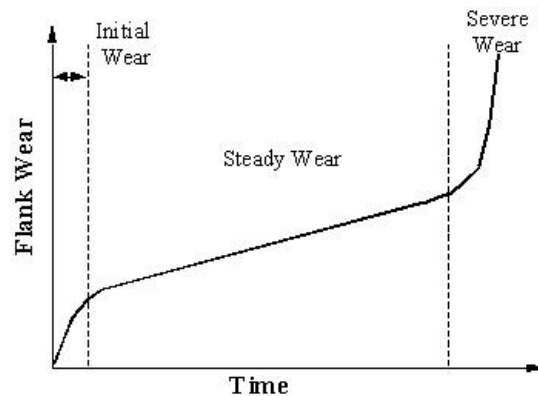


Fig: 1.16 Graph showing typical stages of tool wear in normal cutting situation

Initial wear region:

Caused by micro-cracking, surface oxidation and carbon loss layer, as well as micro-roughness at the cutting tool tip in tool grinding (manufacturing). For the new cutting edge, the small contact area and high contact pressure will result in high wear rate. The initial wear size is $V_B=0.05-0.1$ mm normally.

Steady wear region:

After the initial (or preliminary) wear (cutting edge rounding), the micro-roughness is improved, in this region the wear size is proportional to the cutting time. The wear rate is relatively constant.

1.2.5 Reduction of Tool Wear with Application of Magnetic Field in Machining

Tool wear reduction has always been a focus in research into machining processes. As productivity and cost are closely related to tool life, a small increase in tool life can greatly reduce the amount of machine down time for tool replacements, and also the cost of grinding and resetting the worn tool. Currently, the most common method to reducing wear is to separate the surfaces by the use of fluid or solid lubricants. The second general approach is to modify materials and material properties. Examples of this would include creating special materials and alloys for cutting tools and also hardened layers at material surfaces. In the papers by Mohamed El Mansori [12, 13], it was shown that beneficial effects on the application of magnetic field in various machining processes has been demonstrated. Many of these experiments often involve application of the magnetic field to both work piece and tool. And studies using pulse and alternating magnetic field were performed as well.

1.3 Surface Structure and Properties

Surface roughness is an important measure of product quality since it greatly influences the performance of mechanical parts as well as production cost. Surface roughness has an impact on the mechanical properties like fatigue behavior, corrosion resistance, creep life, etc. Before surface roughness, it is also necessary to discuss about surface structure and properties, as they are closely related. Upon close examination of the surface of a piece of metal, it can be found that it generally consists of several layers (Figure 1.20).

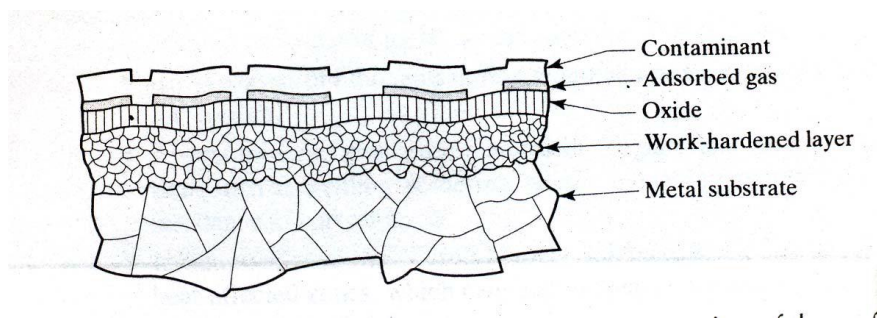


Fig: 1.17 Schematic of a cross-section of the surface structure of metals
(Courtesy:ANSI B46.1 - 1962)

1.3.1 Surface Topography

Outermost layers of all machined surfaces display a great number of both macro geometrical and micro-geometrical deviations from the ideal geometrical surface. Surface roughness refers to deviation from the nominal surface of the third up to sixth order. Order of deviation is defined in international standards. First and second-order deviations refer to form, i.e. flatness, circularity, etc. and to waviness, respectively, and are due to machine tool errors, deformation of the work piece, erroneous setups and clamping, vibration and work piece material inhomogenities. Third and fourth-order deviations refer to periodic grooves, and to cracks and dilapidations, which are connected to the shape and condition of the cutting edges, chip formation and process kinematics. Fifth and sixth-order deviations refer to work piece material structure, which is connected to physical-chemical mechanisms acting on a grain and lattice scale (slip, diffusion, oxidation, residual stress, etc.).

The principal elements of surfaces are discussed below:

- a. **Surface:** The surface of an object is the boundary which separates that object from another substance. Its shape and extent are usually defined by a drawing or descriptive specifications.
- b. **Profile:** It is the contour of any specified section through a surface.
- c. **Roughness:** It is defined as closely spaced, irregular deviations on a scale smaller than that of waviness. Roughness may be superimposed on waviness. Roughness is expressed in terms of its height, its width, and its distance on the surface along which it is measured.
- d. **Waviness:** It is a recurrent deviation from a flat surface, much like waves on the surface of water. It is measured and described in terms of the space between adjacent crests of the waves (waviness width) and height between the crests and valleys of the waves (waviness height). Waviness can be caused by,

- i. Deflections of tools, dies, or the work piece,
- ii. Forces or temperature sufficient to cause warping,
- iii. Uneven lubrication,
- iv. Vibration
- v. Any periodic mechanical or thermal variations in the system during manufacturing operations.

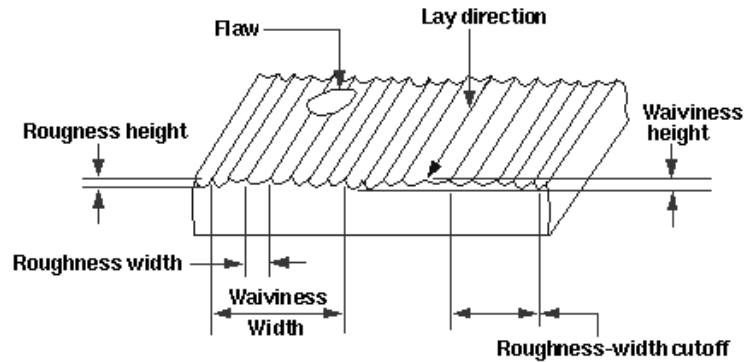


Fig: 1.18 Schematic diagram of surface characteristics (Courtesy:ANSI B46.1 - 1962)

- e. **Flaws:** Flaws, or defects, are random irregularities, such as scratches, cracks, holes, depressions, seams, tears, or inclusions.
- f. **Lay:** Lay, or directionality, is the direction of the predominant surface pattern and is usually visible to the naked eye.

1.3.2 Factors Affecting the Surface Finish

Whenever two machined surfaces come in contact with one another the quality of the mating parts plays an important role in the performance and wear of the mating parts. The height, shape, arrangement and direction of these surface irregularities on the work piece depend upon a number of factors such as:

- A) The machining variables which include
 - a) Cutting speed
 - b) Feed, and
 - c) Depth of cut.
- B) The tool geometry
 - Some geometric factors which affect achieved surface finish include:
 - a) Nose radius
 - b) Rake angle
 - c) Side cutting edge angle, and
 - d) Cutting edge.
- C) Work piece and tool material combination and their mechanical properties
- D) Quality and type of the machine tool used,
 - E) Auxiliary tooling, and lubricant used, and
 - F) Vibrations between the work piece, machine tool and cutting tool.

1.3.3 Roughness Parameters

Each of the roughness parameters is calculated using a formula for describing the surface. There are many different roughness parameters in use, but R_a is the most common. Other common parameters include R_z , R_q , and R_{sk} . Some parameters are used only in certain industries or within certain countries. For example, the R_k family of parameters is used mainly for cylinder bore linings. Since these parameters reduce all of the information in a profile to a single number, great care must be taken in applying and interpreting them. Small changes in how the raw profile data is filtered, how the mean line is calculated, and the physics of the measurement can greatly affect the calculated parameter. The details of different surface roughness parameters are given in Appendix A.

1.3.4 Factors Influencing Surface Roughness in Turning

Generally, it is found that the factors influencing surface roughness in turning are:

- i.* **Depth of cut:** Increasing the depth of cut increases the cutting resistance and the amplitude of vibrations. As a result, cutting temperature also rises. Therefore, it is expected that surface quality will deteriorate.
- ii.* **Feed:** Experiments show that as feed rate increases surface roughness also increases due to the increase in cutting force and vibration.
- iii.* **Cutting speed:** It is found that an increase of cutting speed generally improves surface quality.
- iv.* **(iv)Engagement of the cutting tool:** This factor acts in the same way as the depth of cut.
- v.* **Cutting tool wears:** The irregularities of the cutting edge due to wear are reproduced on the machined surface. Apart from that, as tool wear increases, other dynamic phenomena such as excessive vibrations will occur, thus further deteriorating surface quality.
- vi.* **Use of cutting fluid:** The cutting fluid is generally advantageous in regard to surface roughness because it affects the cutting process in three different ways. Firstly, it absorbs the heat that is generated during cutting by cooling mainly the tool point and the work surface. In addition to this, the cutting fluid is able to reduce the friction between the rake face and the chip as well as between the flank and the machined surface. Lastly, the washing action of the cutting fluid is considerable, as it consists in removing chip fragments and wear particles. Therefore, the quality of a surface machined with the presence of cutting fluid is expected to be better than that obtained from dry cutting.
- vii.* **Three components of the cutting force:** It should be noted that force values cannot be set a priori, but are related to other factors of the experiment as well as to factors possibly not included in the experiment, i.e. force is not an input factor and is used as an indicator of the dynamic characteristics of the work piece—cutting tool—machine system.

Finally, the set of parameters including the above mentioned parameters that are thought to influence surface roughness, have been investigated from the various researchers.

1.4 Objectives of the Study

- a) To develop a method for using magnetic (permanent magnet and electromagnet) cutting in turning operation.
- b) To develop a digital image processing technique for the determination of tool wear (Flank and Nose) and compare the developed mechanism with the optical microscope measurement technique.
- c) To study the effect of machining parameters (depth of cut and cutting speed) during magnetic cutting on machinability factors (surface roughness, tool wear, cutting temperature and cutting force) during turning operation using single point cutting tool.
- d) To study the morphology of chip for magnetic and non magnetic cutting.
- e) To establish a comprehensive method for improvement of machinability factors during turning operation of steel.

1.5 Thesis Organization

This thesis is arranged in five chapters. All the details about the study with general information and research background are described in those chapters. A brief summary of each of the chapters are as follows:

The first chapter is the introduction. It contains general description of the process and theory related with the study. The parameters necessary for the study with formulas are described. It also contains general information about insert, magnetism and wear mechanism along with problem statement, methodology and objective of the study.

In chapter two the background of the current study along with the research of contemporary scientists in related fields is described. It gives an idea about the potential of the current project and relates it with the work of others.

Chapter three is titled as experimental setup and procedure. In this section the detailed description of each of the equipment used in the study is provided with specification and pictures. The image processing techniques used in the study for measurement of tool wear and surface roughness are also described in this section.

The Fourth chapter is the results and discussions. This chapter contains the graphs generated based on the experimental data and comparative analysis among different experimental conditions.

Chapter Five is the conclusions and recommendations where the decisions derived from the study are elaborately stated with the scope of future work on this current study.

Review of Relevant Literatures

Introduction

There has been significant amount of research on tool wear mechanism and surface roughness. Some of the important research topics and results are discussed in the following sections. It is to be noted that the discussion is in no way comprehensive as there is a huge volume of research literature in the field.

2.1 General Discussion of Relevant Research

The turning process is one of the most important metalworking processes and is one of the most effective means of reducing a raw work piece to a finished shape. In metal cutting practice, productivity and cost of machining are highly correlated to tool life due to the opportunity cost of machine down time during the replacement or resetting of tool inserts. Thus in attempts to increase tool life of inserts hence increasing productivity, a variety of machining solutions has been introduced over the years. Most of these solutions are based on changes in tool design, process optimization or the use different insert grades with different types of wear resistant coatings.

Tool wear, the gradual failure of cutting tools due to regular use, is an inevitable impediment in machining processes [14]. High speed machining uses high cutting speed and feed rate and ultimately generates high cutting temperature which not only reduces tool life but also impairs the product quality, which indirectly represents a significant portion of the machining costs [15]. Nevertheless, the proper selection of tool material and cutting conditions can reduce tool wear to an acceptable rate and thus, increase tool life. Therefore, it is important to address the factors generally affecting the tool wear mechanism in turning operation [16-19].

Tool wear is of many different types and also depend on the type of tool material chosen and the cutting conditions used. For this study, flank wear, measured as the

maximum land wear " V_{Bmax} " was investigated. For continuous turning the maximum tool wear land width (V_{Bmax}) shows a near linear increase with cutting distance after initial rapid wear. Flank wear typically results due to erosion of the flank face and excessive chipping on flank side of tool. Such flank wear compromises the stability of the cutting edge, causing reduction dimensional tolerance and tool life, increased roughness, and tool breakage in the extreme case.

2.1.1 Contemporary Research about Tool Wear

Tool wear has been extensively studied for almost all machining processes. Braghini et al [20] studied the wear behaviour of Polycrystalline Cubic Boron Nitride (PCBN) and cemented carbide tool in end milling of hardened steels. They discovered that the minimal wear mechanism was a combination of adhesion and abrasion. It was also stated that wear occurred predominantly on the flank face. Kumar et al [21] investigated the wear morphology of alumina based ceramic tools in the machining of hardened stainless steel and noticed that the flank wear affected tool life at lower speed.

Ghani et al [22] researched on the performance of TiN coated carbide inserts in semi-finish and finish end milling of hardened tool steel at high cutting speeds. Their results compared the effectiveness of TiAlN inserts under preheated room temperature conditions with the performance of the same tool material under room temperature condition. Once factor in the variation of performance was concluded to be tool wear. Amin et al. [23] proposed a predictive model for the estimation of tool life under different cutting conditions in end milling of tool steel using TiAlN (Titanium Aluminum Nitride).

Tool design focuses on specialized inserts which can fulfil the unique cutting conditions. However, this will result in extra tool cost and specialized training to determine the specific insert needed under a unique condition. Process optimization relies on establishing a simple functional dependency between input process variables (cutting

conditions, tool geometry etc) and output parameters (amount of tool wear, tool life etc) and adjusting the cutting conditions accordingly. This trial and error process is usually time consuming and requires constant fine-tuning. The other common process depends on the application of hard and thin wear resistant coatings to improve the tool life of inserts. Nevertheless, problems such as sudden failure of coatings and poor adhesion between thin surface coatings and insert material remains to be a challenge.

In their investigation on tool flank wear, Takeyama and Murata [24] argued that the amount of tool flank wear is given by the sum of the wear due to abrasion and temperature sensitive diffusion. They considered abrasion to be proportional to the cutting distance and independent of tool temperature. Diffusion was considered to be temperature dependant and the wear rate could be represented by Arrhenius type equation. In [24], tool temperature, tool life and tool wear rate results were obtained when machining steel and cast iron using P10 grade WC tools. It was shown that the experimental results for temperatures above 800°C could be represented well by equations thus indicating that wear of tested tools was dominated by diffusion.

Oxley [9] and his co-workers [25-26] have shown that experimental tool life values could be used in conjunction with temperature values determined from a machining theory. When compared with pure empirical methods, the theoretical method appears far more effective in predicting tool life as it allows tool geometrical parameters and cutting conditions to be combined into the single parameter of temperature. This approach was initially applied to orthogonal and oblique [10] conditions with plane face tools. Later it was extended to tools with restricted contact and commercial chip grooves [27] with considerable success. It is noteworthy that in the investigations, diffusion was considered to be the dominant tool wear mechanism.

Wear mechanisms abrasion and oxidation of WC tools were considered by Hastings and Oxley [9] and Trent and Wright [10]. They have pointed out that, when machining steel work materials, these mechanisms are unlikely to be dominant under the conditions normally used in practice (i.e. at relatively high cutting speeds). This is due to

(i) the insufficient amount of abrasives present in the work material, (ii) insufficient hardness of abrasives to abrade WC and (iii) inability to detect any significant signs of abrasive wear in extensive metallurgical studies. However, there are certain conditions under which abrasive wear of WC tools have been observed.

Adhesive wear of WC tools has also been investigated. Kitagawa et al. [27] assumed that, under practical conditions, wear of WC tools was due to adhesion, that wear rate could be represented by a relation and that wear should increase with the normal stress on the tool flank. This is one of the major drawbacks of these studies since reliable experimental results or an analytical method to determine this stress is not yet available. Another is that the predicted results indicate elastic contact at flank/work interface in spite of experimental evidence of plastic contact reported by Trent and Wright [10]. Moreover, Iwata et al. [28] showed that adhesion between WC and steel (hence adhesive wear rate) becomes a maximum around 600 °C and thereafter falls off rapidly with further increase in temperature.

2.1.2 Contemporary Research about Surface Roughness

Surface roughness represents the dimensional accuracy of the finished product and is one of the most important quality requirements of the finished product. The productivity of a machining process is not only determined by the use of low cost-high performance alloys, but also by the capability to transform a specific steel alloy to the required surface finish and geometry by machining at sufficiently high speed . Therefore, in most machining situations, minimization of surface roughness is a prime issue. It is to be noted that zero surface roughness is a machining impossibility, as there is always some inherent limitations of the machine, machine operator, and machining process. Therefore it is more practical to investigate ways to optimize the machining process parameters in order to attain minimal surface roughness; roughness as close as possible to the nominal value required.

Lin et al. [29] adopted an abdicative network to construct a prediction model for surface roughness and cutting force. Once the process parameters: cutting speed, feed rate

and depth of cut were given; the surface roughness and cutting force could be predicted by this network. Regression analysis was also adopted as second prediction model for surface roughness and cutting force. Comparison was made on the results of both models indicating that adductive network was found more accurate than that by regression analysis. Investigation was also carried out for the prediction of surface roughness in finish turning operation by developing an empirical model through considering working parameters: work piece hardness (material), feed, cutting tool point angle, depth of cut, spindle speed, and cutting time. Data mining techniques, nonlinear regression analysis with logarithmic data transformation were employed for developing the empirical model to predict the surface roughness.

Lee and Chen [30] highlighted on artificial neural networks using a sensing technique to monitor the effect of vibration produced by the motions of the cutting tool and work piece during the cutting process developed an on-line surface recognition system. The authors employed tri-axial accelerometer for determining the direction of vibration that significantly affected surface roughness.

Kirby et al. [31] developed the prediction model for surface roughness in turning operation. The regression model was developed by a single cutting parameter and vibrations along three axes were chosen for in-process surface roughness prediction system. By using multiple regression and Analysis of Variance a strong linear relationship among the parameters (feed rate and vibration measured in three axes) and the response (surface roughness) was found. The authors demonstrated that spindle speed and depth of cut might not necessarily have to be fixed for an effective surface roughness prediction model.

Özel and Karpaz [32] studied for prediction of surface roughness and tool flank wear by utilizing the neural network model in comparison with regression model. The data set from measured surface roughness and tool flank wear were employed to train the neural network models. Predictive neural network models were found to be capable of better predictions for surface roughness and tool flank wear within the range in between

they were trained. They also carried out theoretical and experimental studies to investigate the intrinsic relationship between tool flank wear and operational conditions in metal cutting processes using carbide cutting inserts. The authors developed the model to predict tool flank wear land width which combined cutting mechanics simulation and an empirical model. The study revealed that cutting speed had more dramatic effect on tool life than feed rate.

Sing and Kumar [33] studied on optimization of feed force through setting of optimal value of process parameters namely speed, feed and depth of cut in turning of EN24 steel with TiC coated tungsten carbide inserts. The authors used Taguchi's parameter design approach and concluded that the effect of depth of cut and feed in variation of feed force were affected more as compare to speed.

Ahmed [34] developed the methodology required for obtaining optimal process parameters for prediction of surface roughness in Aluminium turning. For development of empirical model nonlinear regression analysis with logarithmic data transformation was applied. The developed model showed small errors and satisfactory results. The study concluded that low feed rate was good to produce reduced surface roughness and also the high speed could produce high surface quality within the experimental domain. Abburi and Dixit [35] developed a knowledge-based system for the prediction of surface roughness in turning process. Fuzzy set theory and neural networks were utilized for this purpose. The authors developed rule for predicting the surface roughness for given process variables as well as for the prediction of process variables for a given surface roughness. Zhong et al. [36] predicted the surface roughness of turned surfaces using networks with seven inputs namely tool insert grade, work piece material, tool nose radius, rake angle, depth of cut, spindle rate, and feed rate.

Mahmoud and Abdelkarim [37] studied on turning operation using High-Speed Steel (HSS) cutting tool with 45° approach angle. This tool showed that it could perform cutting operation at higher speed and longer tool life than traditional tool with 90° approach angle. The study finally determined optimal cutting speed for high production

rate and minimum cost, tool life, production time and operation costs. Doniavi et al. [38] used response surface methodology (RSM) in order to develop empirical model for the prediction of surface roughness by deciding the optimum cutting condition in turning. The authors showed that the feed rate influenced surface roughness remarkably. With increase in feed rate surface roughness was found to be increased. With increase in cutting speed the surface roughness decreased. The analysis of variance was applied which showed that the influence of feed and speed were more in surface roughness than depth of cut.

Kassab and Khoshnaw [39] examined the correlation between surface roughness and cutting tool vibration for turning operation. The process parameters were cutting speed, depth of cut, feed rate and tool overhanging. The experiments were carried out on lathe using dry turning (no cutting fluid) operation of medium carbon steel with different level of aforesaid process parameters. Dry turning was helpful for good correlation between surface roughness and cutting tool vibration because of clean environment. The authors developed good correlation between the cutting tool vibration and surface roughness for controlling the surface finish of the work pieces during mass production. The study concluded that the surface roughness of work piece was observed to be affected more by cutting tool acceleration; acceleration increased with overhang of cutting tool. Surface roughness was found to be increased with increase in feed rate.

Al-Ahmari [40] developed empirical models for tool life, surface roughness and cutting force for turning operation. The process parameters used in the study were speed, feed, depth of cut and nose radius to develop the machinability model. The methods used for developing aforesaid models were Response Surface Methodology (RSM) and neural networks (NN). Natarajan et al. [41] presented the on-line tool wear monitoring technique in turning operation. Spindle speed, feed, depth of cut, cutting force, spindle-motor power and temperature were selected as the input parameters for the monitoring technique. For finding out the extent of tool wear; two methods of Hidden Markov Model (HMM) such as the Bar-graph Method and the Multiple Modelling Methods were used. A decision fusion centre algorithm (DFCA) was used for increasing the reliability of this output

which combined the outputs of the individual methods to make a global decision about the wear status of the tool. Finally, all the proposed methods were combined in a DFCA to determine the wear status of the tool during the turning operations.

Sahoo et al. [42] studied for optimization of machining parameters combinations emphasizing on fractal characteristics of surface profile generated in CNC turning operation. It was concluded that feed rate was more significant influencing surface finish in all three materials. It was observed that in case of mild steel and aluminium feed showed some influences while in case of brass depth of cut was noticed to impose some influences on surface finish. The factorial interaction was responsible for controlling the fractal dimensions of surface profile produced in CNC turning.

Lan et al. [43] considered four cutting parameters: speed, feed, depth of cut, and nose runoff varied in three levels for predicting the surface roughness of CNC turned product. Thamma [44] constructed the regression model to find out the optimal combination of process parameters in turning operation for Aluminium 6061 work pieces. The study highlighted that cutting speed, feed rate, and nose radius had a major impact on surface roughness. Smoother surfaces could be produced when machined with a higher cutting speed, smaller feed rate, and smaller nose radius.

Biswas et al. [45] studied that on-line flank wear directly influenced the power consumption, quality of the surface finish, tool life, productivity etc. The authors developed a model for prediction of the tool wear. From the orthogonal machining of aluminium with high-speed steel tool for various rake angles, feed and velocity the experimental data were obtained and input along with other machining parameters ratio between cutting force and tangential forces was collected. These were used to predict the tool wear. The final parameters of the model were obtained by tuning the crude values obtained from mountain clustering method by using back-propagation learning algorithm and finally predicted the flank wear with reasonable accuracy and proved it to be a potent tool in estimating flank wears on-line.

2.1.3 Contemporary Research about Magnetic Cutting

Bagchi and Ghosh [46,47] seem to be the first investigators to have studied the effect of an EMF created by a magnetic field on the wear characteristics of cutting HSS tools while machining mild steel. Flank wear was measured and a wear gain factor (wear decrease) due to the applied magnetic field was considered. They found that within the range of speeds investigated, the gain factor was always found to be positive. This improvement depended both on magnetic field intensity and cutting speed although there were particular cutting speeds at which the extended tool life was maximum, irrespective of field intensity.

To provide some reasons of why a magnetized cutting tool has greater life, Chakrabarti proposed a qualitative model in which he assumed a physical reorientation of the elements of the magnets [48]. Although the results of the modeling analysis were encouraging, the model itself was subject to question. Two years later, Pal and Gupta [49] investigated the effect of an alternating magnetic field on the wear behavior of HSS drills in drilling gray cast iron and malleable cast iron under dry cutting condition. In the case of gray iron, the alternating magnetic field was applied both on tool and work piece simultaneously using a solenoid. In drilling malleable iron, the same solenoid was used but instead of encircling the job, it was placed on top of the SG iron block so that the magnetic field was mainly applied on the tool. The authors observed that considerable increase in the tool lifetime has been achieved for both test configurations. Some possible reasons for this improvement have been suggested although no theoretical explanations for the experimental observations have been given. This has been attempted by Muju and Ghosh [50] who present a physical model to explain some results obtained when conducting tool wear experiments with magnetized HSS turning tools on mild steel and brass. The wear experiments consisted of the use of mild steel tools to cut aluminum. Additional tests with the mild steel tools rubbing against brass and mild steel were also performed. The tools were magnetized using a D.C. source and an auxiliary tool was used to keep the machined surface fresh. In their observations, they found an increase in tool life by approximately 40% and a reduction of the size of wear particles, but no phase

change. The authors discussed the effects of an external magnetic field from a mechanical point of view. Their analysis was performed as a phenomenological approach based on dislocation mobility during a two body interaction in the presence of an external magnetic field. It follows from this literature analysis that if tool life improvement by a magnetic field has been proven, it is still difficult to state with certainty what process is leading to such an improvement. Recently the effect of external electromagnetic force has been proven to provide better characteristics of products in case of turning and milling operation [51].

In this project a magnet (permanent and electromagnet) in turning of a shaft made of steel was used in different cutting conditions by changing the cutting speed and depth of cut in three experimental conditions: without magnet, with permanent magnet and with electro magnet. The measurements of tool wear and surface roughness were carried out by using digital image processing techniques. The results obtained in the image processing method were verified by physical experimental data.

The use of magnetic treatment to improve the tool life of inserts has many attractive features. The treatment usually involves low intensity, easy to produce and control magnetic field that are applied at room temperature. However, the use of magnetic field to improve tool life is still not widely appreciated and is underexploited in today's industry. Hence the main emphasis of this report is to ascertain that an application of magnetic field will result in an improvement in tool life of inserts and surface roughness of work piece.

2.2 Problem Statement

This thesis presents the details of improvement of machinability of mild steel using magnetic cutting during turning operation. Improvement of machinability was evaluated in terms of tool life, surface roughness and chip morphology. Poor machinability can result in poor dimensional accuracy of the work-piece, reduction of tool life, and damage to the machine. This is formed because of vibration phenomena during machining because of the instability of the system formed by machine tool structure and metal-cutting process. In this study, magnets were used to avoid the adverse effects and its effect on machinability was investigated. The application of magnetic field will produce a damping effect which reduces the vibrations experienced by the cutting inserts. This in turns leads to an increase in the tool life of inserts [19]. This would then bring about significant cost savings towards the cost of production as it will reduce machine down time during replacement and the cost of grinding and resetting worn tools. Improvements in tool life and surface finish were observed during magnetic cutting of the mild steel. An obvious change in the chip behaviour was also present. These observations further enhance the possibility of using this magnetic cutting to improve tool life and reduce surface roughness.

2.3 Scope of current work

Literature depicts that a considerable amount of work has been carried out by previous investigators for reducing tool wear and improving surface quality by several techniques including magnetic cutting. The present study investigates the effect of new arrangements of electromagnetic fields and also permanent magnetic field. To study the effect in a wide range several cutting conditions have been used in the experiment. Newly developed image processing techniques have been used for measurement of tool wear and surface roughness. The study can lead to the following outcomes:

- a) An effective magnetic cutting process for turning operation of mild steel.
- b) A cost effective digital image processing technique for determining tool wears of single point cutting tool.
- c) Reduction of tool wears during turning leading to lower production cost.
- d) Improvement of surface roughness resulting in higher product quality.
- e) Better understanding of chip morphology in different cutting conditions.

Experimental Setup and Procedures

Introduction

The primary idea behind the research endeavour was to study the effect of two magnetic cutting environments at different cutting conditions. The two magnetic environments, one with permanent magnet another with electromagnet, were used to determine optimum setting for the attainment of minimum tool wear and surface roughness. Finally, these findings were also compared to normal non magnetic cutting results for better observation

The whole process of the experimentation can be shown as the flowchart given below:

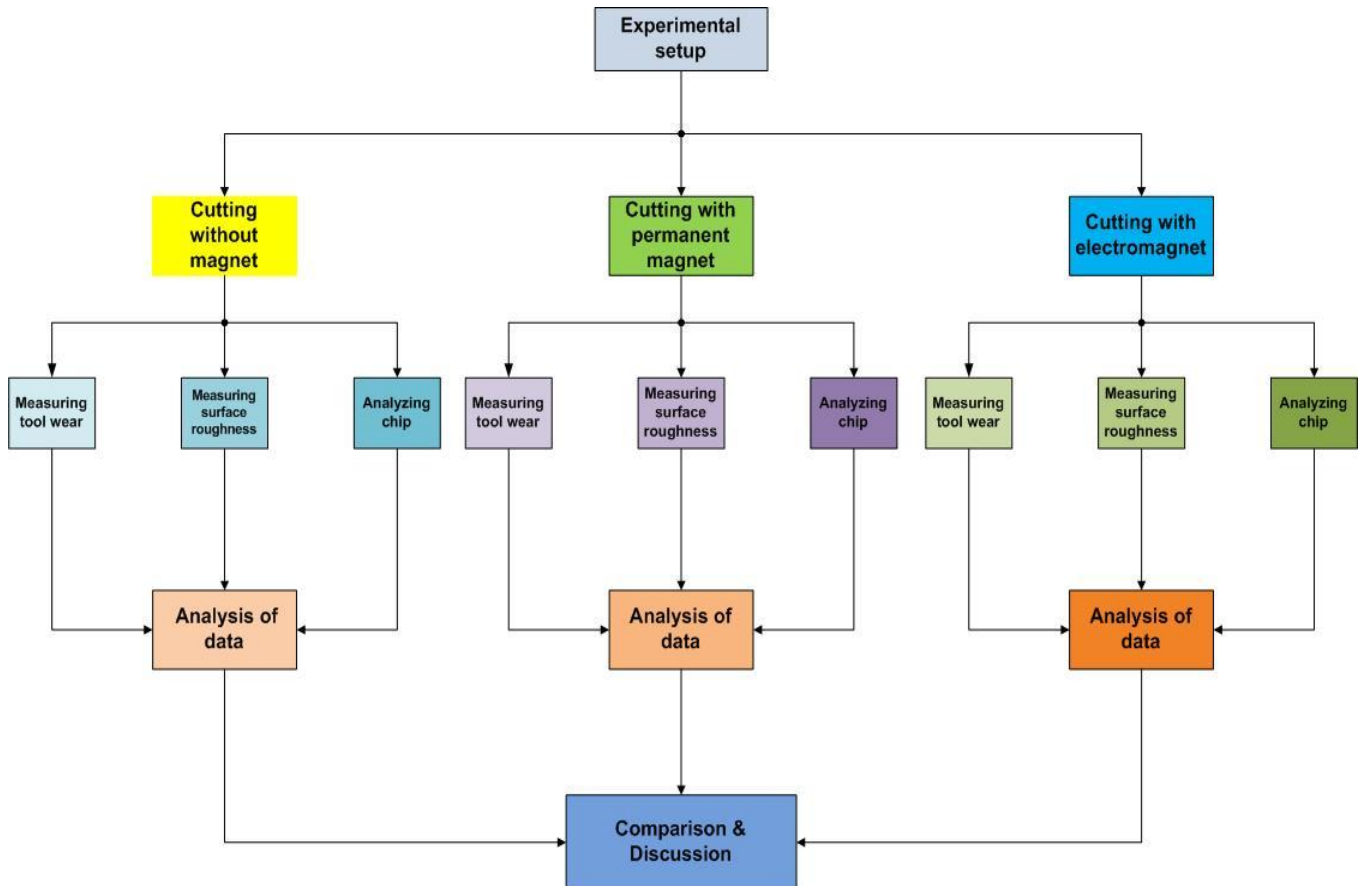


Fig: 3.1 Flow sequence of the experimentation

3.1 Experimental Setup

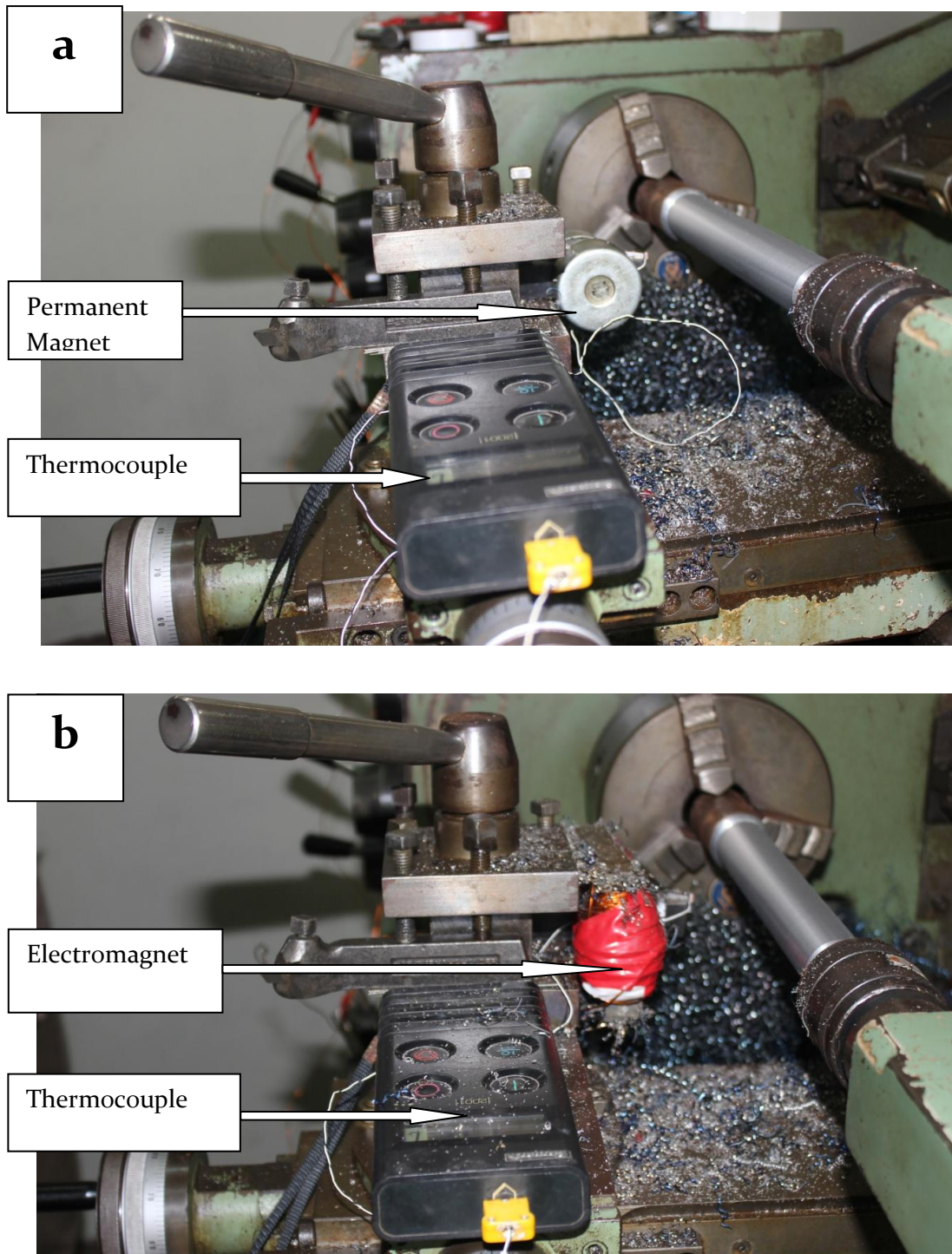


Fig: 3.2 Photographs of experimental setup for a) permanent magnet, b) electromagnet

3.2 Process Variables and Their Values

In the present experimental study, spindle speed, feed rate and depth of cut have been considered as process variables. The process variables with their units (and notations) are listed in Table 3.1.

Process Variables			
Spindle Speed (RPM)	Spindle Speed (m/min)	Feed (f) (mm/rev)	Depth of cut (D) (mm)
530	66.56	0.095	0.5, 0.75, 1.0
860	108.016	0.095	0.5, 0.75, 1.0
1400	175.84	0.095	0.5, 0.75, 1.0

Table: 3.1 Process variables and their values

3.3 Equipments and Apparatus Used

Centre Lathe

Manufactured by: GATE INC. (United Kingdom)

Model: L-1/180

Optical Microscope

The model of the microscope used for the DIP technique is Metallurgical Microscope MMB2300. Figure 3.3 and table 3.3 give more details of the microscope.

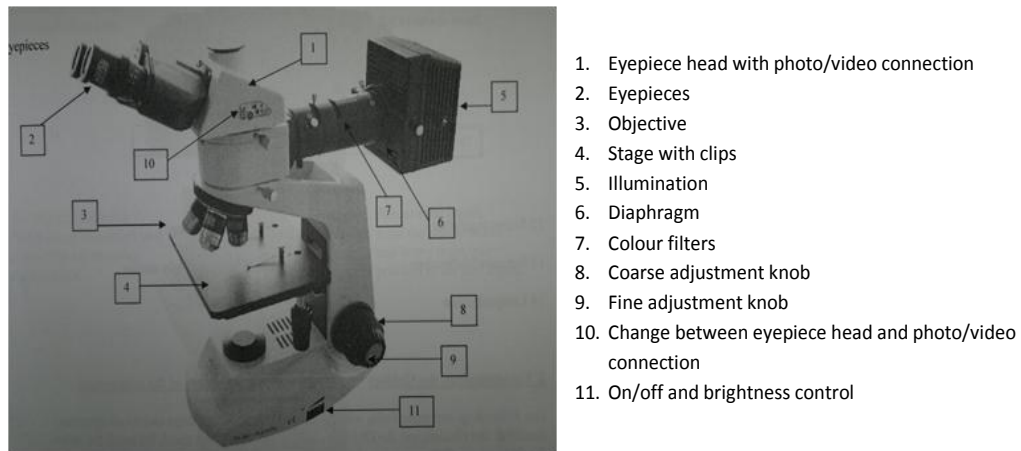


Fig: 3.3 Photograph and details of the optical microscope

Plano eyepieces	10X
Lenses	Plan achromatic 4X,10X,40X
Magnification	40 to 400
Filter	Blue
Power supply	90 to 240 VAC
Fuse	3.15 A
Illumination	Built in lamp 6V 30W, bright-field condenser
Stage moving range	132 x 140 mm
Photo-/video-mounting	Photo-adapter with eyepiece Video-adapter with eyepiece
Weight	10kg net, 15kg cross

Table: 3.2 Detail specification of the microscope

Cutting Tool Used

Tool: Tungsten carbide coated insert

Model: TX 20

Dimension: 10mm × 10mm × 5mm

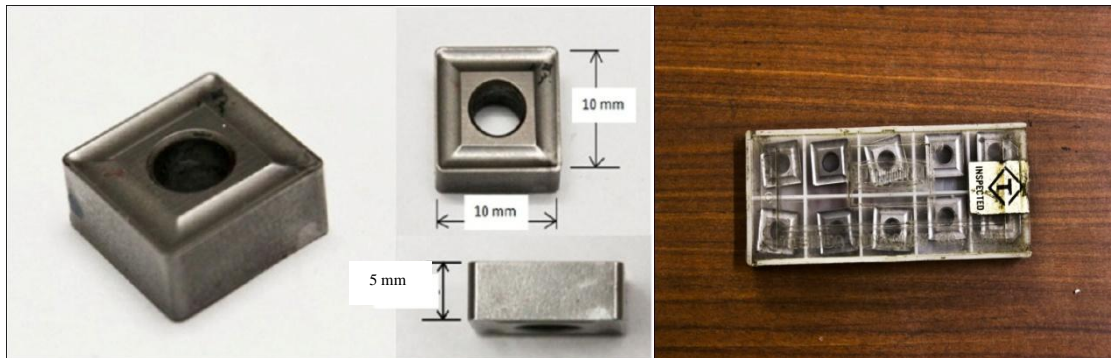


Fig: 3.4 Photograph of Insert with dimension

Work Piece Used

Mild steel shafts (Diameter 40mm and length 250mm) were used as the work piece material of the experiments.

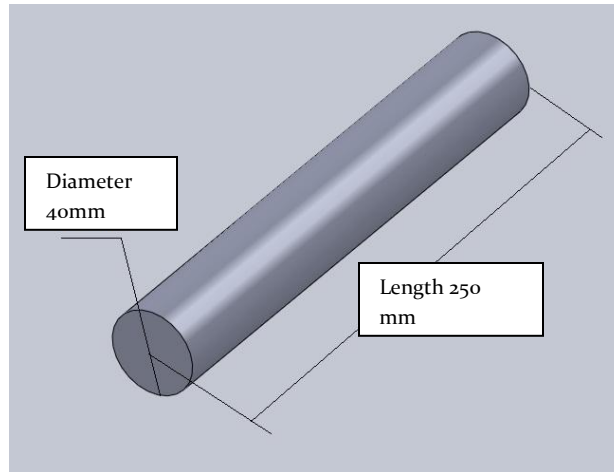


Fig: 3.5 CAD model of Work piece with dimension

A sample of the work piece was tested in the laboratory to find out the chemical composition. The result is given in table 3.4. The base metal is iron (Fe).

CONTENTS	PERCENTAGE
CARBON (C)	0.25
SILICON (Si)	0.15
MANGANESE (Mn)	0.75
SULPHUR (S)	0.045
PHOSPHORUS (P)	0.023

Table: 3.3 Chemical composition of the mild steel used in the experimentation

Magnetic Setup Used in the Experiments

Permanent Magnet

A permanent magnet is an object made from a material that is magnetized and creates its own persistent magnetic field. Materials which can be magnetized and are strongly attracted to a magnet, are called ferromagnetic (or ferrimagnetic). These include iron, nickel, cobalt, some alloys of rare earth metals, and some naturally occurring minerals such as lodestone. Although ferromagnetic (and ferrimagnetic) materials are the only ones attracted to a magnet strongly enough to be commonly considered magnetic, all

other substances respond weakly to a magnetic field, by one of several other types of magnetism.

For this study ferrite magnets were used as permanent magnet. Hard ferrite magnets are produced with iron oxide and barium or strontium oxide. The raw materials are mixed together and normally pre sintered, to generate the magnetic phase. The pre sintered mixture then gets crushed. The resulting powder gets pressed together (wet or dry) either in a magnetic field (an - isotropic) or without a magnetic field (isotropic) and in the end sintered. Due to the low cost of the raw material, hard ferrite magnets are the cheapest magnet type out of the actual supply of magnets. Ferrites have a very good electrical isolation effect and are hard to demagnetize even in strong external magnetic fields. The properties of the magnet used in this study are given in table 3.4.

Parameter	Unit	Value
Recoil permeability	G	1.05-1.30
Curie temperature	°C	450
Coefficient of demagnetization to temperature	°C ⁻¹	0.2% (0-100 °C)
Coefficient of demagnetization coercive force to temperature	°C ⁻¹	0.2%-0.5% (0-100 °C)
Density	gm/cm ³	4.7-5.0
Resistivity	°C ⁻¹	≥106
Hardness		480-580

Table: 3.4 Detail specification of permanent magnet

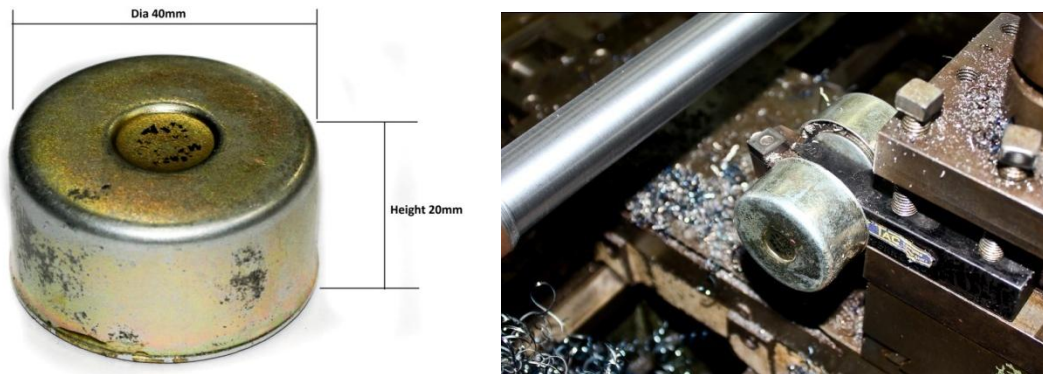


Fig: 3.6 Photograph of permanent magnet used in the study

Electro Magnet

An electromagnet is a type of magnet in which the magnetic field is produced by the flow of electric current. An electric current flowing in a wire creates a magnetic field around the wire. To concentrate the magnetic field, in an electromagnet the wire is wound into a coil with many turns of wire lying side by side. The magnetic field of all the turns of wire passes through the centre of the coil, creating a strong magnetic field there. A coil forming the shape of a straight tube is called a solenoid. Much stronger magnetic fields can be produced if a "core" of ferromagnetic material, such as soft iron, is placed inside the coil. The ferromagnetic core increases the magnetic field to thousands of times the strength of the field of the coil alone, due to the high magnetic permeability (μ) of the ferromagnetic material. This is called a ferromagnetic-core or iron-core electromagnet.

The material of the core of the magnet (usually iron) is composed of small regions called magnetic domains that act like tiny magnets. Before the current in the electromagnet is turned on, the domains in the iron core point in random directions, so their tiny magnetic fields cancel each other out, and the iron has no large scale magnetic field. When a current is passed through the wire wrapped around the iron, its magnetic field penetrates the iron, and causes the domains to turn, aligning parallel to the magnetic field, so their tiny magnetic fields add to the wire's field, creating a large magnetic field that extends into the space around the magnet. The larger the current passed through the wire coil, the more the domains align, and the stronger the magnetic field is. Finally all the domains are lined up, and further increases in current only causes slight increases in the magnetic field; this phenomenon is called saturation.

In this study an electromagnet was manufactured by using mild steel core and insulated copper wire. Instead of using a solid mild steel core, several layers of mild steel sheets were used to make the core. This arrangement ensures minimum eddy current loss. Insulated copper wire with 200 turns made up each coil.

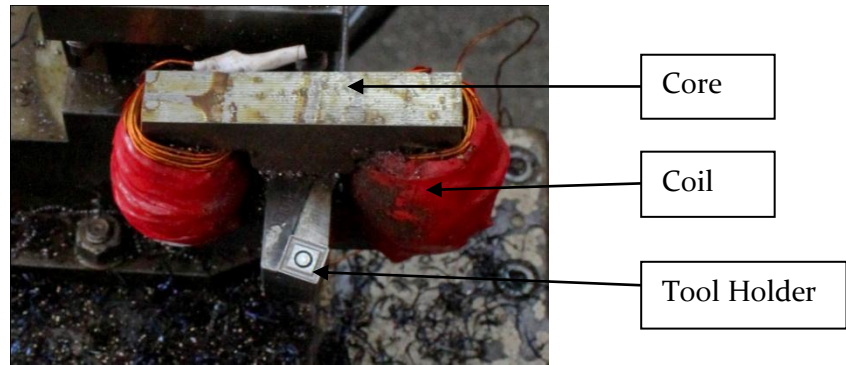


Fig: 3.7 Photograph of electro magnet used in the study

In total 37 laminated sheets were used to produce the core with total thickness of 18.5mm. The length and height of the core is 96mm and 80mm respectively. A schematic diagram of the setup with detailed dimension is shown below:

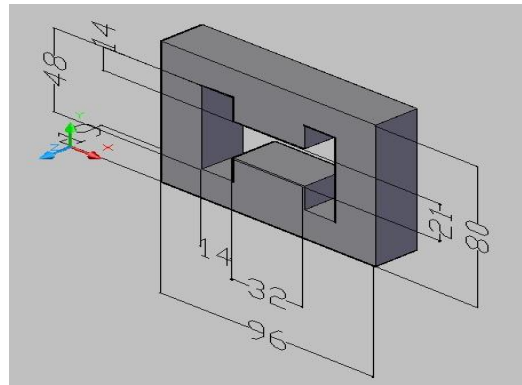


Fig: 3.8 CAD Model of the core of electromagnet

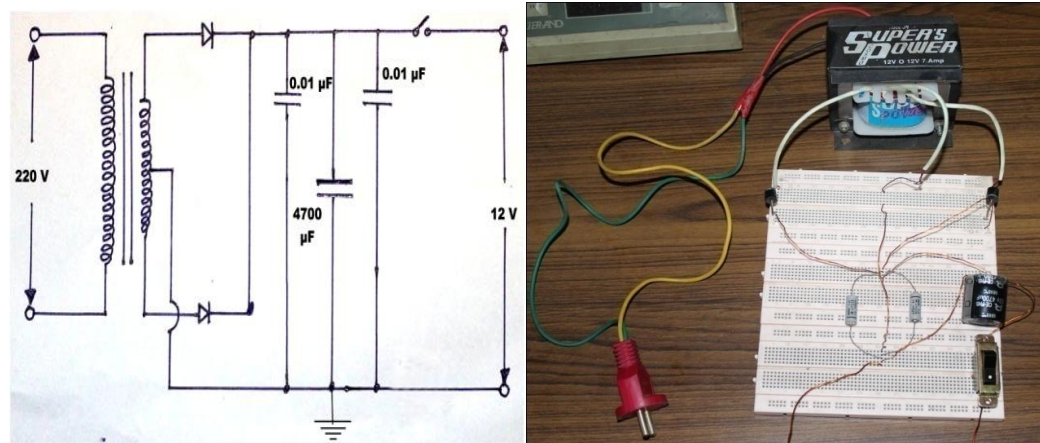
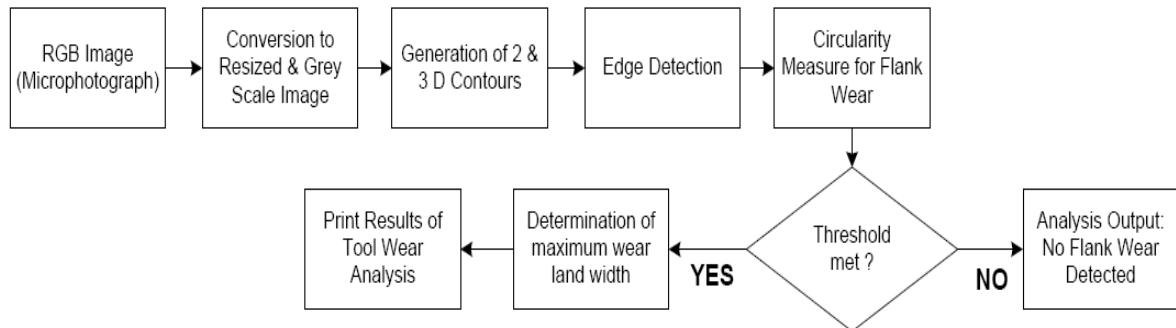


Fig: 3.9 Photograph of electrical Circuit to produce electromagnetic field

3.4 Measurement Techniques

3.4.1 Measurement of Tool Wear

The sequence used in the analysis is illustrated by figure 3.10 below. The flank wear observed were always hemispherical in shape and thus, utilization of image



processing for wear analysis was plausible.

Fig: 3.10 Process logic sequence flowchart for measuring tool wear

Digital image processing comprises the application of computer algorithm and logic to process and analyze digitized images. It is a subcategory of digital signal processing and has many advantages over analog image processing, such as: application of a wider range of algorithms to the input data and avoidance of signal distortion build-ups. An additional advantage is that images are defined over two or more dimensions, in digital image processing, and thus, can be easily modeled in the form of multidimensional systems in software dealing with Matrices, like MATLAB. For their analysis, the authors used MATLAB 2008a image processing toolbox, which can efficiently process the samples' images, in n by m 2-D matrices form.

The microphotograph of interest, obtained at 10x zoom, was obtained and saved as an RGB digital image. The image is subsequently resized and converted to grayscale for standardization in comparison and reducing the calculation load by a third,

respectively. The surface topography and contour, in 2 and 3-D respectively, were then generated using the algorithm developed by Patwari et al. [52].

The resized grayscale image was then analyzed for edge detection. The sharp edge of the tool, defined by the principal and auxiliary flank surfaces, was clearly identified by the algorithm along with the measure of its uniform straightness. The algorithm then was then used to detect and evaluate the circularity of the flank wear, which manifests as small craters. The principal axis of the crater was then determined in number of pixels. This pixel information along with the edge detection and original tool dimensions were then used to calculate the maximum flank wear land width, „ V_{Bmax} ,“ in millimeters.

The results of the wear analysis are then compared by the software against a ‘threshold’ land wear value, obtained from Patwari et al. [52] work, to determine whether the wear is a flank wear. This is achieved by a decision subroutine in the software. The utility of this screening process for flank wear is that most tools display other types of wear such as: built-up edge, rake wear, and edge wear etc. which are not very significant to cutting edge stability. Depending upon the evaluation of the decision subroutine, the software outputs either that ‘no flank wear is detected’ or that ‘flank wear detected’ along with the calculated value of land wear V_{Bmax} . The same analysis was conducted for eight different lengths of cut and compared with the results obtained by Patwari et al. [67].

A new measure, called the circularity metric ‘ CM ’, was developed to detect and analyze flank tool wear land width V_B . The metric evaluates the extent to which feature in the tool’s image is circular and decides that it is a flank wear if the metric threshold of 0.80 was reached. Once the wear is detected the algorithm then determines the length of the wears principal axis in pixels; which is subsequently converted to millimetres by the process already mentioned above. Equation (1), below, is the mathematical definition of the circularity metric used.

$$CM = \frac{4\pi(area)}{(Perimeter)^2} \quad (3.4)$$

Figure 3.11, below, shows the sample results of image processing for tool (with flank wear) used for turning with length of cut 800 mm.

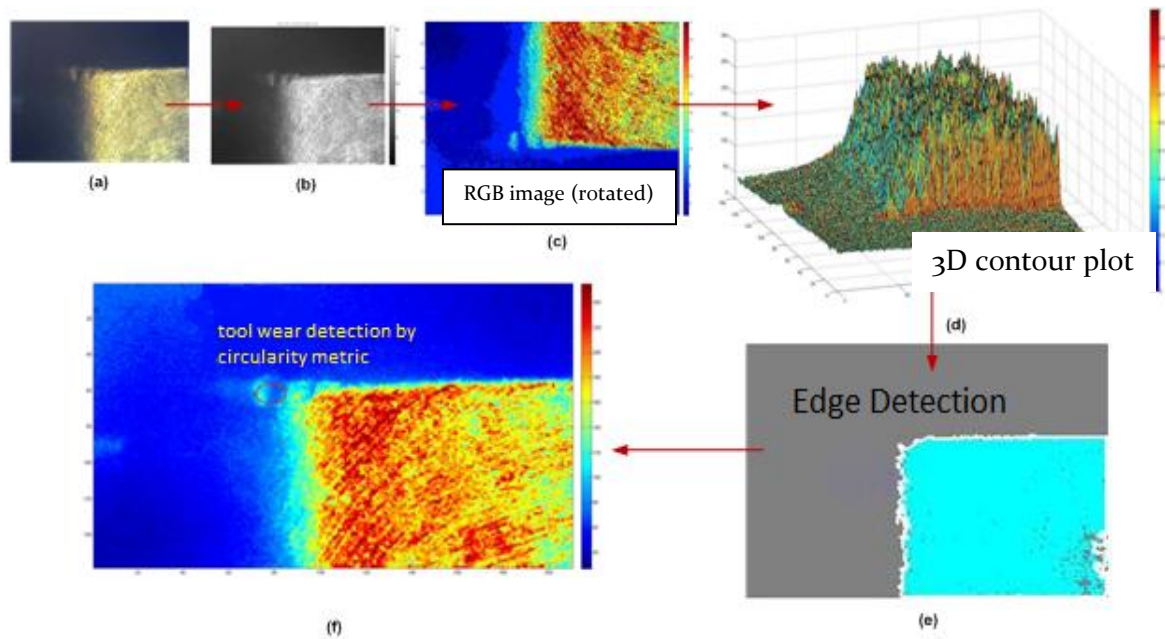


Fig: 3.11 Image processing result sample for measuring tool wear [52]

3.4.2 Measurement of Surface Roughness

The image processing technique for determining surface roughness is described below:

1. The microphotographs of finished work piece are taken using optical microscope. For maintaining same quality and environment in all photographs same setup with same magnification and illuminating conditions were used.
2. The photographs are converted to grey scale and then to binary images in order to speed up the calculation process. As the process is dependent on the intensity of the reflected light from the surface to the microscope it is convenient to convert the image to greyscale image in order to compare the intensity of each point with others.

The binary image stores the values of each point as binary values. This way it is easier to analyze the image later.

3. The binary images are then analyzed using a digital image processing algorithm to generate profile plot and coloured contour plot.
4. First the program adds up all the values of each point over the whole region and then finds out the average value. This average value is the average surface roughness of the work piece.
5. Then a profile plot is generated by plotting the average value of light intensity on each plane against distance. This helps to understand the waviness of the surface in two dimensional views.
6. Next a coloured contour plot of the whole region is generated to observe the location of peak points and bottom points. The contour colour map thus gives an overall idea of the surface quality.
7. Finally a 3D contour plot of the surface is generated for the whole region to reconstruct the real surface in the software. This 3D contour plot represents as the 3D model of the actual surface that has been taken in the study.

The whole sequence is illustrated by the following flowchart (figure 3.12) and by figure 3.13.

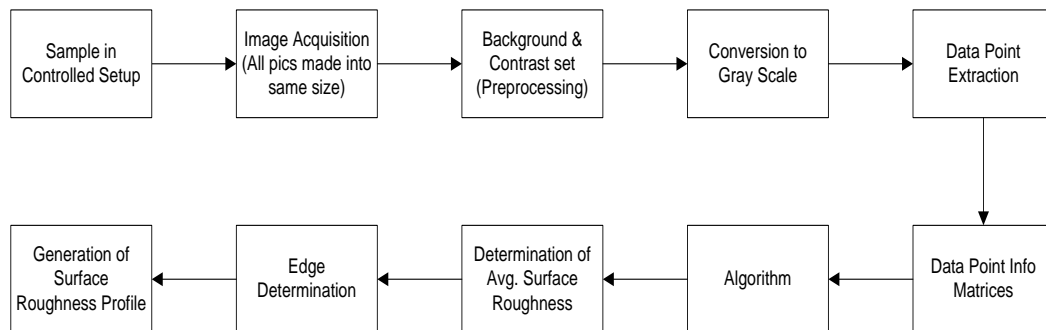


Fig: 3.12 Flow diagram of image processing for surface roughness

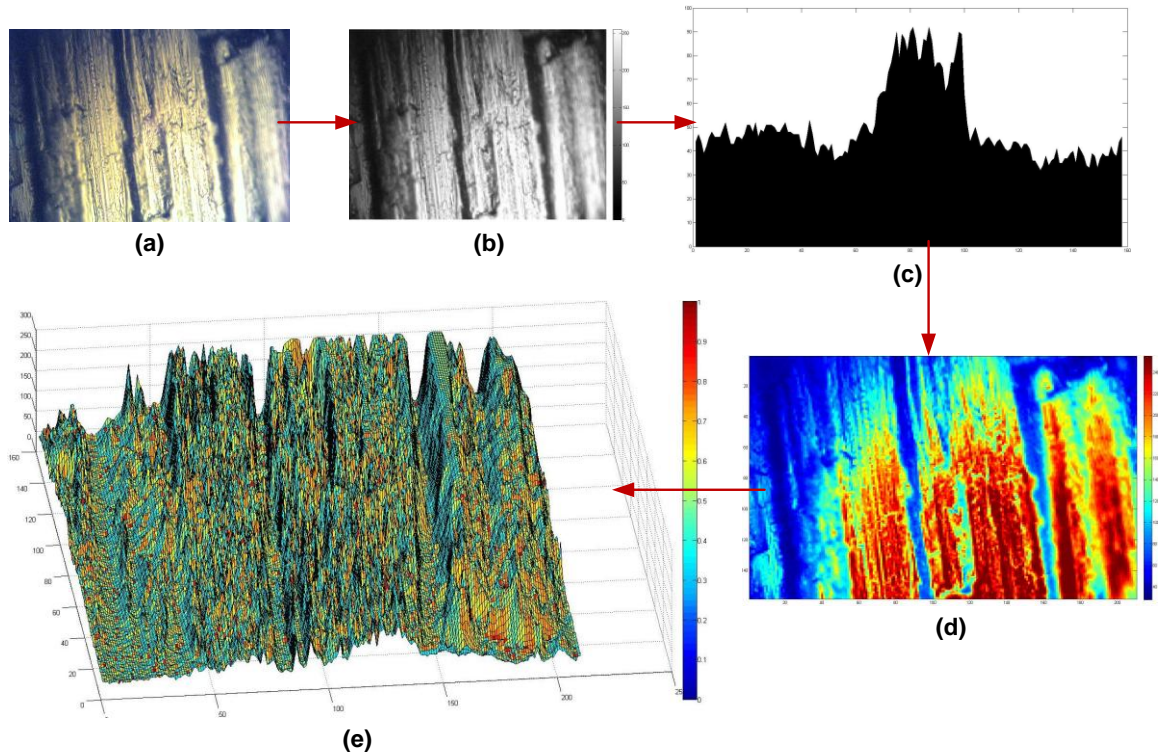


Fig: 3.13 DIP results (work-piece surface roughness, without magnet) (a) 10x zoom RGB microphotograph, (b) greyscale, (c) profile plot, (d) 2-D coloured contour plot, (e) 3-D coloured contour plot[53]

3.4.3 Observation of Chip Behaviour

The chips formed during turning were mainly investigated and it has been found that at some specific cutting conditions chip formation presents extreme cases of secondary and primary chip serration. Firstly, the chip at different cutting conditions were collected, labeled and kept accordingly. Then each chip was mounted using a mixture of resin and hardener. The mixture was stirred for about one minute and left to solidify. The solidified mixture is called mounting. The next step is to grind the mounting surface in order to reveal the chip to the surface. Various grade of abrasive paper are used starting with grade 240 followed by 400, 800 and 1200. In order to remove the scratches on the surfaces, the mounting is then polished using alumina solution starting from grain size 6.0μ , followed by 1.0μ , 0.3μ and 0.01μ . As a safety precaution, before polishing; the mounting is viewed under the microscope to ensure that the chip is visible on the surface.

Finally, nitol is applied to the surface to reveal the grain boundaries of the ferrite and pearlite. Then the mounting is ready to be viewed under the microscope to capture the structure of the chip.



Fig: 3.14 Photograph of samples of mounted chip

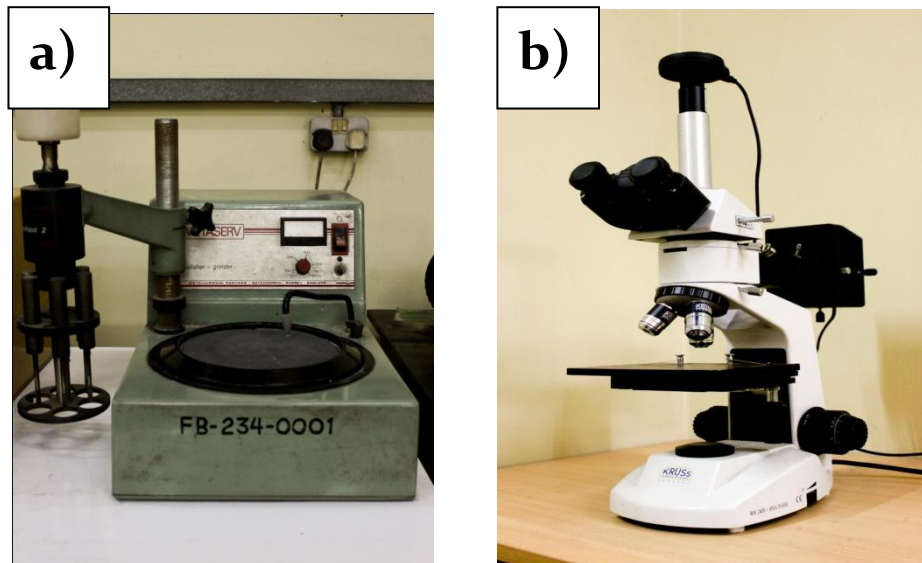


Fig: 3.15 Photograph of instruments used for chip analysis. a) Polishing wheel, b) optical microscope

3.4.4 Measurement of Temperature

To measure the temperature of the tip of the insert a digital thermocouple was used. The hot end of the thermocouple was welded to the tip of the insert. Readings were taken from the display of the thermocouple after cutting 200mm at different cutting speed and depth of cut.

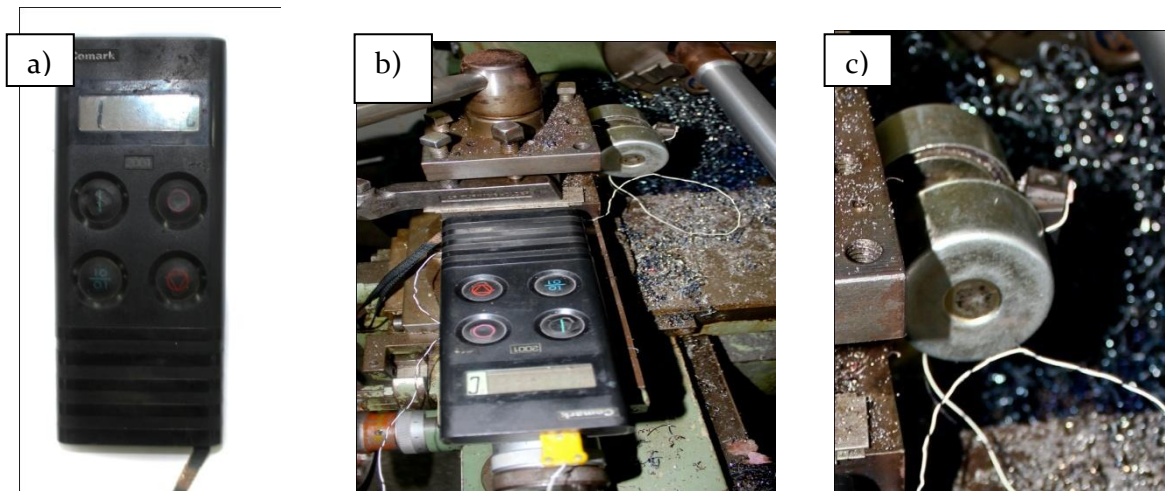


Fig: 3.16 Photograph of arrangement for measuring cutting temperature a) thermocouple b) experimental setup c) thermocouple hot end attached with insert tip

3.4.5 Measurement of Cutting Force

To measure the cutting force a digital strain meter was used. Two strain gauges (Mfg- JP Tech, model- PA13-062AB-120 EN, gauge factor- 2.07) were attached to the tool holder. A half Wheatstone bridge circuit was used to connect the strain gauges to the digital strain meter. One strain measure was attached on top portion of the tool holder to measure the tension and one was attached on the bottom side to measure the compression. These two strain meters acted as two active arms of the bridge. The other two resistors of the bridge circuit were activated internally in the strain meter. The connection and the circuit diagram are shown in the following section.

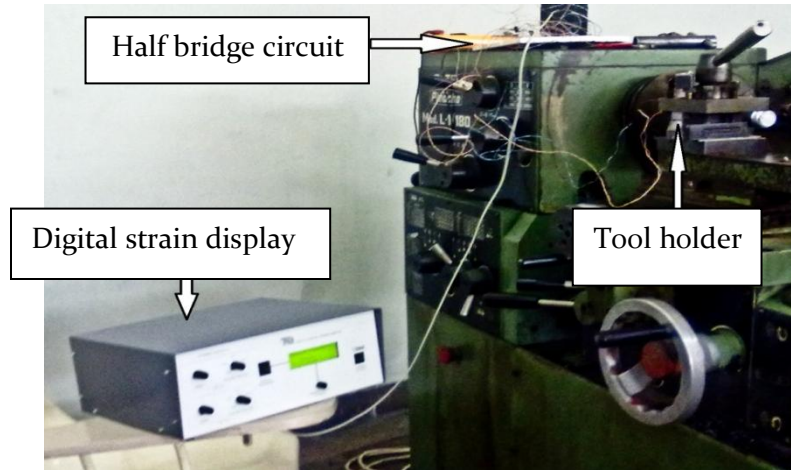


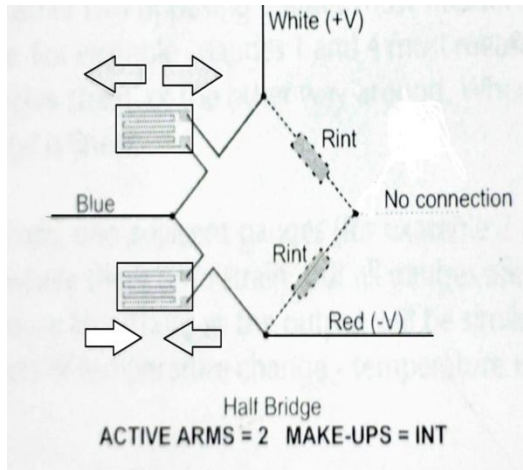
Fig: 3.17 Photograph of arrangement for measuring cutting force with half bridge circuit and strain meter

The strain meter measured the strain on the tool holder because of tangential cutting force in micro strain. Later this strain was related to force using Young's formula. The empirical equation shows a proportional relationship in between strain and force. Later these data were plotted.



Fig: 3.18 Photograph of SM 1010 Digital Strain Display

The circuit diagram of the half bridge circuit with the connection terminal to strain meter is shown below:



Rint- ‘make up’ resistors inside (built into) the digital strain display

Fig: 3.19 Photograph of Circuit used to connect strain gauges to the strain meter [54]

There were four wires in the input cable of the strain display. They had four different colours. The white wire was attached to the power line and the red wire was connected to the ground. The blue wire was connected in between the strain gauges. As the dummy or make up resistors were built into the strain gauge so no connection was required to the green wire. The specifications of the strain display are given in the table below:

Item	Details
Standard strain display range	+/- 10000 $\mu\epsilon$
Dynamic strain range	+/- 2000 $\mu\epsilon$
Gauge factor range	1.9 to 2.3
Nominal warm up time	10 minutes
Connections	Quarter, half & full bridge
Channels	16 (14 standard & 2 extra dynamic outputs)

Table: 3.5 Technical details of SM1010 digital strain display [54]

Introduction

Different analyses have been done based on the data recorded through the experimentation process. Comparisons of tool wear, surface roughness, chip behaviour, cutting temperature and cutting force have been studied in several cutting conditions and different cutting environments.

4.1 Distribution of Magnetic Field

To evaluate the distribution of magnetic force line in the field surrounding the cutting environment simulations were done using MATLAB to compare between the permanent magnet and electro magnet condition. These two results are shown below:

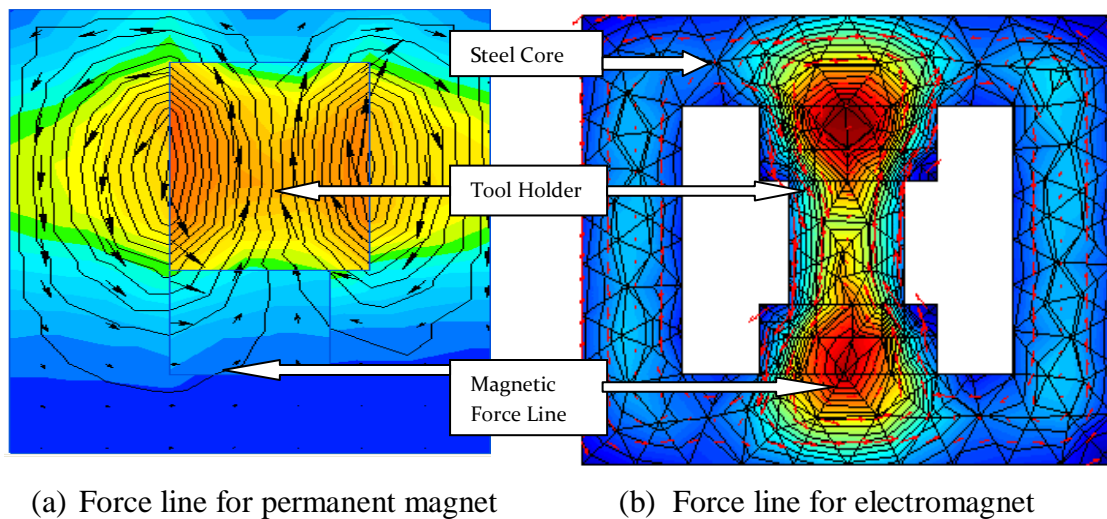


Figure: 4.1 Comparison of field distribution between permanent magnet and electromagnetic condition

It is clearly visible from the diagram that in case of electromagnetic condition the force lines are more concentrated. This is because of the steel core around the tool holder. The core minimizes the loss of force line and directs the force line towards tool holder,; as a result, better properties of the product are obtained in case of electromagnetic cutting condition.

4.2 Effect of Magnetic Field on Tool Wear

At first the image processing tool for determining flank wear was developed and verified. The results of the analysis were compared with those previously determined by Patwari et al. [52], who used Kruss metallurgical microscope's analysis software to determine V_{Bmax} . Table 4.1 lists the average accuracy and repeatability of the analysis technique. From the table, it was observed that, the accuracy was higher for greater wear or larger wear land V_{Bmax} .

No.	Cut Length (mm)	Wear measured by optical process (mm)	Wear measured by simulation (mm)	Error %
1	0	0	0	0
2	200	0	0	0
3	400	0.0057	0.0063	10.52631579
4	500	0.0281	0.0298	6.049822064
5	600	0.0323	0.031	-4.024767802
6	700	0.0374	0.036	-3.743315508
7	800	0.0393	0.039	-0.763358779
8	1000	0.0412	0.04105	-0.36407767
Avg. Error % =				3.183957201

Table: 4.1 Accuracy and repeatability of the automated tool wear analysis technique

The image processing technique for tool wear measurement showed good accuracy and consistency. It was observed that the technique was simple, fast, and economical. The only major investment is the requirement for an optical microscope and laptop, hardware that is readily available in most modern industries or research institutes. The shortcoming observed was that the software was less precise in evaluating tool wear when the flank land wear was very small ($V_{Bmax} < 0.3$ mm approx.). For detection of larger tool flank wear the accuracy of the system was markedly improved. The consistency to detect tool wear, however, was always 100%, as shown by the first two data points. The explanation for this behaviour is that the software relies on contrast difference or grey level intensity variation to detect and evaluate tool wear. Hence, when small amount of wear is concerned, the contrast is less, which leads to increased chances of error.


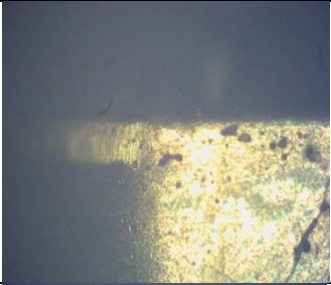
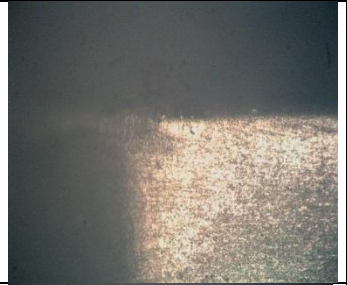
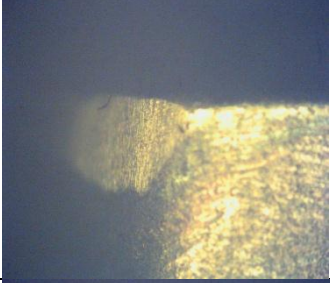
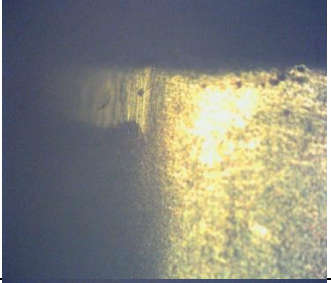

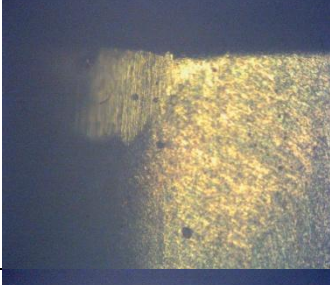
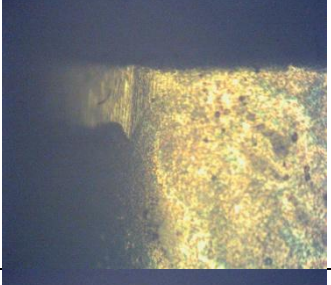

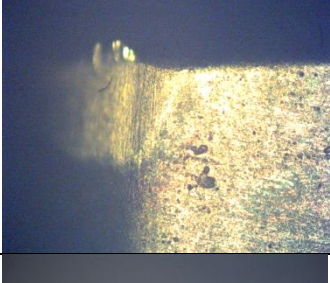
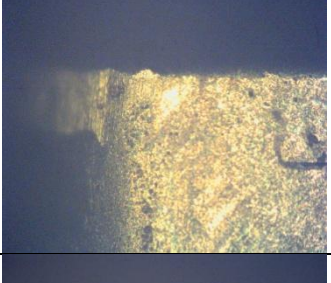

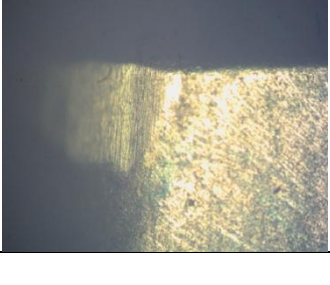
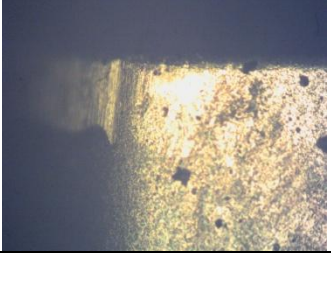
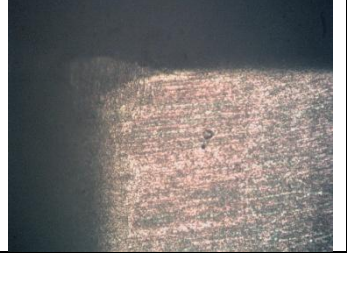
DOC 0.75 mm, RPM 860	Non magnet	Permanent magnet	Electro magnet
After cutting 200 mm			
After cutting 400 mm			
After cutting 600 mm			
After cutting 800 mm			
After cutting 1000 mm			

Table: 4.2 Sample photographs of tool wear taken at 860 RPM and 0.75 DOC under different cutting environment with constant feed at 0.095 mm/rev.

The values of tool wear found in different cutting conditions under different cutting environments have been plotted to compare between each of the cases. Some samples of the generated graphs are shown below:

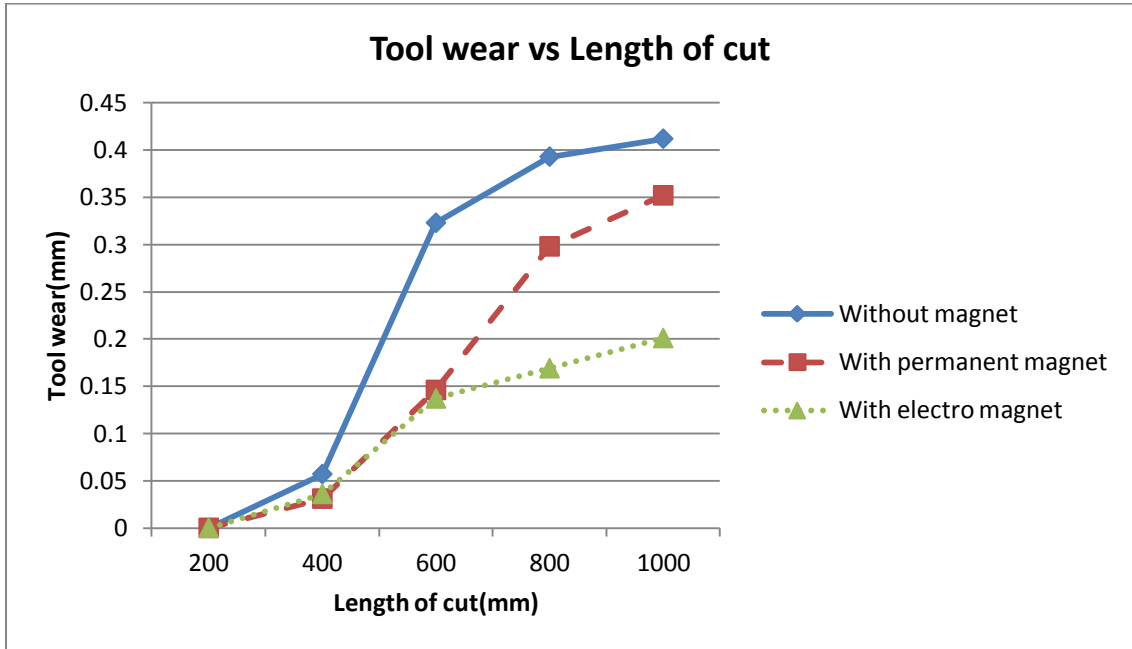


Figure: 4.2 Comparison of tool wear at 530rpm and depth of cut 0.5 mm

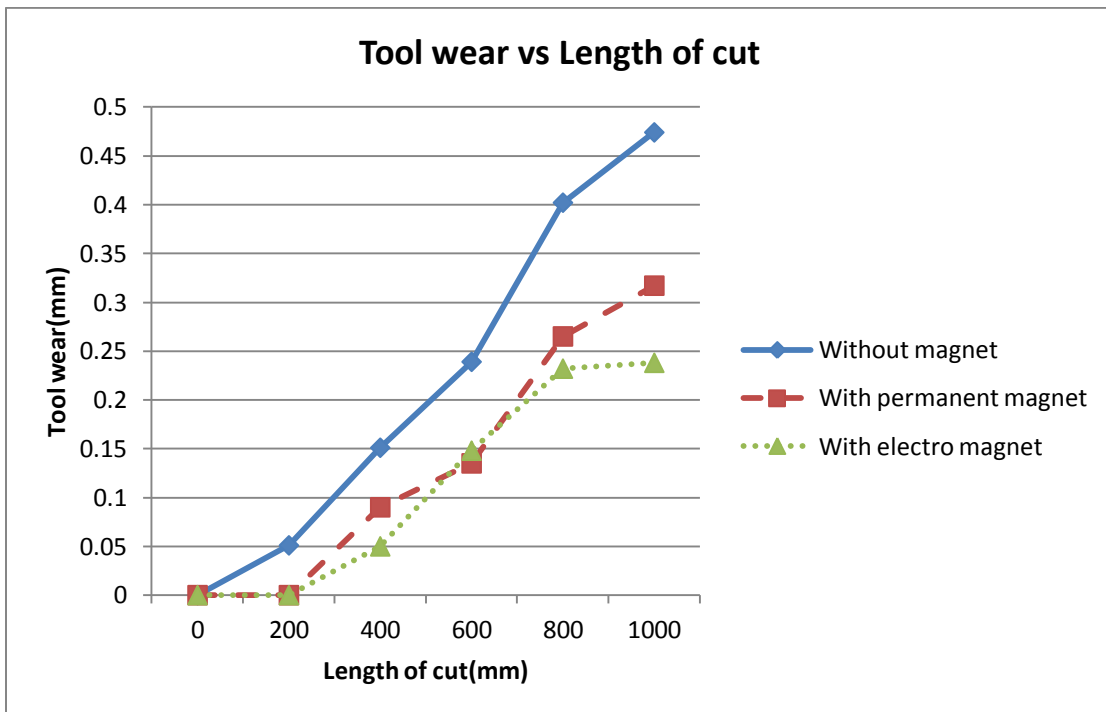


Figure: 4.3 Comparison of tool wear at 860rpm and depth of cut 0.5 mm

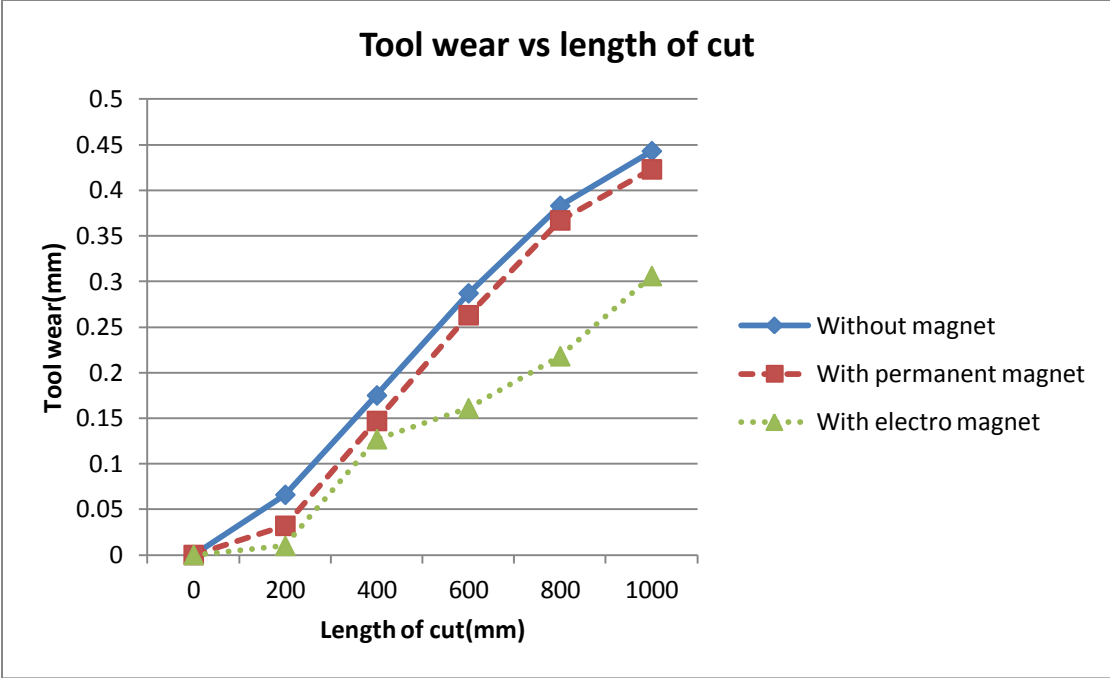


Figure: 4.4 Comparison of tool wear at 1400rpm and depth of cut 0.5 mm

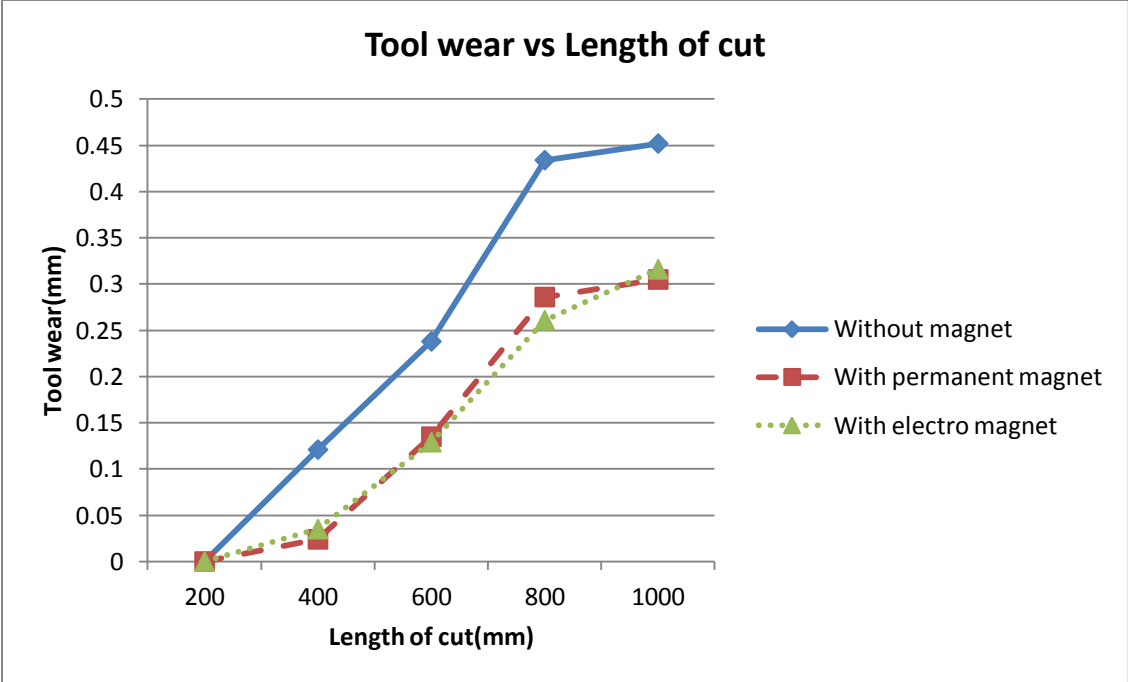


Figure: 4.5 Comparison of tool wears at 530rpm and depth of cut 0.75 mm

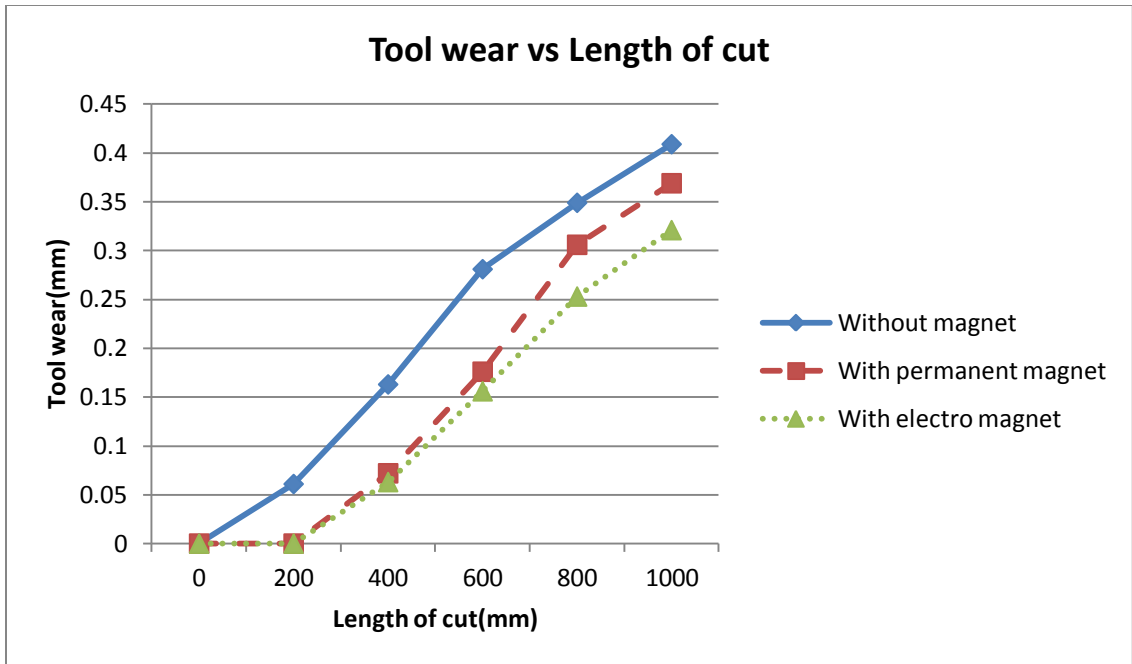


Figure: 4.6 Comparison of tool wears at 530rpm and depth of cut 1.0 mm

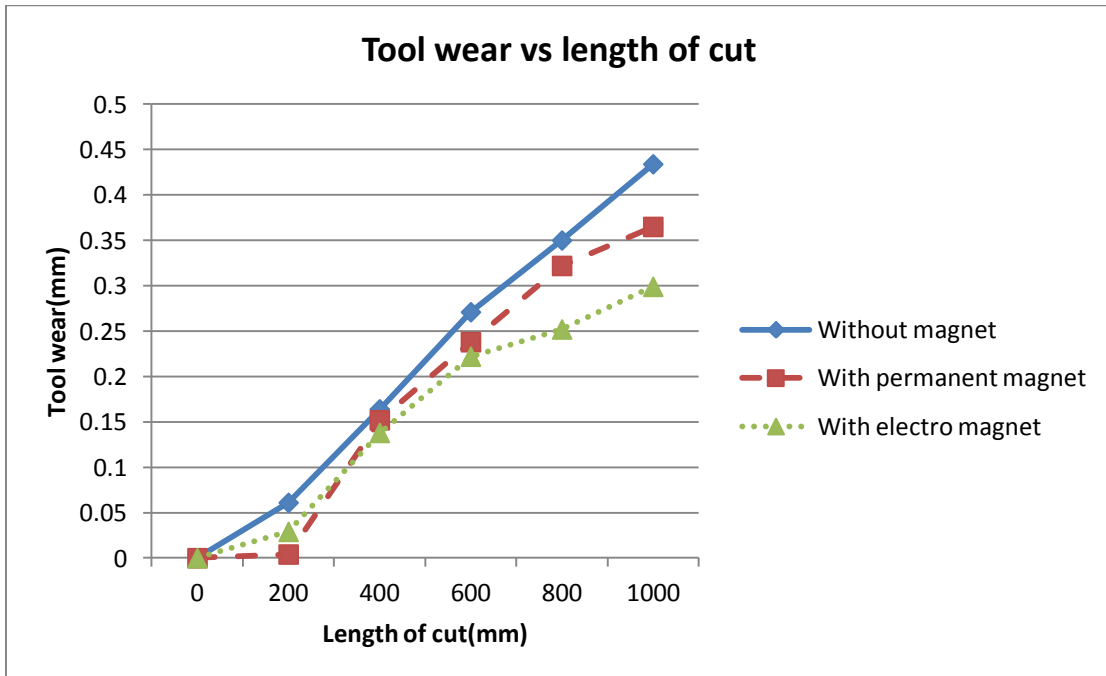


Figure: 4.7 Comparison of tool wears at 860rpm and depth of cut 0.75 mm

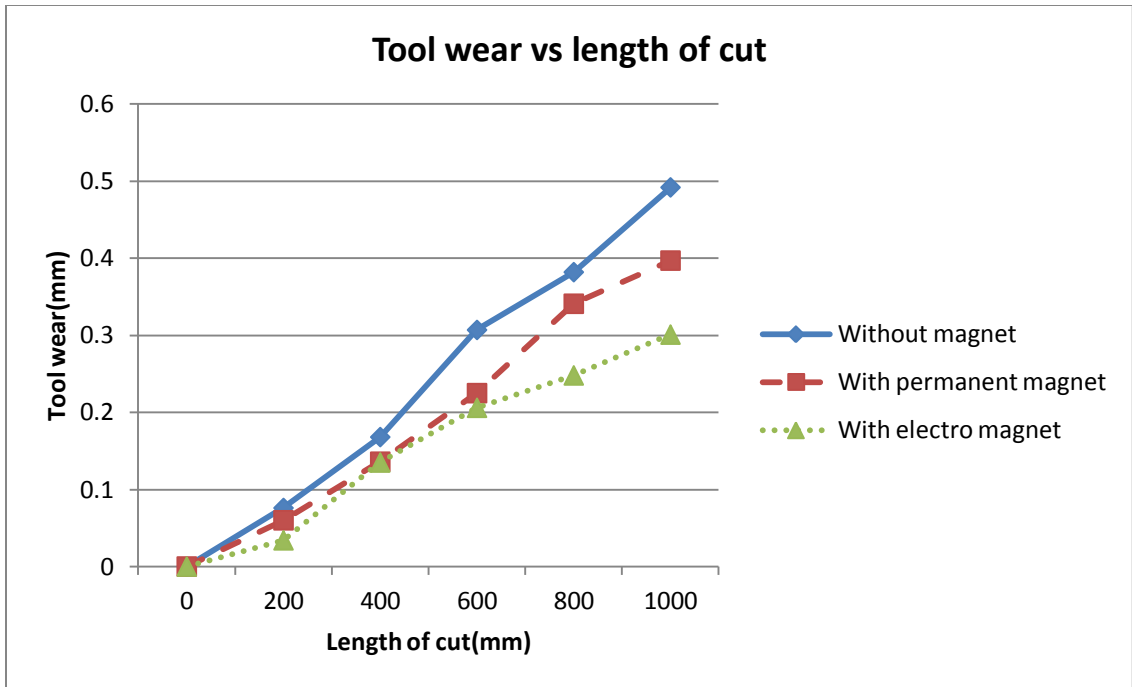


Figure: 4.8 Comparison of tool wears at 860rpm and depth of cut 1.0 mm

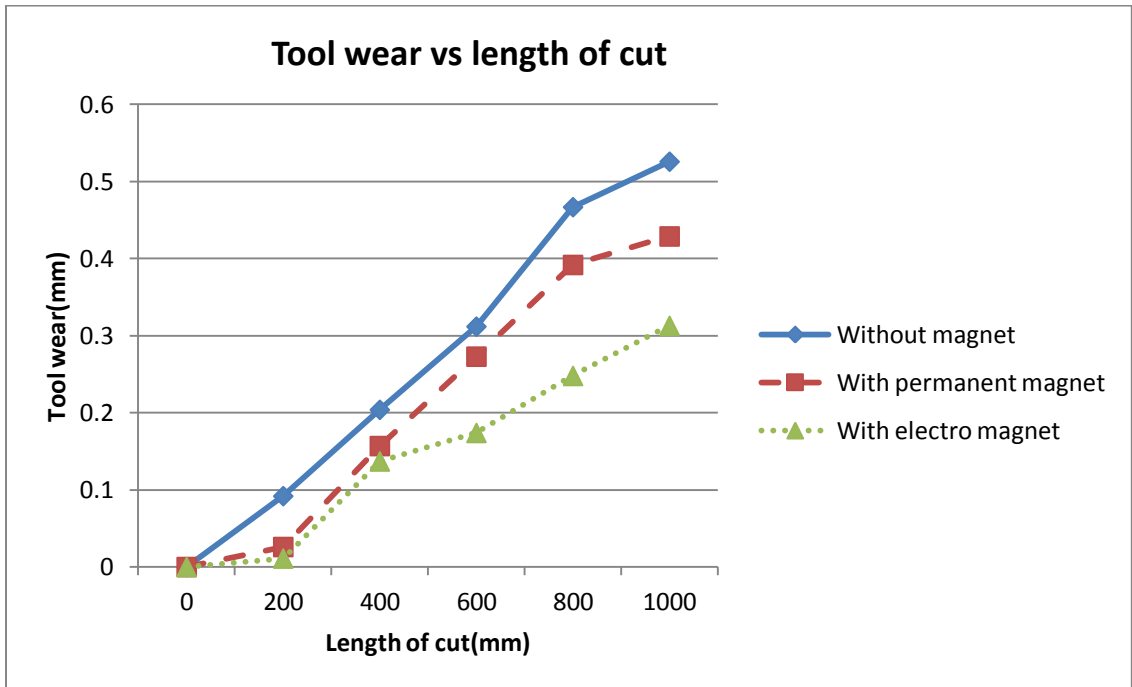


Figure: 4.9 Comparison of tool wears at 1400rpm and depth of cut 0.75 mm

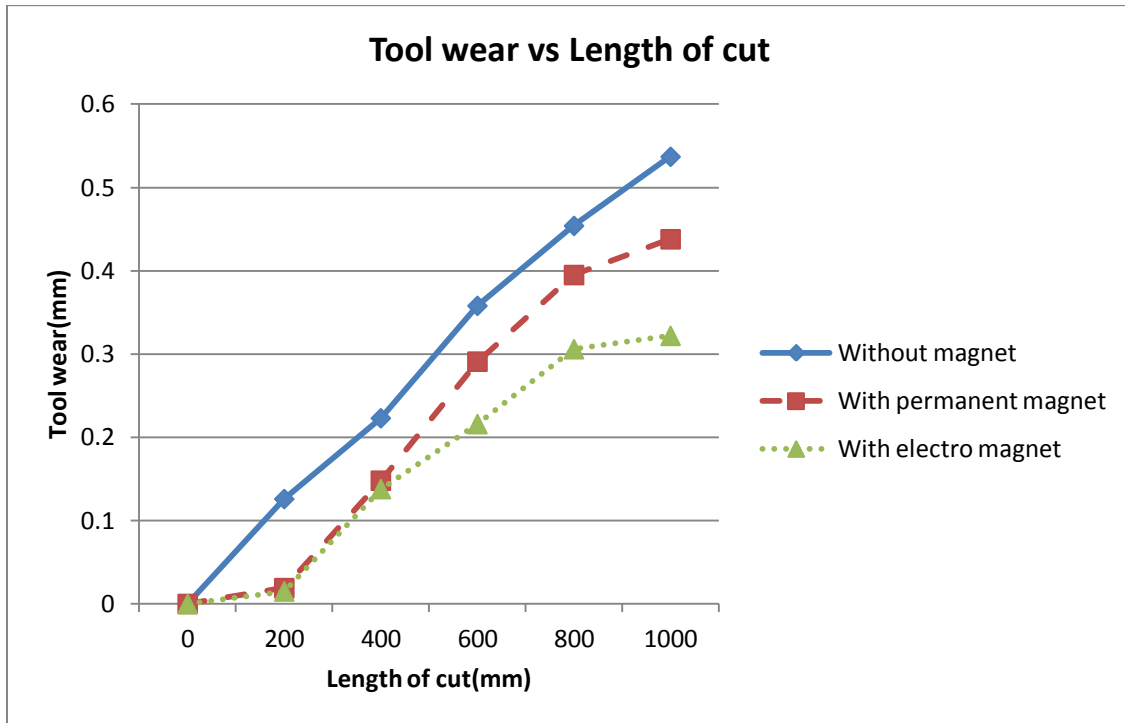


Figure: 4.10 Comparison of tool wears at 1400rpm and depth of cut 1.0 mm with constant feed.

It can be observed from the above graphs that, the tool wear with the application of magnetic field is reduced as compared to without the application of magnetic field. For example, at 530 rpm and 0.5 mm depth of cut, tool wear reaches maximum wear limit 0.3 mm after cutting around 550 mm in case of no magnetic condition. But for permanent magnet condition the cutting length is around 800 mm and for electromagnetic condition this is more than 1000mm. This trend is observed in all the experiments done in this study. The applied magnetic field affects the cutting mechanism as discussed earlier. The tool wear is significantly reduced in case of electro magnet. This may be due to the concentration of more magnetic flux in cutting point of the insert which leads to built up edge at the tip of the insert. This built up edge protects the insert from wear. It can also be observed that in all the environment tool wear increases with the increase of depth of cut. In all depth of cut magnetic condition shows less tool wear and it is least in electromagnetic condition. Tool wear also increases with the increase of

speed. In this case also tool wear reduces when external magnetic field is applied and the result significantly improves in case of electromagnetic condition. To observe the effect of depth of cut in each cutting conditions at a certain cutting speed the following graphs have been generated:

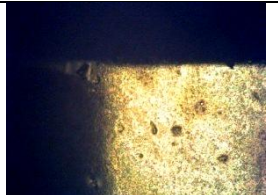

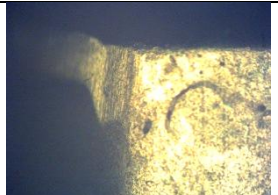






	DOC 0.5mm	DOC 0.75mm	DOC 1.0 mm
Non Magnet			
Permanent Magnet			
Electro Magnet			

Table: 4.3 Sample photographs of tool wear at Different depth of cut under different cutting environment

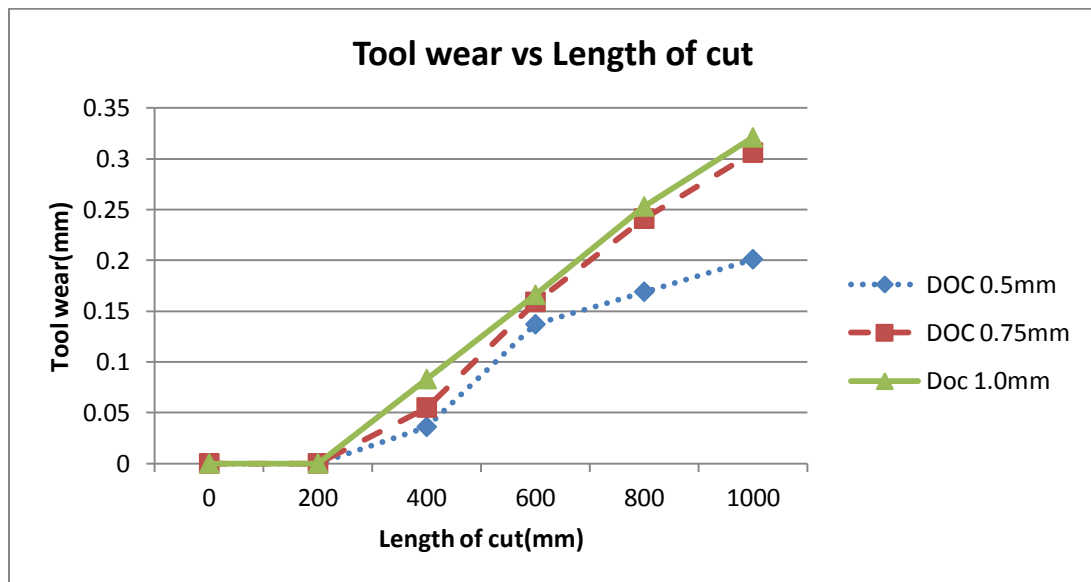


Figure: 4.11 Comparison of tool wear at 530rpm in electromagnetic condition with different depths of cut

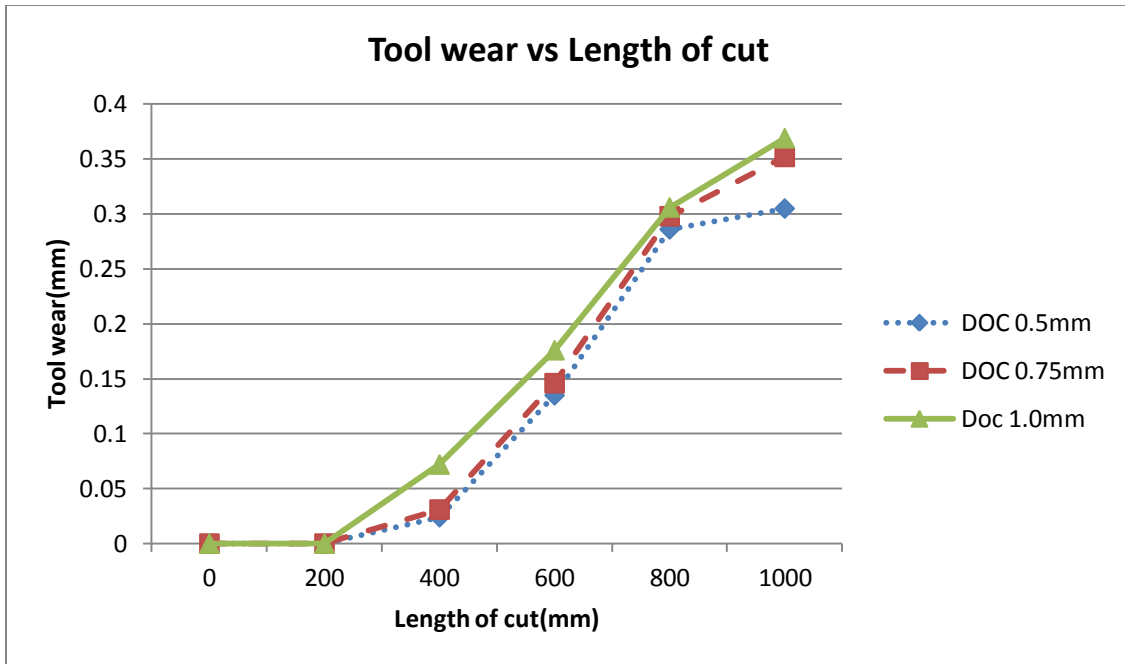


Figure: 4.12 Comparison of tool wear at 530rpm in permanent magnetic condition with different depths of cut

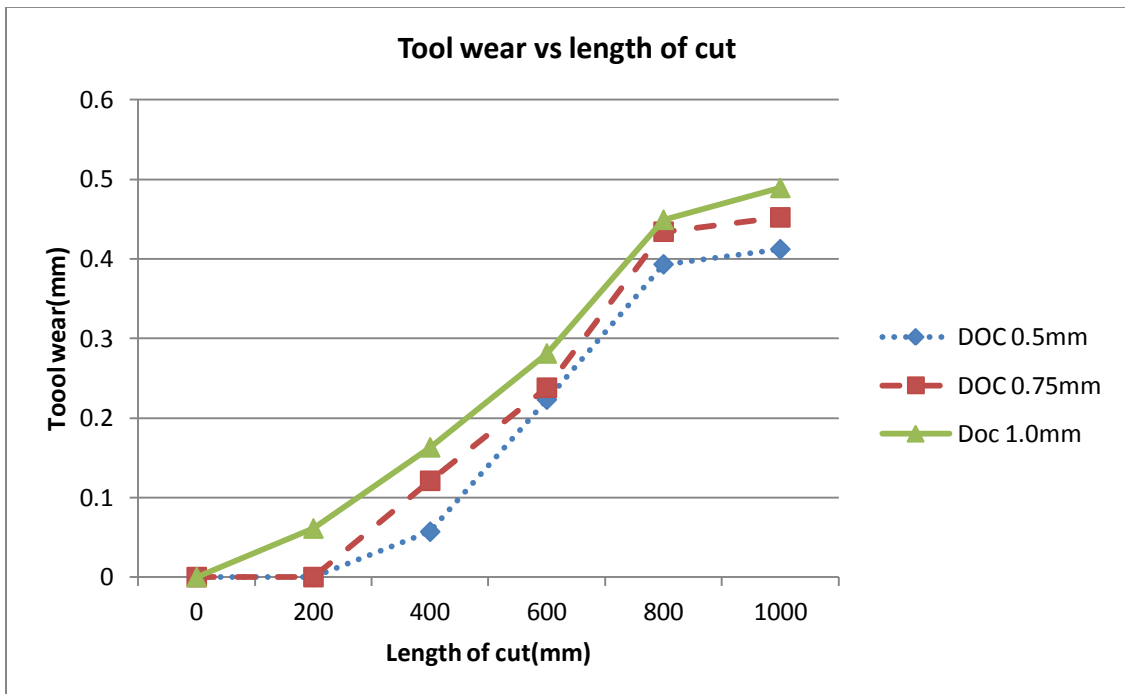


Figure: 4.13 Comparison of tool wear at 530rpm in without magnet condition with different depths of cut

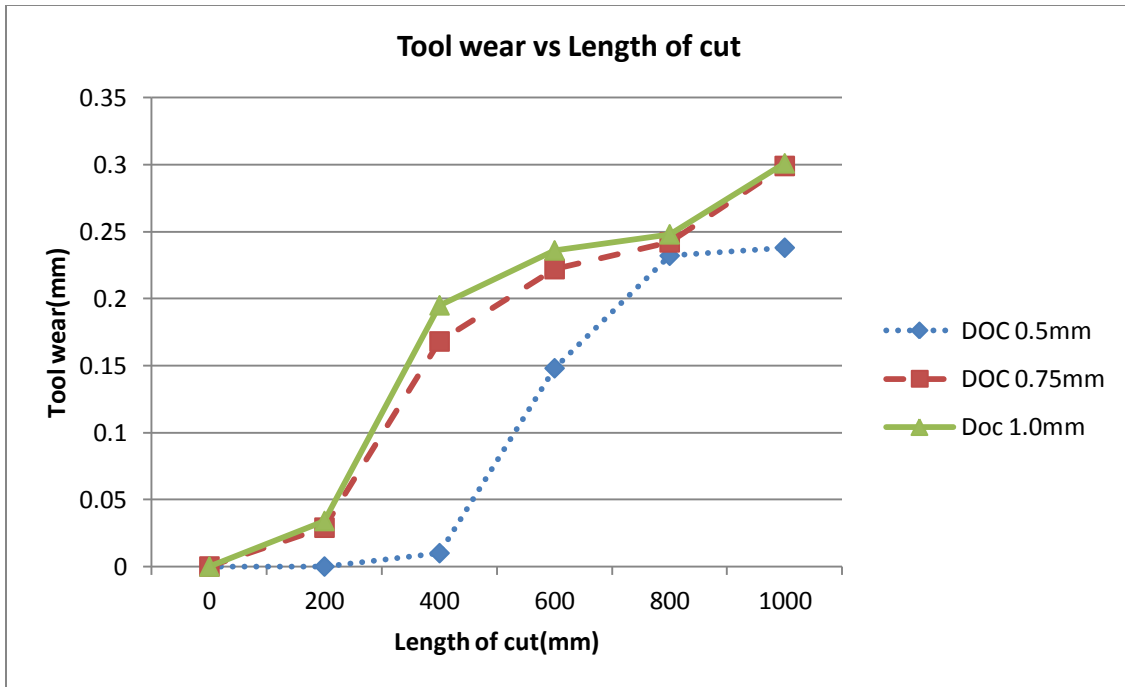


Figure: 4.14 Comparison of tool wears at 860rpm in electromagnetic condition with different depths of cut

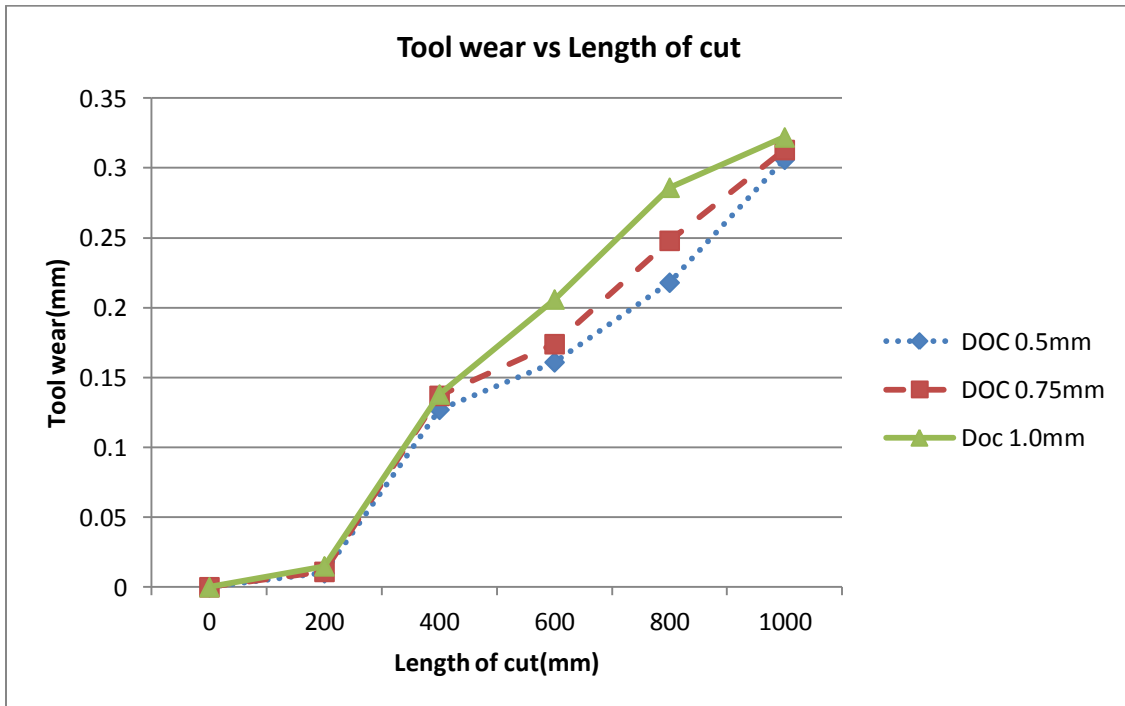


Figure: 4.15 Comparison of tool wears at 1400rpm in electromagnetic condition with different depths of cut

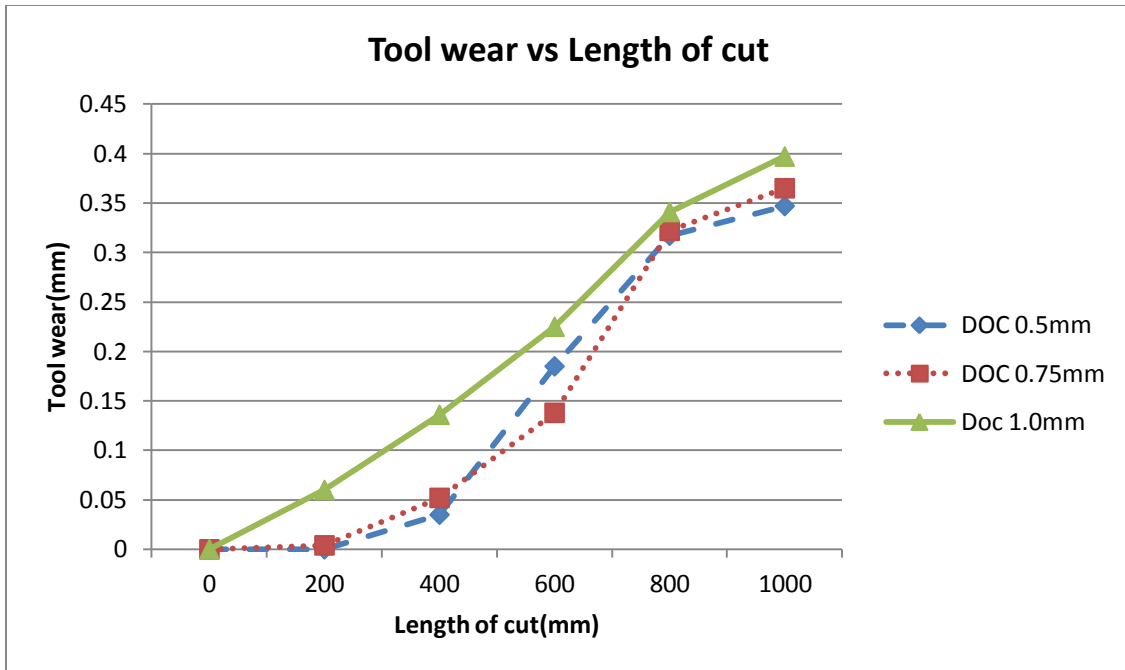


Figure: 4.16 Comparison of tool wears at 860rpm in permanent magnetic condition with different depths of cut

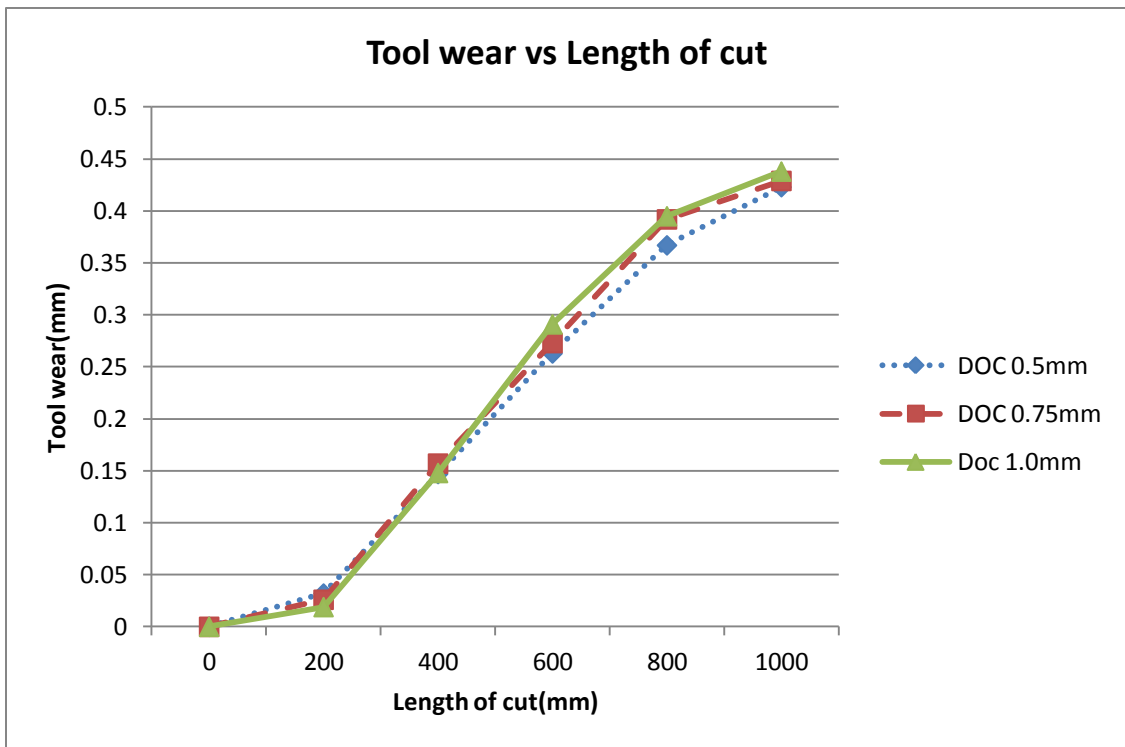


Figure: 4.17 Comparison of tool wears at 1400rpm in permanent magnetic condition with different depths of cut

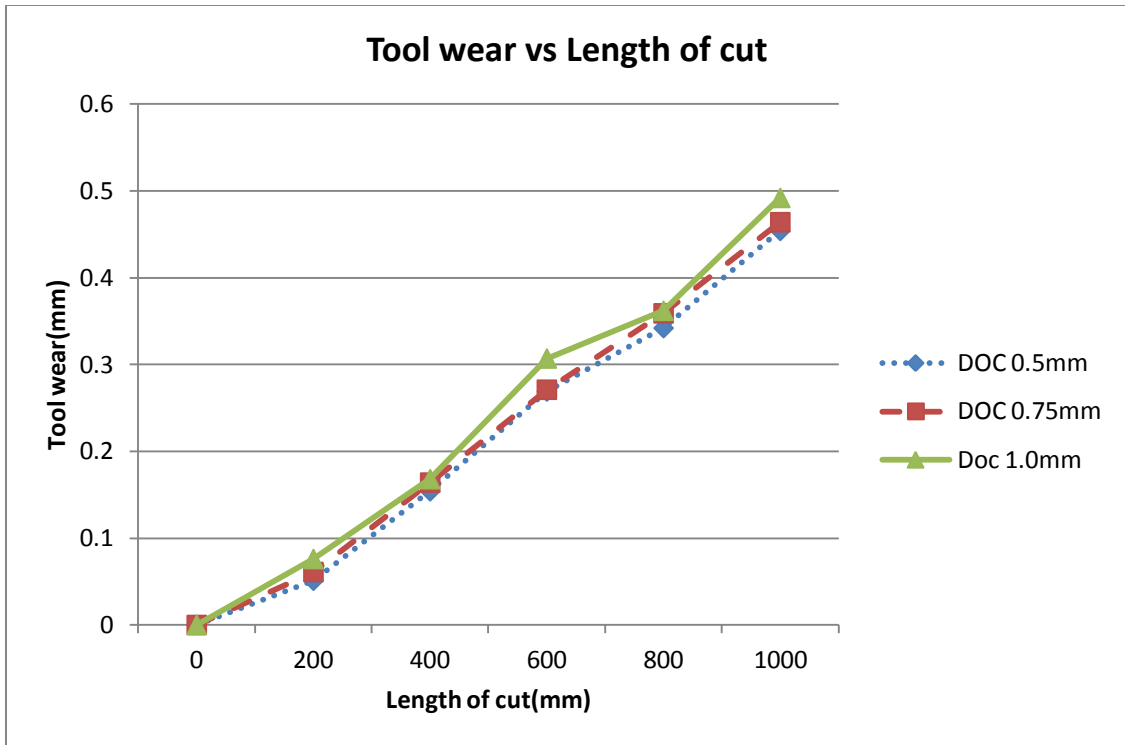


Figure: 4.18 Comparison of tool wears at 860rpm in without magnet condition with different depths of cut

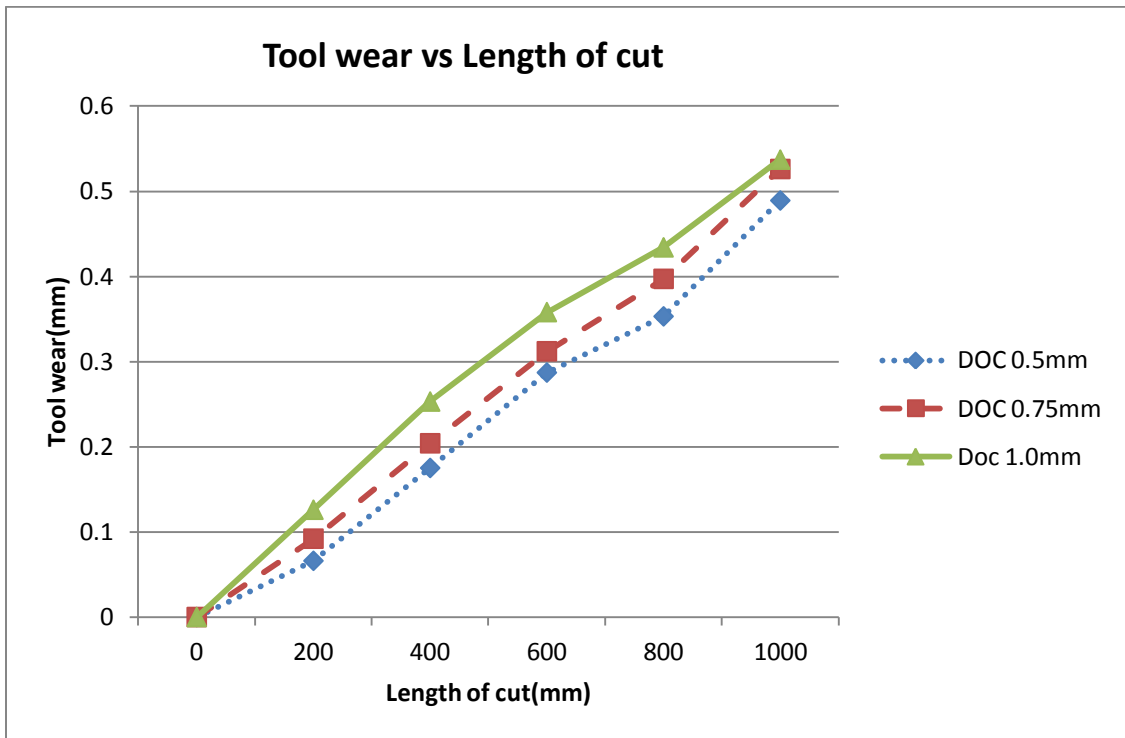


Figure: 4.19 Comparison of tool wears at 1400rpm in without magnet condition with different depths of cut

From the graphs provided above it can be observed that with increase of depth of cut the flank wear of the insert gradually increases. For example in case of electromagnetic condition at 530 RPM the tool wear for 0.5mm, 0.75mm and 1.0mm depth of cut were 0.201mm, 0.306mm and 0.321mm respectively after cutting 1000mm. Similar increase of tool wear is also seen in case of permanent magnet and without magnet condition. It has been observed that as the cutting speed increases the effect of depth of cut on tool wear gradually decreases. For this reason the lines for tool wear are separated in 530RPM, but quite close in 1400RPM. This effect is least in electromagnetic condition which results in large difference among tool wear at different depth of cut with increase of speed. In case of permanent magnet and without magnet condition the difference between tool wear at different depth of cut with the increase of cutting speed is similar. The lines almost coincide with each other in these cases. But the point to remember is that the overall values of the tool wear in case of permanent magnet is quite less in compare to without magnet cutting condition. Based on these it can be said that electromagnetic cutting condition is better in case of larger depth of cut.

For observing the effect of cutting speed on tool wear in different cutting condition tool wear vs. length of cut were plotted at certain depth of cut in each cutting environment. These graphs show the effect of increase in cutting speed on tool wear at a certain depth of cut. Graphs were generated for all the cutting environments: without magnet condition, Permanent magnet condition and electro magnet condition. For comparison among them, the generated graphs are given below:

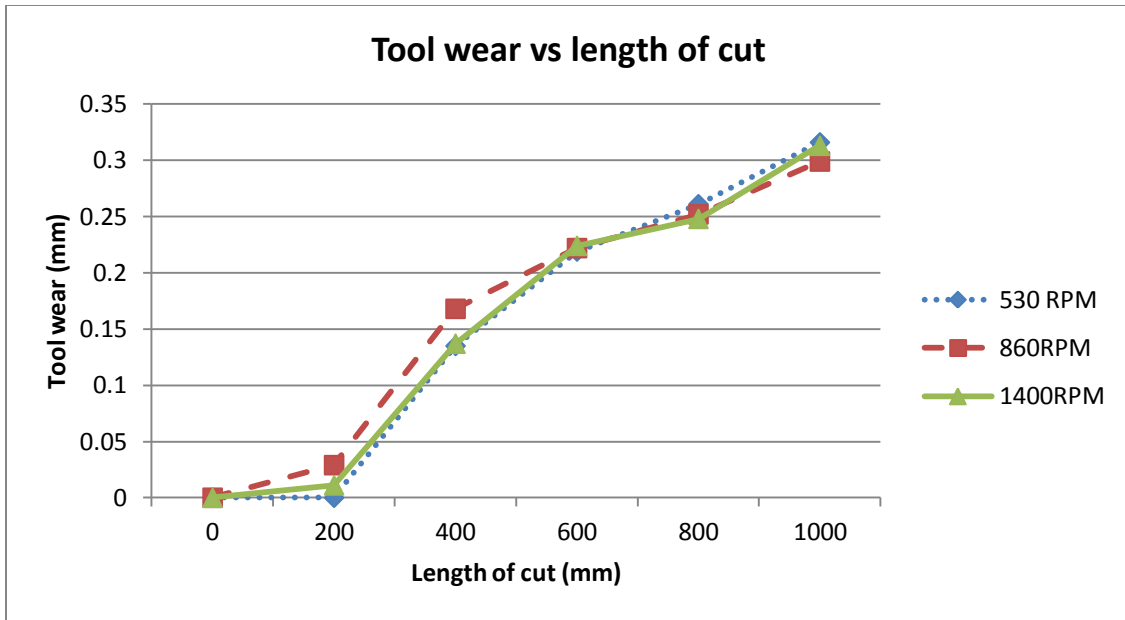


Figure: 4.20 Comparison of tool wear at 0.75mm DOC in electromagnet condition with different cutting speeds

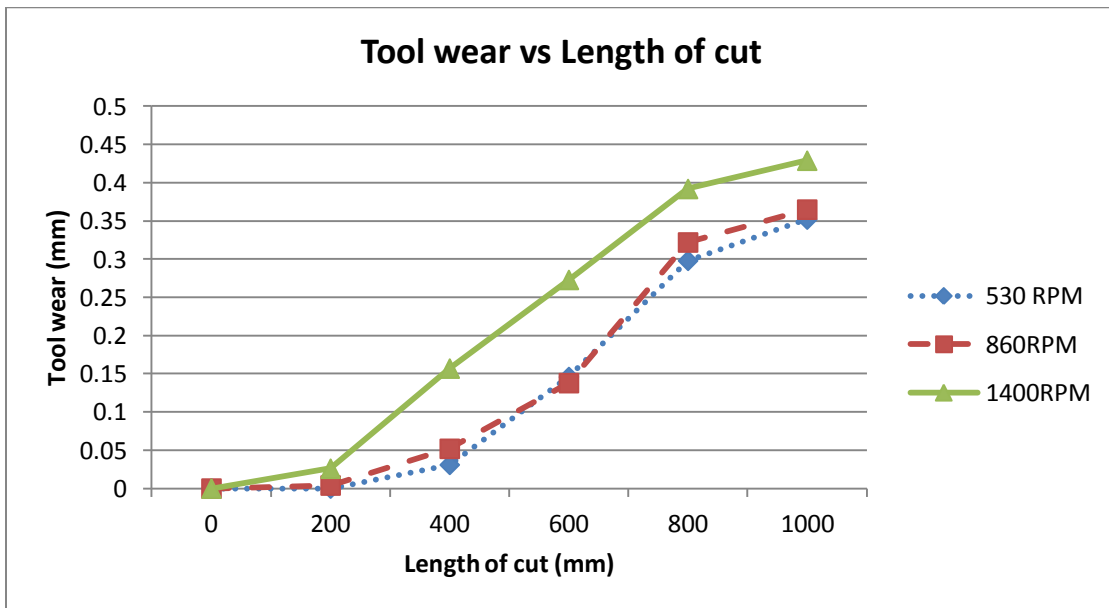


Figure: 4.21 Comparison of tool wear at 0.75mm DOC in permanent magnet condition with different cutting speeds

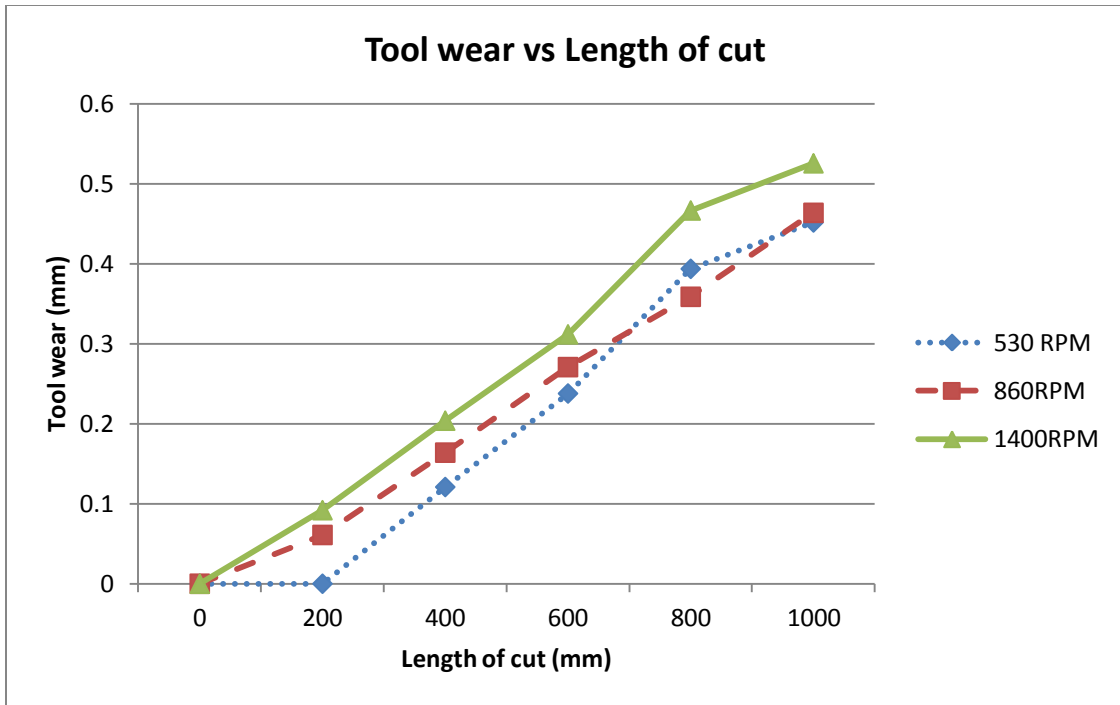


Figure: 4.22 Comparison of tool wear at 0.75mm DOC in without magnet condition with different cutting speeds

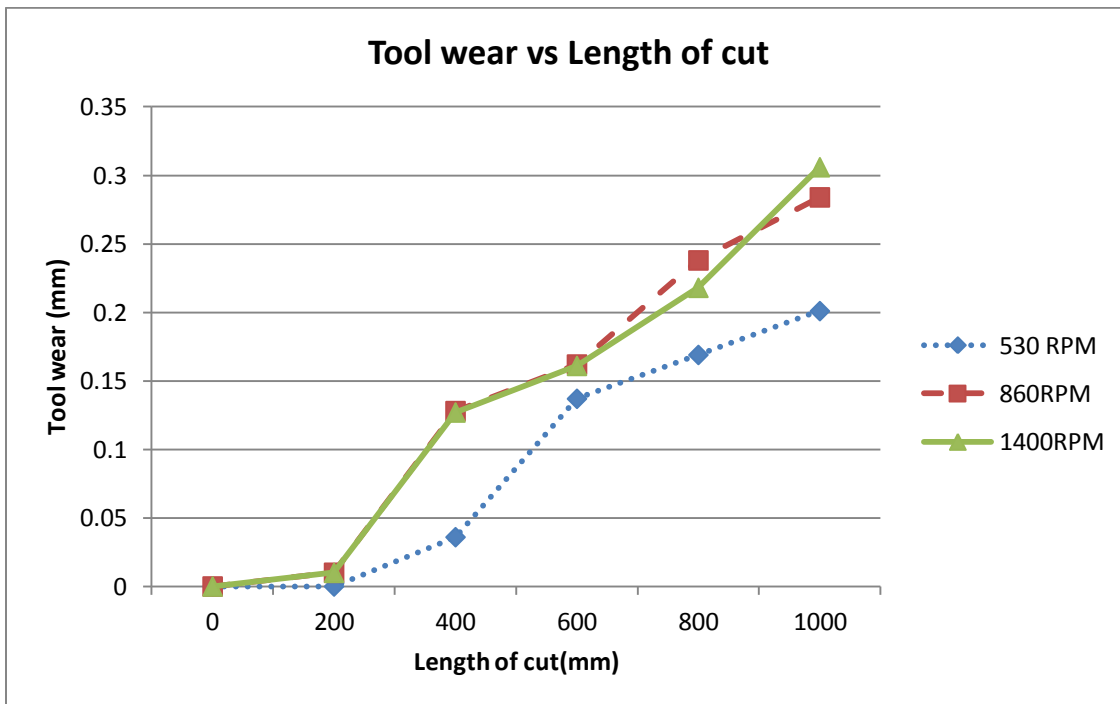


Figure: 4.23 Comparison of tool wears at 0.5mm DOC in electromagnet condition with different cutting speeds

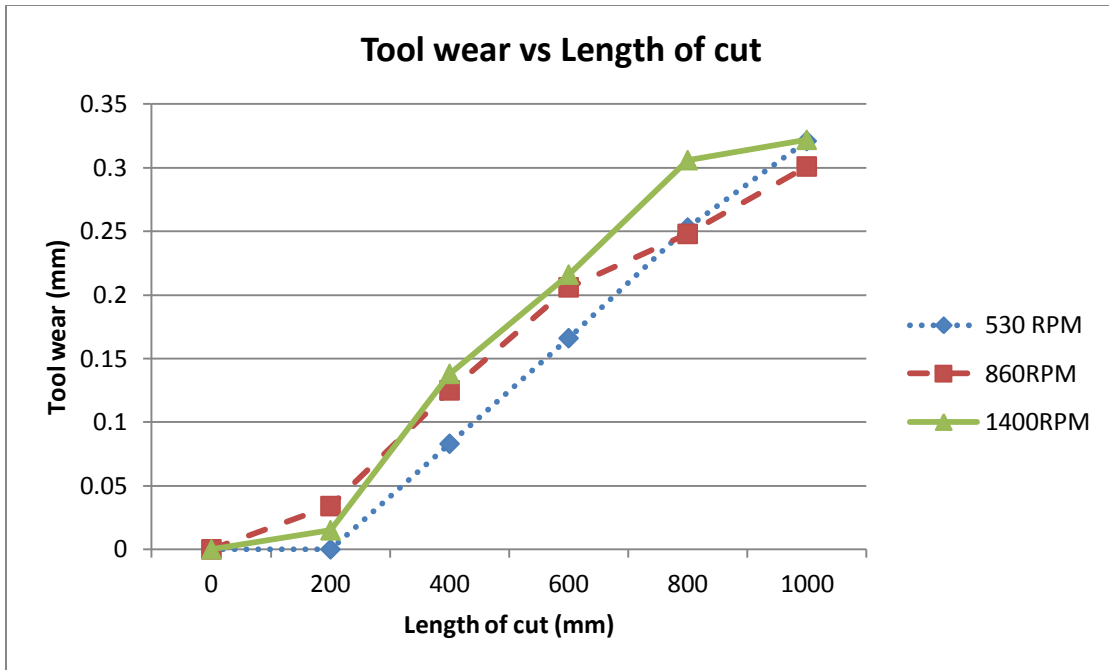


Figure: 4.24 Comparison of tool wears at 1.0mm DOC in electromagnet condition with different cutting speeds

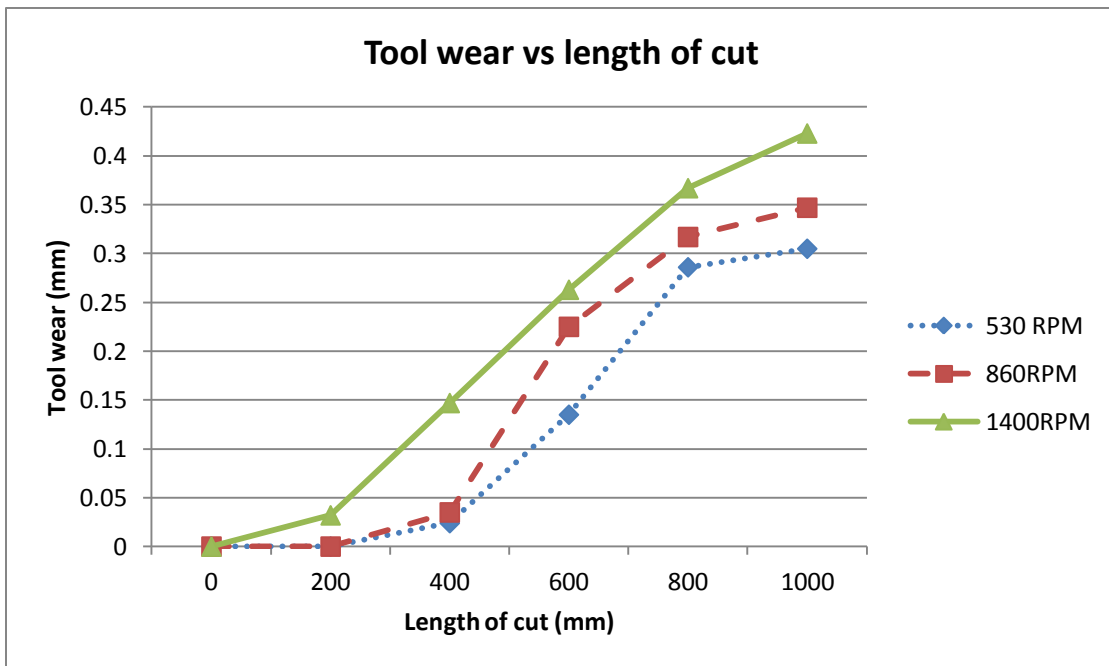


Figure: 4.25 Comparison of tool wears at 0.5mm DOC in permanent magnet condition with different cutting speeds

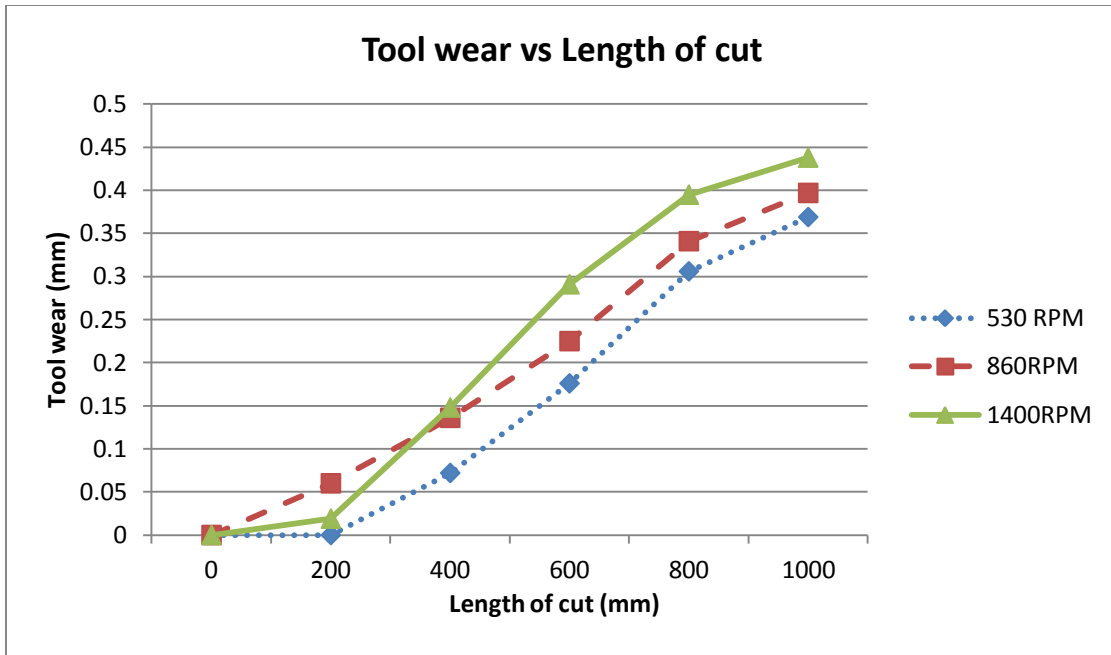


Figure: 4.26 Comparison of tool wears at 1.0mm DOC in permanent magnet condition with different cutting speeds

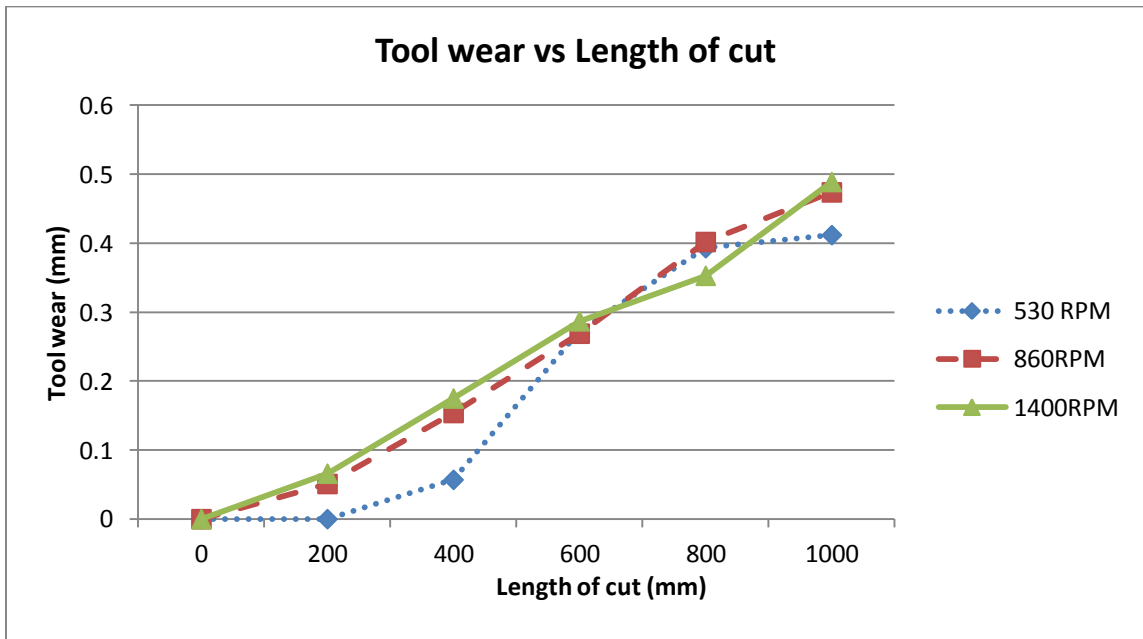


Figure: 4.27 Comparison of tool wears at 0.5mm DOC in without magnet condition with different cutting speeds

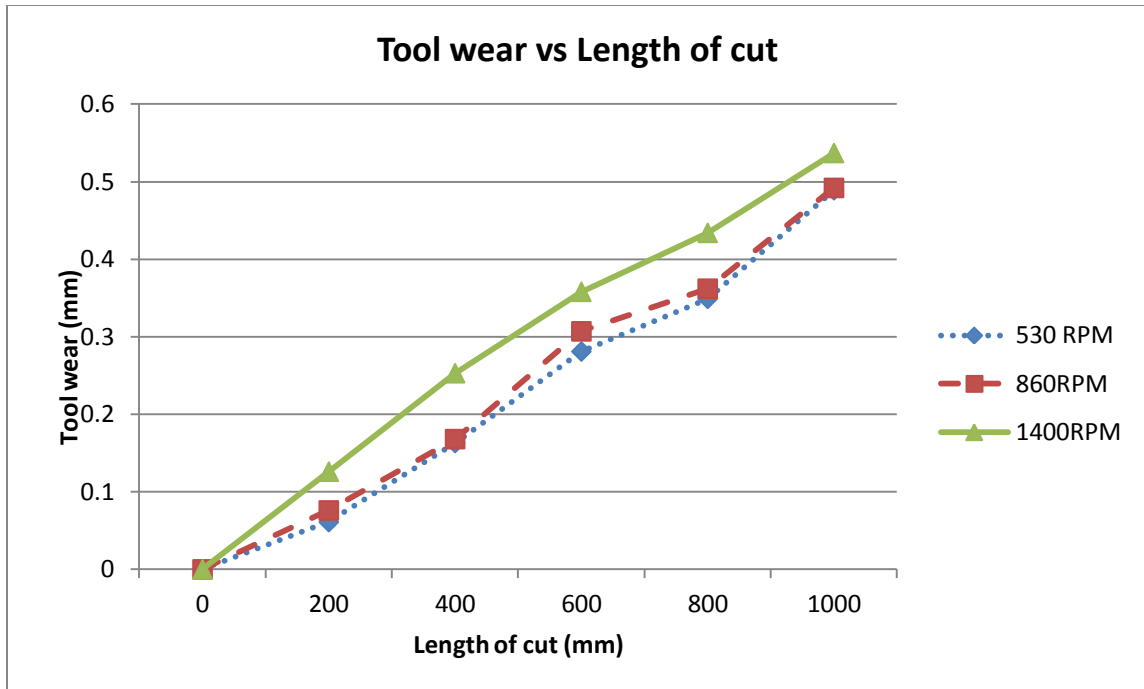


Figure: 4.28 Comparison of tool wears at 1.0mm DOC in without magnet condition with different cutting speeds

From the graphs (figure 4.20-4.28) it can be observed that with the increase of cutting speed the tool wear increases in all cases. This is because with the increase of cutting speed the cutting force and heat generation increase which result in greater tool wear. For electromagnetic condition tool wear is quite low at 0.5mm depth of cut. But in case of larger depth of cut the difference is reduced. In case of permanent magnet at 0.5mm depth of cut the tool wear show quite similar characteristics over 530RPM-860RPM range. As larger depth of cut this difference is increased. The overall value of tool wear in case of permanent magnet is larger compared to the electromagnetic condition. In case of without magnet condition at lower depth of cut and lower speed the tool wear is almost similar. With the increase of speed, the tool wear also increases. At larger depth of cut the difference between the values of tool wear at each cutting speed gradually increases.

In all the graphs some points may deviate from the ideal position. This may occur due to any error in the experimental setup or measurement. It is difficult to reproduce same experimental condition every time when the number of experiment is quite high. The accuracy of tool wear measurement also depends on the quality of the capture image. As tool wear occurs on the edge of insert it is very difficult to focus at the exact point of the maximum flank wear. Because of these reasons some points in the graphs may have dislocated. But as each experimental condition is compared against several numbers of other experimental conditions and the characteristic of each graphs is almost similar to the ideal cases the minor dislocation of some points have little effect on the overall result.

4.3 Effects of Magnetic Field on Surface Roughness

After cutting 1000mm at certain cutting speed and depth of cut the work piece was detached from the lathe and an image of the surface of the work piece was taken using the microscope. These images were then processed in MATLAB to calculate the average roughness value of the surface. From the sample pictures (fig 4.29 and 4.30) it is clearly visible that with the application of external magnetic field the surface characteristics changes.

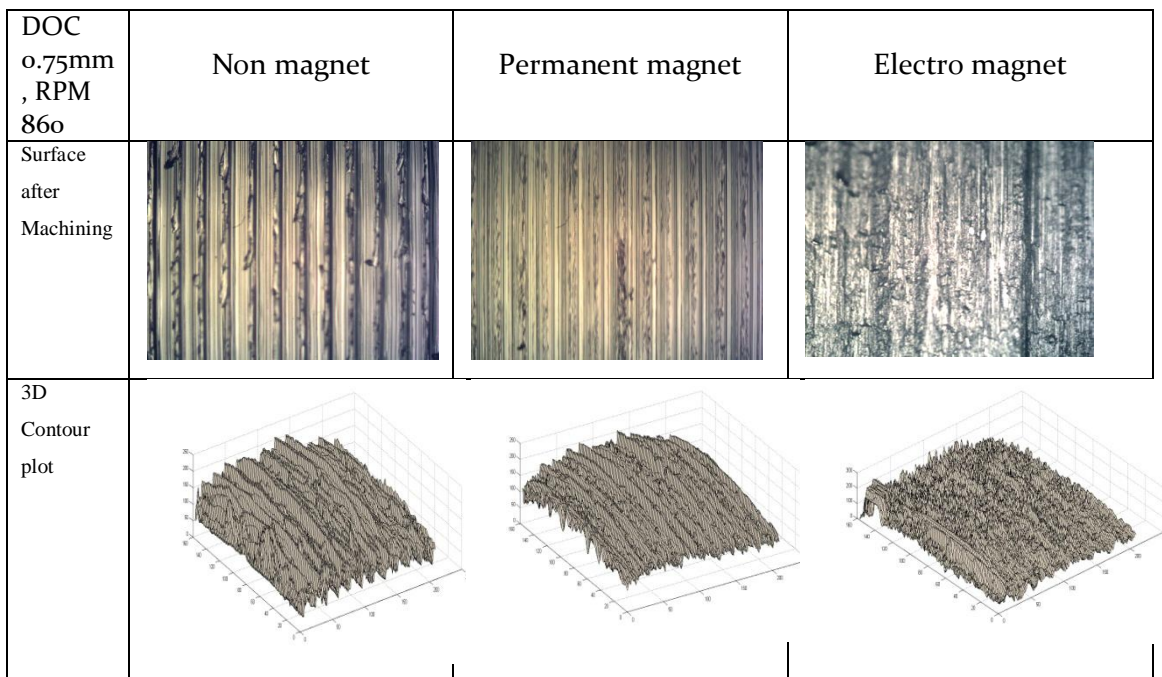


Figure: 4.29 Contour plot of the machined surface under different conditions

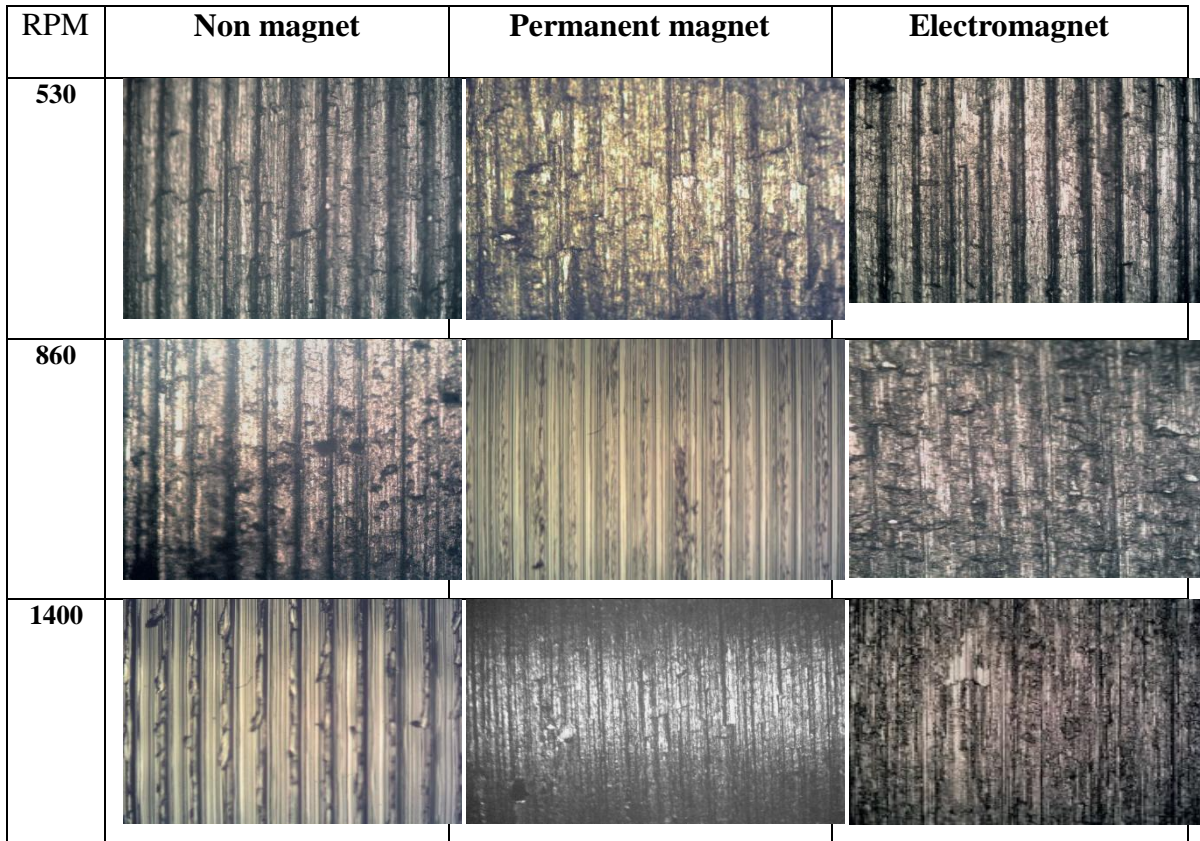


Fig 4.30 Sample photographs of surfaces of the work piece at different cutting speed at 0.5 Depth of cut after cutting 1000mm

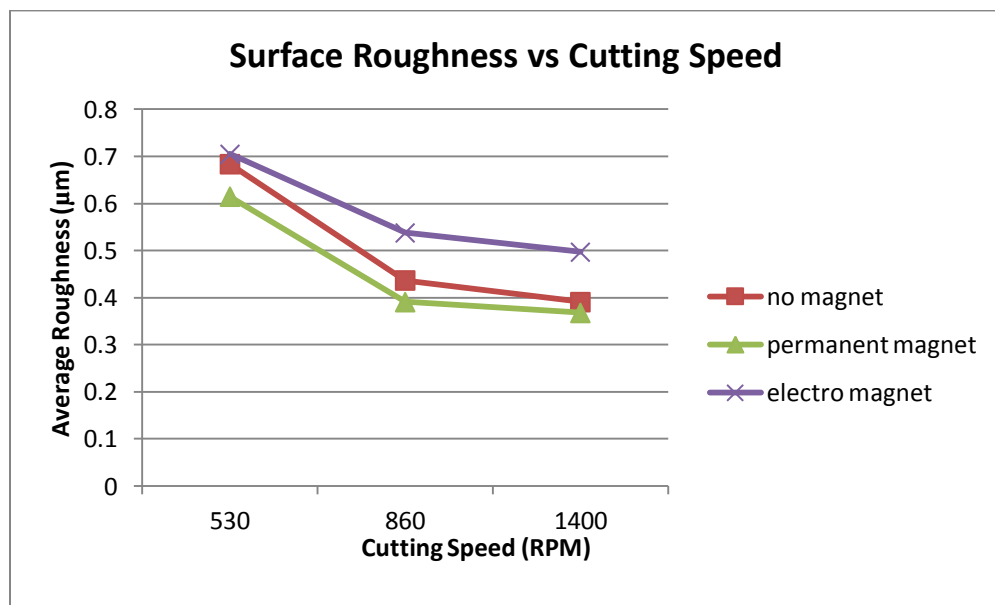


Figure: 4.31 Comparison of surface roughness at 0.5mm DOC and different cutting environment

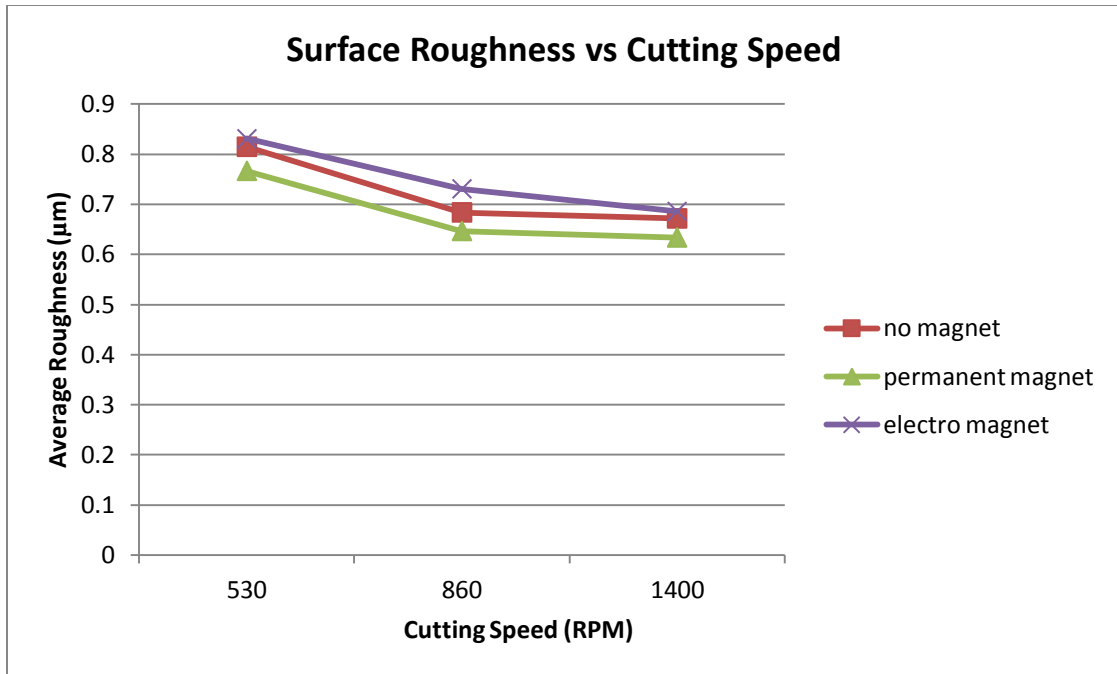


Figure: 4.32 Comparison of surface roughness at 0.75mm DOC and different cutting environment

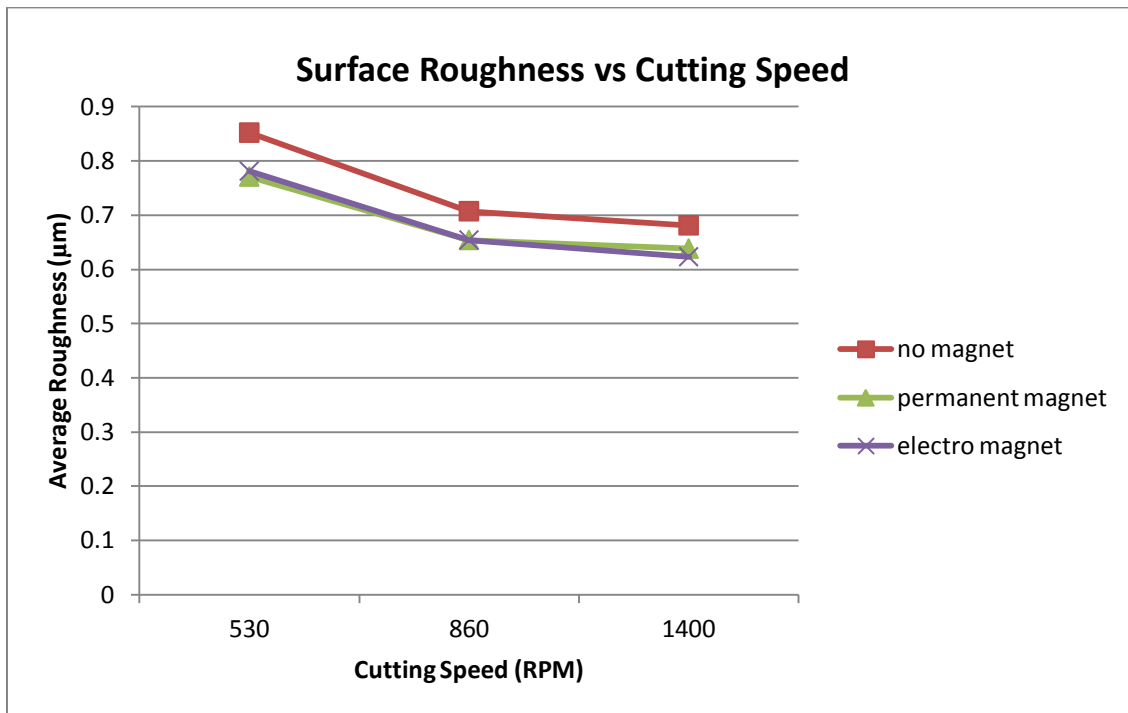


Figure: 4.33 Comparison of surface roughness at 1.0mm DOC and different cutting environment

From the charts a comparative idea about surface roughness at each cutting conditions in different cutting environment can be obtained. As shown in the figure surface quality is best in permanent magnet condition in all the cases. An interesting fact found in the experiment is that, at lower depth of cut (0.5mm and 0.75mm) the surface roughness in electromagnetic condition is higher than the other two conditions. But in 1.0mm depth of cut the roughness quality in electromagnetic condition significantly improves. This phenomenon can be explained by the formation of built up edge. In case of electromagnetic condition the flux density at the tip of insert is higher. This helps the accumulation of metal powder produced in the cutting action on the tip of insert. This powder forms a coating on the cutting tool which is known as built up edge. Because of high flux density the chance of built up edge formation is higher in electromagnetic condition. This built up edge scratches the surface of the work piece in lower cutting speed and depth of cut. At higher depth of cut the built up edge breaks away so the scratches on the work piece is reduced. As a result the surface quality is significantly improved in higher depth of cut in case of electromagnet.

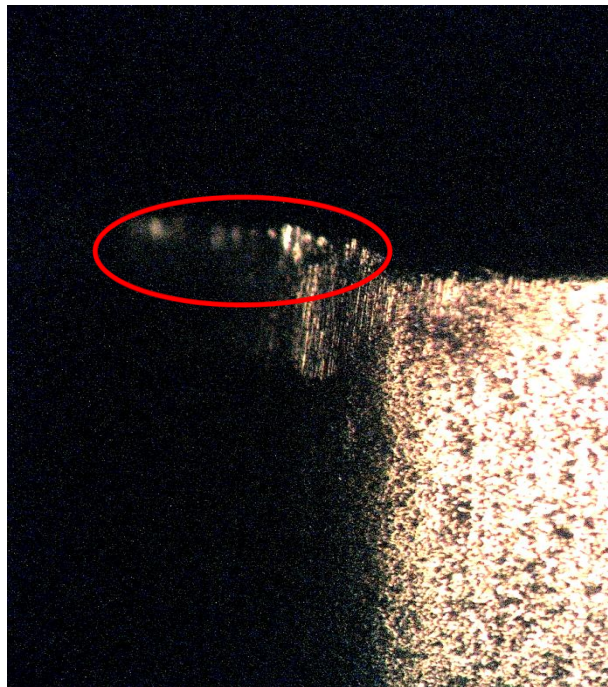


Figure: 4.34 A sample photograph of built up edge taken in electromagnetic cutting condition at 530 RPM and 0.5mm depth of cut

4.4 Effect of Magnetic Field on Cutting Temperature

When external magnetic field is applied, magnetic flux is generated both around tool and work piece. As the work piece rotates the fluxes cut each other and generate eddy current on the surface of the work piece. This eddy current results in higher temperature. The more the temperature increases the more the mechanical properties of the work piece changes. In this study the temperature after 200mm length of cut was measured in different magnetic conditions at different cutting speed and depth of cut.

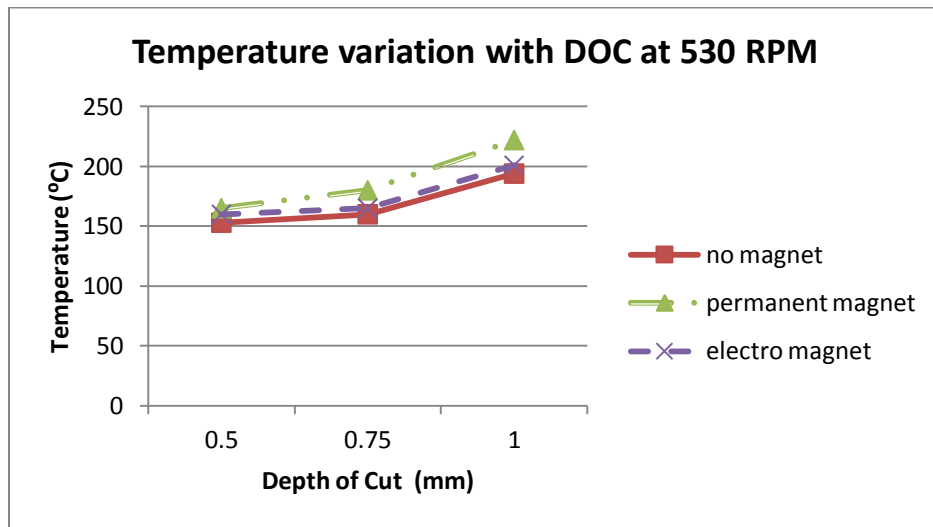


Figure: 4.35 Variation of temperature with depth of cut at 530rpm after 200mm cut

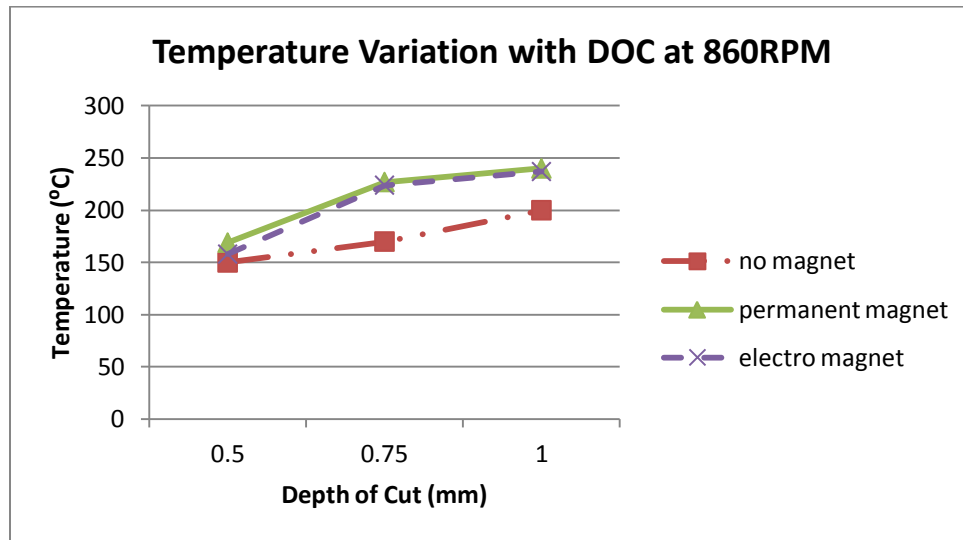


Figure: 4.36 Variation of temperature with depth of cut at 860rpm after 200 mm cut

From the graphs it can be easily observed that use of external magnetic field increases the cutting temperature. The temperature is relatively higher when permanent magnet is used. The temperature gradually increases with the increase of depth of cut. In case of electromagnetic condition the increase in cutting temperature is less in lower cutting speed but increases significantly at higher cutting speed. For investigating the change of cutting temperature with respect to cutting speed the following graphs were generated:

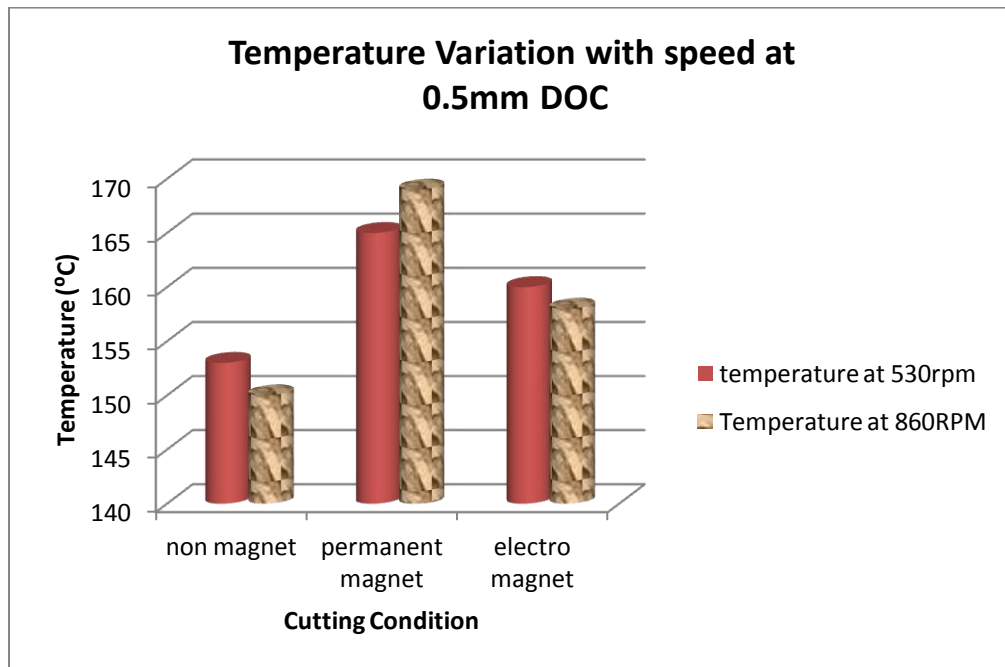


Figure: 4.37 Variation of temperature with depth of cut at 0.5mm DOC after 200mm cut

In all cases the cutting temperature increases with the increase of cutting speed. However the graphs show that the increase in cutting temperature is higher for permanent magnet when depths of cut were 0.5mm and 0.75 mm. When the depth of cut was increased to 1.0 mm the highest temperature was recorded for electromagnet condition.

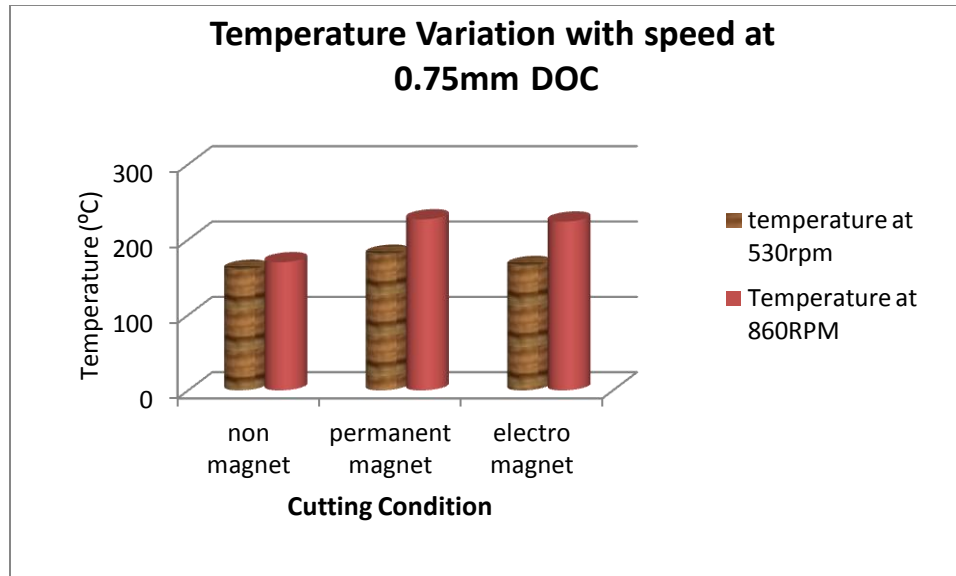


Figure: 4.38 Variation of temperature with depth of cut at 0.75mm DOC after 200 mm cut

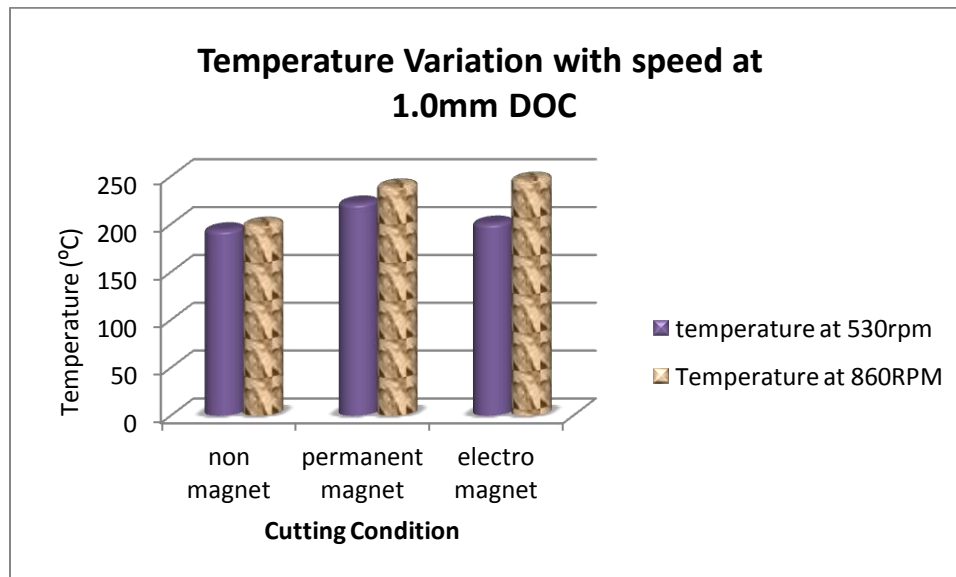


Figure: 4.39 Variation of temperature with depth of cut at 1.0mm DOC after 200 mm cut

The increase in temperature results in softening of the surface of the work piece. The more the temperature the more softening effect will occur. This phenomena leads to decrease in tool wear, cutting force and improvement of surface quality in case of magnetic cutting.

4.5 Effect of Magnetic Field on Chip Behaviour

After cutting 1000mm with an insert the chip for each cutting condition were collected for analysis. The characteristics of chip produced in non magnetic, permanent magnetic and electromagnetic conditions were then compared to study chip behavior in each case. Mainly the continuity, tooth formation and shrinkage coefficient of chip were analyzed for comparison.

4.5.1 Continuity of chip

Chip collected in each cutting environment showed different continuity. Chip produced in non magnetic condition were generally discontinuous and loosely packed. Whereas the chip produced in electromagnetic cutting were continuous and very closely packed. For permanent magnet the length of the chip was moderate.


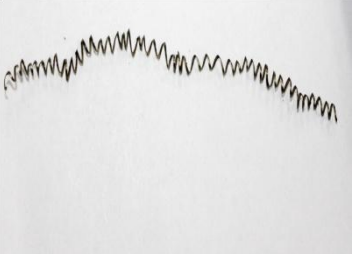
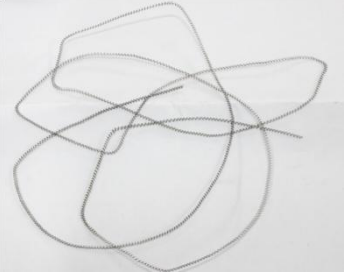
Non magnetic condition	Permanent magnet condition	Electromagnetic condition
		
Very short and discontinuous chip	Medium length chip	Very long and continuous chip

Figure: 4.40 Photograph of continuity of chip at different magnetic conditions

4.5.2 Tooth formation

Figure 4.21 below shows a schematic view of the chip showing where the chips were sectioned (along the line A-A) to be observed under the microscope. This sectioning

is done in order to observe more clearly the chip serration. The lengthwise cross-section view of the chips under optical microscope is shown in Figure 4.21.

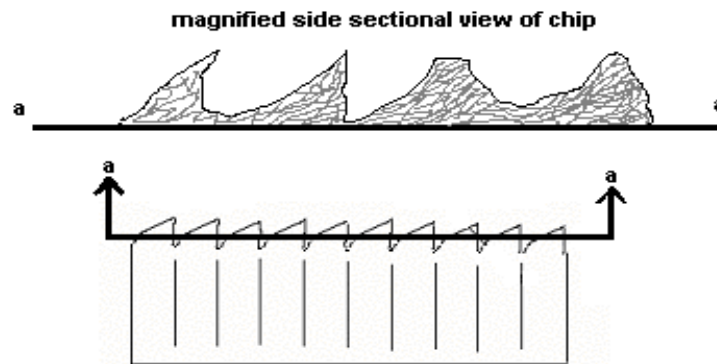


Figure: 4.41 Section of chip formed at different cutting conditions [Patwari et. el. 2010]


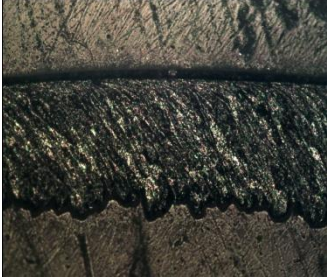
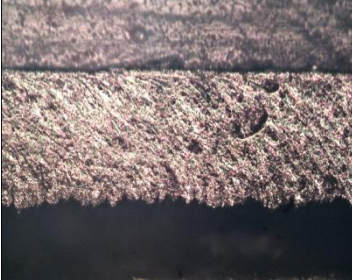
Non magnetic condition	Permanent magnet condition	Electromagnetic condition
		

Figure: 4.42 Cross section view of chip formed at different cutting conditions obtained at 530 rpm and 0.5mm DOC

From Fig 4.22 it is clearly visible that the tooth of serrated chip is larger in case of non magnetic cutting. The size decreases from permanent magnet to electromagnet. This phenomenon is a clear indication of change in vibration characteristic of the system in different condition. The enlarged view of the teeth in different conditions is given in fig 4.23.

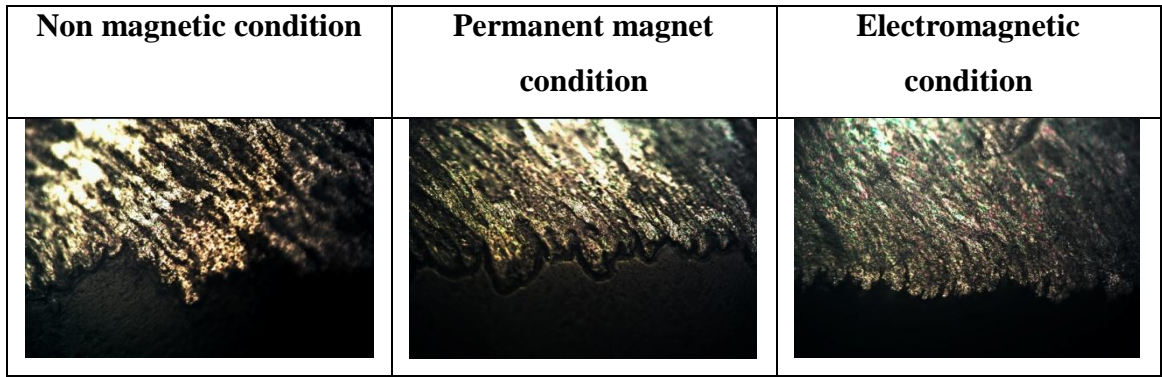


Figure: 4.43 Enlarged view of tooth of chip formed at different cutting conditions obtained at 530 rpm and 0.5mm DOC

4.5.3 Shrinkage Co efficient

Finally the shrinkage co efficient of chip was calculated. First the circumference of the work piece was measured. This indicated the theoretical length of chip after one revolution. Next the actual length of the chip was measured. Finally the chip shrinkage co efficient, K was determined using the following formula:

$$K = \frac{\text{Theoretical (uncut) length of chip}}{\text{Actual length of chip}}$$

After the measurement of actual and theoretical length for each case the following data were found:

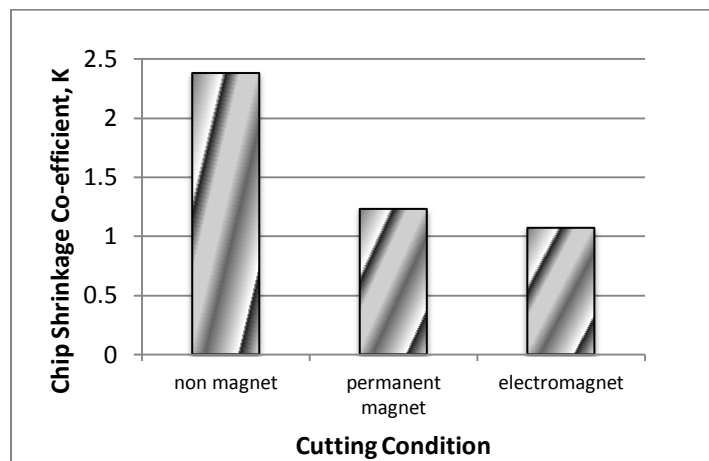


Figure: 4.44 Change of shrinkage co efficient at different cutting conditions

4.5.4 Colour of Chip

It was observed that the colour of the chip produced in different cutting conditions were different. This change of colour is due to the variation of temperature at different cutting environment. In non magnetic cutting the temperature was less, so the chip retained the original metallic colour. With the increase of temperature in permanent magnet condition the colour of the chip turned golden whereas for electromagnet condition the chip were severely affected by the higher temperature and became violet colour.




Non magnetic condition	Permanent magnet condition	Electromagnetic condition
		

Figure: 4.45 Photograph of different colour of chip at different conditions

4.6 Effect of Magnetic field on Cutting Force

The strain in the tool holder under different cutting conditions in different cutting speeds were recorded and then plotted. The value of the strain was measured in micro strain at an interval of thirty seconds. Five readings were taken for each of the experimental condition and from that the average strain was obtained. The depth of cut was kept constant and the RPM of the machine was changed. Later data were taken at different depth of cut while keeping the cutting speed constant. For obtaining the value of tangential cutting force from the strain of the tool holder the Young's formula for rigidity

of material was used. In that formula the value of the Young's modulus was taken as 210 GPa based on the material of the tool holder. The area was taken as the cross section of the tool holder (2cm X 2cm). So a relationship between the force and the strain was found. This relationship shows proportionality between the tangential cutting force and the strain of the tool holder. Finally after obtaining the values of the force graphs were plotted to compare the result at different experimental conditions.

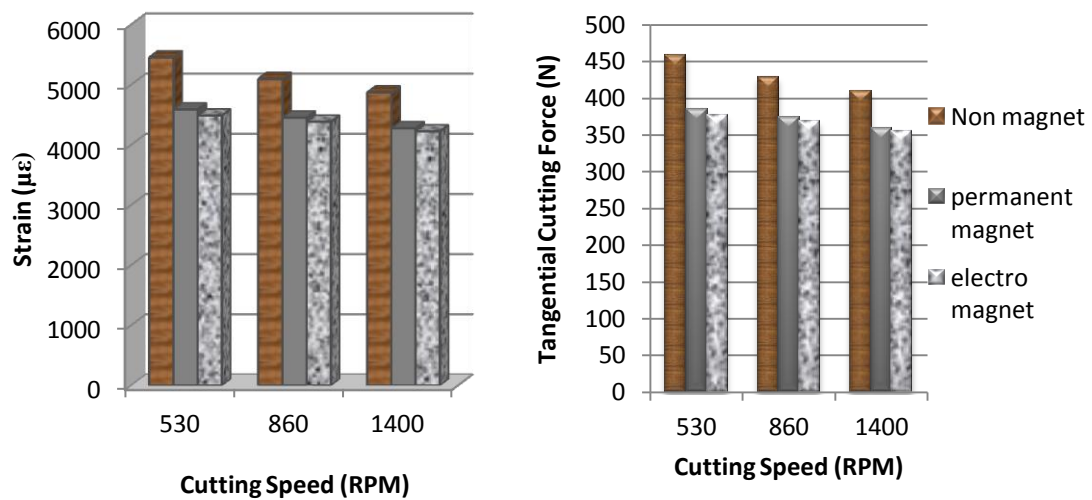


Figure: 4.46 Change of strain of tool holder and tangential cutting force with respect to Cutting Speed

From the graph it is clearly visible that tangential cutting force decreases as magnetic field is applied to the cutting mechanism. Although there is no significant change in the cutting force in between permanent magnet and electro magnet cutting conditions, but the reduction of cutting force after applying the magnetic field is important.

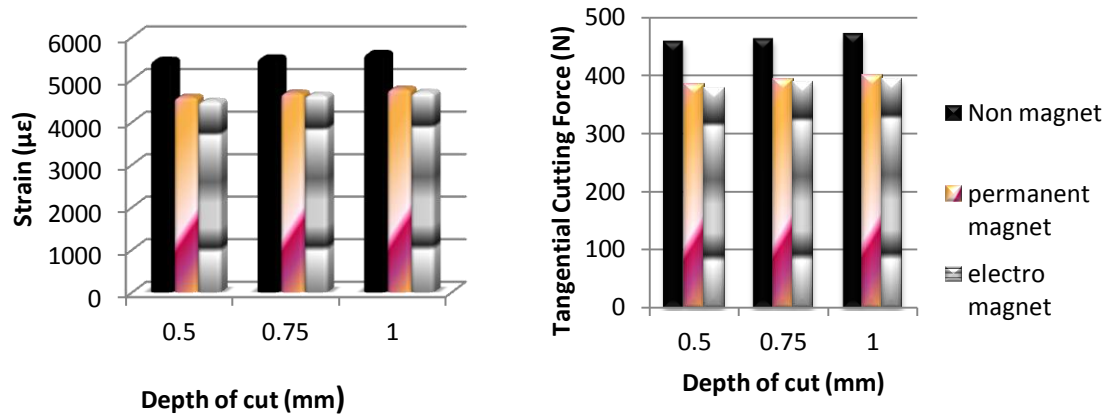


Figure: 4.47 Change of strain of tool holder and tangential cutting force with respect to depth of cut

From the charts the characteristics of change of strain on tool holder and tangential cutting force have been observed. It is observed that when the depth of cut was kept constant the cutting force gradually decreased with the increase in cutting speed. Whereas when the cutting speed was kept constant, the cutting force increased with the increase of depth of cut. This trend was found in all three experimental (non magnet, permanent magnet and electro magnet) conditions. But the result clearly indicates that there has been a decrease in cutting force when the external magnetic (for both permanent magnet and electromagnet) field is applied to the system.

Conclusions and Recommendations

5.1 Conclusions

From this study the following conclusions can be drawn:

1. It is observed that the application of magnetic fields has significant effect in improving the tool life of the WC Coated carbide insert used in turning. Trends can also be seen where increasing magnetic field strengths correspond to better improvements in tool life. On an average 15% - 20% improvement of tool life in case of permanent magnet and 20% -25% improvement of tool life in case of electromagnet.
2. The values of surface roughness are lower in case of permanent magnet cutting condition. 15% - 20% reduction in average surface roughness when permanent magnetic field is applied. Electro magnet shows similar improvement at higher speed and depth of cut.
3. With the application of external magnetic field a rise in cutting temperature has been observed. Around 30-35 °C increase of cutting temperature with application of permanent magnet and 20-30 °C increase in case of electromagnet .
4. There has been a significant change of cutting force with application of external magnetic field. The cutting force decreases around 15% when permanent magnetic field is applied. For electromagnetic field the decrease is around 20%.
5. Improvement of chip serration condition and change in visual characteristics like color, continuity, chip shrinkage coefficient also occur with the application of external magnetic field.
6. Establishment of an innovative DIP technique to measure tool flank wear and comparison of this process with the optical microscope measurement technique. This innovative DIP technique can be successfully used in measurement of tool flank wear in turning operation.

The results of this study present the effect of external magnetic field on different machinability parameters. The results are obtained for specific range of machining parameters and specific experimental arrangement. Beyond this limit different relationship among the variables can be obtained. This study concentrates on the effect of magnetic field on tool wear, surface roughness, cutting temperature, cutting force and chip morphology in low and medium range of cutting force at certain depths of cut and experimental conditions.

5.2 Recommendations

1. Experiments with Different Materials

The experiment conducted in this project used only mild steel, a ferrous and conducting material. Experiments using other materials that is conducting and non-ferrous, or non-conducting and ferrous, can be done to gain further understanding in the mechanism behind the reduction of tool wear by the application of magnetic field.

2. Practical Usage of External Magnetic Fields

Since magnetic fields are capable of improving tool life, there is great potential in using it to reduce costs for the manufacturing industry. Add-ons can be designed to provide external magnetic fields on currently existing machining equipments. New machinery can also be designed to be fitted with magnetic devices to apply an external magnetic field on the work piece and/or tool to improve tool wear. However, having an additional magnetic device would subsequently increase energy usage. Thus, it should be evaluated first if the improvements in tool life can justify the increase in operating costs. Also, meticulous design is required to keep the magnetic field isolated from the rest of the machinery to prevent any possible interference with its internal workings.

3. Experiments with different feed rate

Feed is an important machining parameter. Due to the limitation of the machine feed was kept constant in this study. But the effect of change of feed on different magnetic conditions can also be observed by carrying out similar experiments at different feed.

4. Experiments with different magnetic conditions

This study only included one setup for permanent magnet and one setup for electro magnet. Experiments can be done using different magnetic field strength and configuration. This will help to find a better design for improving the desired result. Also this will help to understand the cutting mechanism in magnetic environment better.

5. Development of mathematical model

Based on this study, a mathematical model can be generated to predict the tool wear and surface roughness in any cutting condition in the range. To increase the accuracy of the model new sets of experiments can be introduced. An optimization model will provide the best machining parameters for obtaining any desired result.

References

1. Hastings, W.F., and Oxley, P.L.B, "Predicting tool life from fundamental work material properties and cutting conditions", *Annals of the CIRP*, pp. 33–38(1976).
2. Opitz, H. and Konig, W., "On the wear of cutting tools", *Proceedings of the 8th International MTDR Conference*, pp. 173–190(1967).
3. Wright, P.K, "Correlation of tool wear mechanisms with slip line fields for cutting in: K. Ludema (Ed.)", *Wear of Materials, ASME*, pp. 482–488(1981).
4. Shaw, M.C., "*Metal Cutting Principles*", Clarendon Press, Oxford (1984).
5. Kurimoto, T. and Barrow, G., "The influence of aqueous fluids on the wear characteristics and life of carbide cutting tools", *Annals of the CIRP*, pp. 19– 25 (1982).
6. Usui, E., "Progress of predictive theories in metal cutting", *International Journal of Japan Society of Mechanical Engineers*, Vol. 31 (2), pp. 363–369 (1998).
7. Taylor, F.W., "On the art of metal cutting", *Trans. ASME*, Vol. 28, pp. 31– 350(1907).
8. Childs, T.H.C., Maekawa, K., Obikawa, T. and Yamane, Y., "*Metal Machining: Theory and Applications*", Arnold Publications, 2000.
9. Oxley, P.L.B., "*The Mechanics of Machining: An Analytical Approach to Assessing Machinability*", Ellis Horwood, Chichester, (1989).
10. Trent, E.M. and Wright, P.K, "*Metal Cutting*", 4th Edition, Butterworth-Heinemann, Boston, (2000).
11. P. Mathew, "Use of predicted cutting temperatures in determining tool performance", *International Journal on Machine Tools and Manufacture*, Vol. 29 (4), pp.481–497(1989).
12. Mansori, M. El. and Klamecki, B.E., "Magnetic Field Effects in Machining Processes and on Manufactured Part Mechanical Characteristic", *Journal of Manufacturing Science and Engineering*, Vol. 128, pp. 137 – 145 (2006).
13. Mansori, M.El., Pierron, F. and Paulmier, D., "Reduction of tool wear in metal cutting using external electromotive sources", *Surface and Coatings Technology*, Vol. 163 - 164, pp. 472-477(2003).
14. Kalpakjian, S. and Schmid, S.R., "*Manufacturing Processes for Engineering Materials*", 5th Edition, Pearson Education Inc., pp. 440-447(2009).
15. Ginta, T.L, Amin, A.K.M.N. and Patwari, A.U., "Tool Wear Morphology And Chip Segmentation In End Milling Titanium Alloy Ti-6AL-4V", *Proceedings of CUTSE Int. Conference*, (2008).

16. Matsumoto, Y., Hashimoto, F. and Lahoti, G., "Surface Integrity Generated By Precision Hard Turning", *Annals of the CIRP*, Vol. 48(1), pp. 59-62 (1999).
17. Thiele, J. D., and Melkote, S. N., "Effect Of Cutting Edge Geometry And Work piece Hardness On Surface Generation In The Finish Hard Turning Of AISI 52100 Steel," *Journal of Materials Processing Technology*, Vol. 94, pp. 216-226 (1999).
18. Dawson, T. G. and Kurfess, T. R., "Machining Hardened Steel With Ceramic-Coated And Uncoated CBN Cutting Tools", Technical Paper -Society of Manufacturing Engineers, MR 02-156, pp. 1-7 (2002).
19. Özel, T., Hsu, T. K. and Zeren, E., "Effects Of Cutting Edge Geometry, Workpiece Hardness, Feed Rate And Cutting Speed On Surface Roughness And Forces In Finish Turning Of Hardened AISI H13 Steel," *International Journal of Advanced Manufacturing Technology*, (2004).
20. Braghini, A. Jr., and Coelho, R.T, "An Investigation Of The Wear Mechanisms Of Polycrystalline Cubic Boron Nitride (PCBN) Tools When End Milling Hardened Steels At Low/Medium Cutting Speeds," *International Journal on Advanced Manufacturing Technology*, Vol. 17, pp. 244-257 (2001).
21. Kumar, S., Durai, A.R. and Sornakumar, A. "The Effect Of Tool Wear On Tool Life Of Alumina-Based Ceramic Cutting Tools While Machining Hardened Martensitic Stainless Steel," *Journal of Materials Processing Technology*, Vol. 173, pp. 151-156 (2006).
22. Ghani, J.A., Choudhury, I.A. and Hassan, H.H., "Application of taguchi method in the optimization of end milling parameters," *Journal of Materials Processing Technology*, Vol. 145, pp. 84-92 (2004).
23. Amin, A. K. M. N., Hafiz, A. M. K., Lajis, M. A. and Patwari, A. U., "Prediction of tool life and experimental investigation during hot milling of AISI H13 tool steel," *Advanced Materials Research*, Vol. 83-86, pp. 190-197 (2010).
24. Takeyama, H. And Murata, R., "Basic Investigation of Tool Wear", *Trans.ASME, J. Eng. Ind.* Vol. 85, pp. 33-38 (1963).
25. Arsecularatne, J.A., "On prediction of tool life and tool deformation conditions in machining with restricted contact tools", *International Journal of Machine Tools and Manufacture*, Vol. 43, pp. 657-669 (2003).
26. Arsecularatne, J.A., "Prediction of tool life for restricted contact and grooved tools based on equivalent feed", *International Journal of Machine Tools and Manufacture*, Vol. 44, pp. 1271-1282 (2004).

27. Kitagawa, T., Maekawa, K., Shirakashi, T. and Usui, E., “Analytical prediction of flank wear of carbide tools in turning plain carbon steels (part 1)”, *Japanese Society of Precision Engineering*, Vol. 22 (4), pp. 263–269 (1988).
28. Iwata, K., Ashara, J. and Okushima, K., “On the mechanism of built-up edge formation in cutting”, *Annals of the CIRP*, Vol.19 (2), pp. 323–330 (1971).
29. Lin, W. S., Lee B. Y., Wu C. L., “Modeling the surface roughness and cutting force for turning”, *Journal of Materials Processing Technology*, Vol. 108, pp. 286-293(2001).
30. Lee, S. S. and Chen, J. C., “Online surface roughness recognition system using artificial neural networks system in turning operations”, *International Journal of Advanced Manufacturing Technology*, Vol. 22, pp. 498–509 (2003).
31. Kirby, E. D., Zhang, Z. and Chen, J. C., “Development of An Accelerometer based surface roughness Prediction System in Turning Operation Using Multiple Regression Techniques”, *Journal of Industrial Technology*, Vol. 20 (4), pp. 1-8 (2004).
32. Özel, T. and Karpuz, Y., “Predictive modeling of surface roughness and tool wear in hard turning using regression and neural networks”, *International Journal of Machine Tools and Manufacture*, Vol.45, pp. 467–479 (2005).
33. Singh, H. and Kumar, P., “Optimizing Feed Force for Turned Parts through the Taguchi Technique”, *Sadhana*, Vol. 31(6), pp. 671–681(2006).
34. Ahmed, S. G., “Development of a Prediction Model for Surface Roughness in Finish Turning of Aluminium”, *Sudan Engineering Society Journal*, Vol. 52 (45), pp. 1-5 (2006).
35. Abbari, N. R. and Dixit, U. S., “A knowledge-based system for the prediction of surface roughness in turning process”, *Robotics and Computer-Integrated Manufacturing*, Vol. 22, pp. 363–372 (2006).
36. Zhong, Z. W., Khoo, L. P. and Han, S. T., “Prediction of surface roughness of turned surfaces using neural networks”, *International Journal of Advance Manufacturing Technology*, Vol. 28, pp. 688–693(2006).
37. Mahmoud, E. A. E. and Abdelkarim, H. A., “Optimum Cutting Parameters in Turning Operations using HSS Cutting Tool with 45° Approach Angle”, *Sudan Engineering Society Journal*, Vol. 53 (48), pp. 25-30 (2006).
38. Doniavi, A., Eskanderzade, M. and Tahmasebian, M., “Empirical Modeling of Surface Roughness in Turning Process of 1060 steel using Factorial Design Methodology”, *Journal of Applied Sciences*, Vol. 7 (17), pp. 2509-2513 (2007).

39. Kassab, S. Y. and Khoshnaw, Y. K., "The Effect of Cutting Tool Vibration on Surface Roughness of Work piece in Dry Turning Operation", *Engineering and Technology*, Vol. 25(7), pp. 879-889 (2007).
40. Al-Ahmari, A. M. A., "Predictive machinability models for a selected hard material in turning operations", *Journal of Materials Processing Technology*, Vol. 190, pp. 305–311(2007).
41. Natarajan, U., Arun, P. and Periasamy, V. M., "On-line Tool Wear Monitoring in Turning by Hidden Markov Model (HMM)", *Institution of Engineers (India) Journal (PR)*, Vol. 87, pp. 31-35 (2007).
42. Sahoo, P., Barman, T. K. and Routara, B. C., "Taguchi based practical dimension modeling and optimization in CNC turning", *Advance in Production Engineering and Management*, Vol. 3(4), pp. 205-217 (2008).
43. Wang, M. Y. and Lan, T. S., "Parametric Optimization on Multi-Objective Precision Turning Using Grey Relational Analysis". *Information Technology Journal*, Vol. 7, pp.1072-1076 (2008).
44. Thamma, R., (2008), "Comparison between Multiple Regression Models to Study Effect of Turning Parameters on the Surface Roughness", *Proceedings of the IJME International Conference*, ISBN 978-1-60643-379-9, Paper 133, ENG 103, pp. 1-12(2008).
45. Biswas, C. K., Chawla, B. S., Das N. S., Srinivas, E. R. K. N. K., "Tool Wear Prediction using Neuro-Fuzzy System", *Institution of Engineers (India) Journal (PR)*, Vol. 89, pp. 42-46 (2008).
46. Bagchi, P.K., Ghosh, A., "Effect of magnetization on wear characteristics of cutting tools", *Institution of Engineers (India) Journal (PR)*, Vol. 50, pp. 264-269 (1970).
47. Bagchi, P.K., Ghosh, A., "Mechanism of a cutting tool in presence of a magnetic field", *Indian Journal of Technology*, Vol. 9, pp. 165-168 (1971).
48. Chakrabarti, S., "Why Magnetic Cutting Tool Has Greater Life- Probable Cause", ", *Institution of Engineers (India) Journal (PR)*, Vol. 52, pp. 118-123 (1971).
49. Pal, D.K. and Gupta, N.C, "some experimental studies on drill wear in the presence of alternating magnetic field", *Institution of Engineers (India) Journal (PR)*, Vol.53, pp. 195-200 (1973).
50. M.K. Muju, A. Ghosh, "Effect of magnetic field on diffusive wear of cutting tool", *Wear*, Vol. 58, pp. 137-145 (1980).

51. Kang, T. Y., "Effect of Magnetic Field on Tool life in Milling", Thesis- submitted to National University of Singapore (2006/2007).
52. Patwari, A. U., Arif, M. D. and Mahmood, M.N., "An innovative application of Digital Image Processing to Analyze Tool wear in Turning Operation", *Submitted to INRIT 2012*, Thailand (2012).
53. Patwari, A.U., Arif, M. D., Chowdhury, S. I. And Chowdhury, N.A., "Identification of Machined surfaces using Digital Image processing" *International Journal of Engineering*, Issue X (2012), Vol. 1, pp. 213-218 (2012).
54. User Guide of Digital Strain Display, Model- SM 1010, TQ Education and Training Ltd. (2007).

APPENDIX

Appendix A: Guide to Wear

Parameter	Description	Formula
R_a, R_{aa}, R_{yui}	Arithmetic average of absolute values	$R_a = \frac{1}{n} \sum_{i=1}^n y_i $
R_q, R_{RMS}	Root mean squared	$R_q = \sqrt{\frac{1}{n} \sum_{i=1}^n y_i^2}$
R_v	Maximum valley depth	$R_v = \min_i y_i$
R_p	Maximum peak height	$R_p = \max_i y_i$
R_t	Maximum Height of the Profile	$R_t = R_p - R_v$
R_{sk}	Skew ness	$R_{sk} = \frac{1}{nR_q^3} \sum_{i=1}^n y_i^3$
R_{ku}	Kurtosis	$R_{ku} = \frac{1}{nR_q^4} \sum_{i=1}^n y_i^4$
R_{zDIN}, R_{tm}	average distance between the highest peak and lowest valley in each sampling length, ASME Y14.36M - 1996 Surface Texture Symbols	$R_{zDIN} = \frac{1}{s} \sum_{i=1}^s R_{zi}$, where s is the number of sampling lengths, and R_{zi} is R_t for the i^{th} sampling length.
R_{zJIS}	Japanese Industrial Standard for R_z , based on the five highest peaks and lowest valleys over the entire sampling length.	$R_{zJIS} = \frac{1}{5} \sum_{i=1}^5 R_{pi} - R_{vi}$, where R_{pi} & R_{vi} are the i^{th} highest peak, and lowest valley respectively.

Various surface roughness parameters and their formulae [Courtesy: www.armg.com, 2011]

Appendix B: Data Tables

Length of cut	Without magnet	With permanent magnet	With electro magnet
0	0	0	0
200	0	0	0
400	0.057	0.031	0.036
600	0.323	0.146	0.137
800	0.393	0.298	0.169
1000	0.412	0.352	0.201

Data Table for comparison of tool wear at 530rpm and depth of cut 0.5 mm

Length of cut (mm)	Without magnet	With permanent magnet	With electro magnet
0	0	0	0
200	0	0	0
400	0.121	0.024	0.035
600	0.238	0.135	0.129
800	0.434	0.286	0.261
1000	0.452	0.305	0.316

Data Table for comparison of tool wear at 5300rpm and depth of cut 0.75 mm

Length of cut (mm)	Without magnet	With permanent magnet	With electro magnet
0	0	0	0
200	0.061	0	0
400	0.163	0.072	0.063
600	0.281	0.176	0.156
800	0.349	0.306	0.253
1000	0.409	0.369	0.321

Data Table for comparison of tool wear at 530rpm and depth of cut 1.0 mm

Length of cut (mm)	Without magnet	With permanent magnet	With electro magnet
0	0	0	0
200	0.051	0	0
400	0.151	0.09	0.05
600	0.239	0.135	0.148
800	0.402	0.265	0.232
1000	0.474	0.317	0.238

Data Table for comparison of tool wear at 860rpm and depth of cut 0.5 mm

Length of cut (mm)	Without magnet	With permanent magnet	With electro magnet
0	0	0	0
200	0.061	0.004	0.029
400	0.164	0.152	0.138
600	0.271	0.238	0.222
800	0.35	0.322	0.252
1000	0.434	0.365	0.299

Data Table for comparison of tool wear at 860rpm and depth of cut 0.75 mm

Length of cut (mm)	Without magnet	With permanent magnet	With electro magnet
0	0	0	0
200	0.076	0.06	0.034
400	0.168	0.136	0.135
600	0.307	0.225	0.206
800	0.382	0.341	0.248
1000	0.492	0.397	0.301

Data Table for comparison of tool wear at 860rpm and depth of cut 1.0 mm

Length of cut (mm)	Without magnet	With permanent magnet	With electro magnet
0	0	0	0
200	0.066	0.032	0.01
400	0.175	0.147	0.127
600	0.287	0.263	0.161
800	0.383	0.367	0.218
1000	0.443	0.423	0.306

Data Table for comparison of tool wear at 1400rpm and depth of cut 0.5 mm

Length of cut (mm)	Without magnet	With permanent magnet	With electro magnet
0	0	0	0
200	0.092	0.026	0.011
400	0.204	0.157	0.137
600	0.312	0.273	0.174
800	0.467	0.392	0.248
1000	0.526	0.429	0.313

Data Table for comparison of tool wear at 1400rpm and depth of cut 0.75 mm

Length of cut (mm)	Without magnet	With permanent magnet	With electro magnet
0	0	0	0
200	0.126	0.019	0.015
400	0.223	0.148	0.138
600	0.358	0.291	0.216
800	0.454	0.395	0.306
1000	0.537	0.438	0.322

Data Table for comparison of tool wear at 1400rpm and depth of cut 1.0 mm

Length of cut (mm)	DOC 0.5mm	DOC 0.75mm	Doc 1.0mm
0	0	0	0
200	0	0	0
400	0.036	0.055	0.083
600	0.137	0.159	0.166
800	0.169	0.241	0.253
1000	0.201	0.306	0.321

Comparison of tool wears at 530rpm in electromagnetic condition with different depths of cut

Length of cut (mm)	DOC 0.5mm	DOC 0.75mm	Doc 1.0mm
0	0	0	0
200	0	0.029	0.034
400	0.01	0.168	0.195
600	0.148	0.222	0.236
800	0.232	0.242	0.248
1000	0.238	0.299	0.301

Comparison of tool wears at 860rpm in electromagnetic condition with different depths of cut

Length of cut (mm)	DOC 0.5mm	DOC 0.75mm	Doc 1.0mm
0	0	0	0
200	0.01	0.011	0.015
400	0.127	0.137	0.138
600	0.161	0.174	0.206
800	0.218	0.248	0.286
1000	0.306	0.313	0.322

Comparison of tool wears at 1400rpm in electromagnetic condition with different depths of cut

Length of cut (mm)	DOC 0.5mm	DOC 0.75mm	Doc 1.0mm
0	0	0	0
200	0	0	0
400	0.024	0.031	0.072
600	0.135	0.146	0.176
800	0.286	0.298	0.306
1000	0.305	0.352	0.369

Comparison of tool wears at 530rpm in permanent magnetic condition with different depths of cut

Length of cut (mm)	DOC 0.5mm	DOC 0.75mm	Doc 1.0mm
0	0	0	0
200	0	0.004	0.06
400	0.035	0.052	0.136
600	0.185	0.138	0.225
800	0.317	0.322	0.341
1000	0.347	0.365	0.397

Comparison of tool wears at 860rpm in electromagnetic condition with different depths of cut

Length of cut (mm)	DOC 0.5mm	DOC 0.75mm	Doc 1.0mm
0	0	0	0
200	0.032	0.026	0.019
400	0.147	0.157	0.148
600	0.263	0.273	0.291
800	0.367	0.392	0.395
1000	0.423	0.429	0.438

Comparison of tool wears at 1400rpm in electromagnetic condition with different depths of cut

Length of cut (mm)	DOC 0.5mm	DOC 0.75mm	Doc 1.0mm
0	0	0	0
200	0	0	0.061
400	0.057	0.121	0.163
600	0.223	0.238	0.281
800	0.393	0.434	0.449
1000	0.412	0.452	0.489

Comparison of tool wears at 530rpm in non magnetic condition with different depths of cut

Length of cut (mm)	DOC 0.5mm	DOC 0.75mm	Doc 1.0mm
0	0	0	0
200	0.051	0.061	0.076
400	0.154	0.164	0.168
600	0.269	0.271	0.307
800	0.342	0.359	0.362
1000	0.454	0.464	0.492

Comparison of tool wears at 860rpm in electromagnetic condition with different depths of cut

Length of cut (mm)	DOC 0.5mm	DOC 0.75mm	Doc 1.0mm
0	0	0	0
200	0.066	0.092	0.126
400	0.175	0.204	0.253
600	0.287	0.312	0.358
800	0.353	0.397	0.434
1000	0.489	0.526	0.537

Comparison of tool wears at 1400 rpm in electromagnetic condition with different depths of cut

rpm	no magnet	permanent magnet	electro magnet
530	0.684	0.615	0.705
860	0.437	0.391	0.538
1400	0.391	0.368	0.497

Data table for comparison of surface roughness at 0.5mm DOC and different cutting environments

rpm	no magnet	permanent magnet	electro magnet
530	0.815	0.767	0.831
860	0.684	0.647	0.731
1400	0.672	0.634	0.686

Data table for comparison of surface roughness at 0.75mm DOC and different cutting environments

rpm	no magnet	permanent magnet	electro magnet
530	0.852	0.771	0.781
860	0.707	0.654	0.654
1400	0.681	0.638	0.623

Data table for comparison of surface roughness at 1.0 mm DOC and different cutting environments

DOC (mm)	no magnet	permanent magnet	electro magnet
0.5	153	165	160
0.75	160	180	165
1	194	222	201

Data table variation of temperature with depth of cut at 530rpm after 200mm cut

DOC (mm)	no magnet	permanent magnet	electro magnet
0.5	150	169	158
0.75	170	227	224
1	200	240	237

Data table variation of temperature with depth of cut at 860rpm after 200mm cut

Cutting condition	temperature at 530rpm	Temperature at 860RPM
non magnet	153	150
permanent magnet	165	169
electro magnet	160	158

Data table variation of temperature with depth of cut at 0.5mm DOC after 200mm cut

Cutting condition	temperature at 530rpm	Temperature at 860RPM
non magnet	160	170
permanent magnet	180	227
electro magnet	165	224

Data table variation of temperature with depth of cut at 0.75mm DOC after 200mm cut

Cutting condition	temperature at 530rpm	Temperature at 860RPM
non magnet	194	200
permanent magnet	222	240
electro magnet	201	247

Data table variation of temperature with depth of cut at 1.0mm DOC after 200mm cut

RPM	Non magnet	permanent magnet	electro magnet
530	5452	4586	4485
860	5095	4451	4383
1400	4869	4274	4223

Data table for change of strain of tool holder with respect to Cutting Speed at 0.5 mm DOC

DOC (mm)	Non magnet	permanent magnet	electro magnet
0.5	5452	4586	4485
0.75	5508	4683	4630
1	5612	4776	4695

Data table for change of strain of tool holder with respect to DOC at 530 rpm

RPM	Non magnet	permanent magnet	electro magnet
530	458.8	385.3	376.7
860	428	373.8	368.2
1400	409	359	354.8

Data table for change of tangential cutting force of tool holder with respect to Cutting Speed at 0.5 mm DOC

DOC (mm)	Non magnet	permanent magnet	electro magnet
0.5	458.8	385.2	376.7
0.75	462.7	393.4	388.9
1	471.4	401.2	394.4

Data table for change of tangential cutting force of tool holder with respect to DOC at 530 rpm